

5-2012

BIM MEDIATES IMATINIB-INDUCED APOPTOSIS OF GASTROINTESTINAL STROMAL TUMORS: TRANSLATIONAL IMPLICATIONS

David Reynoso

Follow this and additional works at: https://digitalcommons.library.tmc.edu/utgsbs_dissertations

 Part of the [Medical Molecular Biology Commons](#), [Neoplasms Commons](#), and the [Oncology Commons](#)

Recommended Citation

Reynoso, David, "BIM MEDIATES IMATINIB-INDUCED APOPTOSIS OF GASTROINTESTINAL STROMAL TUMORS: TRANSLATIONAL IMPLICATIONS" (2012). *The University of Texas MD Anderson Cancer Center UTHealth Graduate School of Biomedical Sciences Dissertations and Theses (Open Access)*. 226.
https://digitalcommons.library.tmc.edu/utgsbs_dissertations/226

This Dissertation (PhD) is brought to you for free and open access by the The University of Texas MD Anderson Cancer Center UTHealth Graduate School of Biomedical Sciences at DigitalCommons@TMC. It has been accepted for inclusion in The University of Texas MD Anderson Cancer Center UTHealth Graduate School of Biomedical Sciences Dissertations and Theses (Open Access) by an authorized administrator of DigitalCommons@TMC. For more information, please contact digitalcommons@library.tmc.edu.

BIM MEDIATES IMATINIB-INDUCED APOPTOSIS OF GASTROINTESTINAL
STROMAL TUMORS: TRANSLATIONAL IMPLICATIONS

By

David Reynoso Gaytan, B.S.

Approved:

Russell R. Broaddus, M.D., Ph.D.
Chair, Supervisory Committee

Jonathan C. Trent, M.D., Ph.D.

Emil J. Freireich, M.D., D.Sc.

Edgar T. Walters, Ph.D.

Joseph A. Ludwig, M.D.

Approved:

George Stancel, Ph.D.
Dean, The University of Texas
Graduate School of Biomedical Sciences at Houston

BIM MEDIATES IMATINIB-INDUCED APOPTOSIS OF GASTROINTESTINAL
STROMAL TUMORS: TRANSLATIONAL IMPLICATIONS

A
DISSERTATION

Presented to the Faculty of The University of Texas Health Science Center at Houston
and The University of Texas M. D. Anderson Cancer Center

Graduate School of Biomedical Sciences

in Partial Fulfillment

of the Requirements

for the Degree of

DOCTOR OF PHILOSOPHY

by

David Reynoso Gaytan, B.S.,

Houston, Texas

May, 2012

DEDICATION

This work is dedicated to Adrian and Mia, whose laughter puts life in perspective.

ACKNOWLEDGMENTS

I am foremost grateful for every patient I met as a member of the Sarcoma Medical Oncology team at M. D. Anderson Cancer Center. Though I cannot mention you by name, you inspired me individually, and I hope that I helped a little.

Words cannot express my gratitude for my research advisor and mentor, Dr. Jon Trent, for teaching me the responsibilities of a scientist and clinician, and about balancing life and work. I also thank the faculty who participated diligently in my advisory, examining, and supervisory committees, particularly Dr. Russell Broaddus for serving as my supervisory professor in crunch time. Many thanks to Drs. Emil Freireich, Terry Walters, Joseph Ludwig, Alexander Lazar, Dennis Hughes, and Gary Gallick for so much generous encouragement and advice over the years. I hope to have absorbed some of your collective wisdom, and to be as supportive and nurturing to aspiring scientists as you have been with me.

These studies would not have gone far without the help of my labmates and friends, whom I thank: Dr. Dan Yang, for assisting with the impossible; Drs. Amaury and Sarah Dumont for much thoughtful discussion; Dr. Anthony Conley, for encouraging me at the right times; and Dr. Laura Nolden, for her computer savvy. Because of you, I truly enjoyed my years in graduate research training.

I also thank the people and programs that took a chance on me and made it possible for me to develop as a physician-scientist in Houston: Drs. Dianna Milewicz, Terry Walters, and Russell Broaddus, among others in the M.D./Ph.D. Program at the University of Texas Medical School at Houston, for pushing and prodding me forward; Dr. Victoria Knutson at the Graduate School of Biomedical Sciences for helping me

navigate graduate school, and Dean George Stancel, who supported me generously via a T32 training grant, through the Center for Clinical and Translational Sciences.

I also thank my brothers Miguel and Armando Reynoso for providing me clarity and strength in moments of doubt; my future wife, Leticia Cantu, for her example, love, and support; and my friends, Juan Morales, Joseph Chapa, Ivonne Palacios, Herbert Lindee, Gustavo Garcia, Rene Colorado, and Eugene Galindo, in whose company I caught up on life. Enjoying your company and support was instrumental to this dissertation and to surviving the last seven years.

Finally, I acknowledge my source of unconditional love, support, and motivation for three decades, my parents Micaela Gaytan and Ebodio Reynoso, and my grandparents Hermila Santamaria, Delfina Perez, and Moises Galvan. You let my curiosity and imagination run wild, instilled in me a desire to do well by the world, and showed me, by example, that the best things in life require dedication, hard work, and sacrifice. I thank and admire you.

BIM MEDIATES IMATINIB-INDUCED APOPTOSIS OF GASTROINTESTINAL
STROMAL TUMORS: TRANSLATIONAL IMPLICATIONS

Publication _____

David Reynoso Gaytan, B.S.

Supervisory Professor: Russell R. Broaddus, M.D., Ph.D.

Gastrointestinal stromal tumors (GISTs) are oncogene-addicted cancers driven by activating mutations in the genes encoding receptor tyrosine kinases KIT and PDGFR- α . Imatinib mesylate, a specific inhibitor of KIT and PDGFR- α signaling, delays progression of GIST, but is incapable of achieving cure. Thus, most patients who initially respond to imatinib therapy eventually experience tumor progression, and have limited therapeutic options thereafter. To address imatinib-resistance and tumor progression, these studies sought to understand the molecular mechanisms that regulate apoptosis in GIST, and evaluate combination therapies that kill GISTs cells via complementary, but independent, mechanisms. BIM (**B**cl-2 **i**nteracting **m**ediator of apoptosis), a pro-apoptotic member of the Bcl-2 family, effects apoptosis in oncogene-addicted malignancies treated with targeted therapies, and was recently shown to mediate imatinib-induced apoptosis in GIST. This dissertation examined the molecular mechanism of BIM upregulation and its cytotoxic effect in GIST cells harboring clinically-representative *KIT* mutations. Additionally, imatinib-induced alterations in BIM and pro-survival Bcl-2 proteins were studied in specimens from patients with GIST, and correlated to apoptosis, FDG-PET response, and survival. Further, the intrinsic pathway of apoptosis was targeted

therapeutically in GIST cells with the Bcl-2 inhibitor ABT-737. These studies show that BIM is upregulated in GIST cells and patient tumors after imatinib exposure, and correlates with induction of apoptosis, response by FDG-PET, and disease-free survival. These studies contribute to the mechanistic understanding of imatinib-induced apoptosis in clinically-relevant models of GIST, and may facilitate prediction of resistance and disease progression in patients. Further, combining inhibition of KIT and Bcl-2 induces apoptosis synergistically and overcomes imatinib-resistance in GIST cells. Given that imatinib-resistance and GIST progression may reflect inadequate BIM-mediated inhibition of pro-survival Bcl-2 proteins, the preclinical evidence presented here suggests that direct engagement of apoptosis may be an effective approach to enhance the cytotoxicity of imatinib and overcome resistance.

TABLE OF CONTENTS

DEDICATION.....	iii
ACKNOWLEDGMENTS.....	iv
LIST OF FIGURES.....	xii
LIST OF TABLES.....	xv
LIST OF ABBREVIATIONS.....	xvi
Chapter 1: Introduction.....	1
Gastrointestinal stromal tumors.....	2
KIT and platelet-derived growth factor receptor- α	4
Targeted therapy with imatinib mesylate.....	8
Imatinib delays progression but does not cure advanced GIST.....	9
Imatinib-induced apoptosis in GIST.....	14
The Bcl-2 family of proteins.....	17
Oncogene-addiction and BIM.....	20
Specific aims and significance of study.....	25
Chapter 2: Defining the role of BIM in imatinib-induced apoptosis in GIST cells and patient tumors.....	27
Introduction.....	28
Materials and Methods.....	30
Cell lines and Culture Conditions.....	30
Chemicals, antibodies, and plasmids.....	32
Western Blotting.....	32
Quantitative reverse transcriptase-polymerase chain reaction (RT-PCR) assay.....	33

Apoptosis assays.....	35
Transfection and caspase activity assay	35
Patients and Tumor Specimens.....	36
Immunohistochemical Detection of Apoptosis and Autophagy.....	38
Statistics.....	39
Results.....	40
Inhibition of KIT and PI3K signaling upregulates BIM and activates apoptosis in GIST cells	40
Isoforms BIM-EL, BIM-L, and BIM-S activate apoptosis equally in GIST cells	46
Imatinib treatment causes BIM mRNA upregulation in GIST patients	49
Imatinib downregulates Bcl-2, and upregulates Mcl-1 in GIST patients	52
Imatinib therapy induces tumor cell apoptosis in patients with GIST.....	54
Upregulation of BIM correlates with tumor cell apoptosis in GIST patients.....	56
Imatinib-induced alterations in pro-survival Bcl-2 proteins and apoptosis.....	58
Basal expression of Bcl-2, Bcl-xL, and Mcl-1 and apoptosis	59
Autophagy in imatinib-treated GIST patient samples	60
Bcl-xL upregulation is associated with imatinib-resistance by PET	62
Survival of patients with GIST and the Bcl-2 family	64
Patient and tumor characteristics: MDACC Study ID03-0023	64
Long-term Overall Survival.....	67
Long-term Disease-Free Survival.....	69
Upregulation of BIM is associated with improved DFS in patients with GIST treated with adjuvant imatinib	72

Discussion.....	74
Chapter 3: Synergistic activation of apoptosis by the Bcl-2 Inhibitor ABT-737 and imatinib in GIST cells.....	80
Introduction.....	81
Materials and Methods	84
Chemicals and Antibodies	84
Cell Culture.....	84
Western blot analysis.....	85
Analysis of Cell Proliferation and Viability	86
Propidium Iodide Staining and Cell Cycle Analysis	86
TdT-Mediated dUTP Nick-End Labeling (TUNEL) Assay	87
Ethidium Bromide/Acridine Orange (EB/AO) Apoptosis Assay	89
Data analysis: Statistics and Synergy	89
Results.....	90
ABT-737, but not stereoisomer A793844, inhibits the growth of GIST cells.....	90
ABT-737 and imatinib inhibit GIST cell viability synergistically	94
ABT-737 and imatinib combine to induce apoptosis synergistically	97
ABT-737 induces morphologic features of apoptosis in GIST cells.....	102
ABT-737 and imatinib combine to activate apoptosis and overcome resistance to imatinib in GIST48IM cells	104
Discussion.....	112
Chapter 4: Conclusion and Future Directions	117
Introduction.....	118

Summary of findings	119
Can we predict who will respond to therapy and act accordingly?	122
Can rational combinations of targeted agents cure advanced GIST?	125
Bibliography	128
VITA.....	156

LIST OF FIGURES

Figure 1. KIT/PDGFR- α Structure and Mutation Frequencies	7
Figure 2. Imatinib delays progression but does not cure patients with GIST.....	13
Figure 3. The Bcl-2 Family	19
Figure 4. BIM is suppressed by constitutive oncogene signaling.	23
Figure 5. Inhibition of oncogene signaling upregulates BIM to induce apoptosis.	24
Figure 6. Inhibition of KIT and PI3K activates apoptosis in GIST cells.	42
Figure 7. Inhibition of KIT and PI3K upregulates BIM in GIST cells.....	45
Figure 8. BIM-EL, BIM-L, and BIM-S activate effector caspases in GIST cells.....	48
Figure 9. Imatinib upregulates BIM mRNA in GIST patients.	49
Figure 10. Comparison of BIM upregulation in GISTs treated with imatinib for 3 days and GISTs treated for >3 days.....	51
Figure 11. Imatinib-induced alterations in pro-survival Bcl-2 genes in GIST patients.....	53
Figure 12. Imatinib-induced alterations in pro-survival Bcl-2 genes in GISTs treated with imatinib for 3 days and >3 days.....	53
Figure 13. Imatinib therapy induces tumor cell apoptosis in patients with GIST.	55
Figure 14. Upregulation of BIM correlates with tumor cell apoptosis in GIST patients. .	56
Figure 15. Linear regression analysis of BIM expression and apoptosis.	57
Figure 16. Imatinib-induced alterations in pro-survival Bcl-2 proteins and GIST apoptosis.	58
Figure 17. High basal (pre-imatinib) Bcl-xL mRNA correlates with apoptosis.....	60
Figure 18. Overall survival of patients enrolled in MDACC ID03-0023 study	68

Figure 19. Overall survival by tumor size and primary tumor site in patients enrolled in MDACC ID03-0023 study	68
Figure 20. Disease-free survival, MDACC ID03-0023.....	71
Figure 21. Post-imatinib BIM mRNA level is associated with prolonged DFS in patients with GIST treated with adjuvant imatinib.	74
Figure 22. GIST cells express Bcl-2, Bcl-xL and Mcl-1, the targets of ABT-737.....	91
Figure 23. ABT-737, but not its stereoisomer A793844, significantly inhibits the viability of GIST cells.....	93
Figure 24. ABT-737 and imatinib synergistically inhibit the viability of GIST cells.....	95
Figure 25. Isobologram analysis of synergy for imatinib/ABT-737 combinations with respect to growth inhibition in GIST cells.....	96
Figure 26. ABT-737 and imatinib induce apoptosis synergistically in imatinib-sensitive cells.....	98
Figure 27. Isobologram analyses of synergy with respect to apoptosis for imatinib/ABT-737 combinations in GIST cells.	99
Figure 28. Single-agent and combined effect of ABT-737 and imatinib on caspase/PARP cleavage.	101
Figure 29. The morphologic features of apoptosis are induced by ABT-737 in GIST cells	103
Figure 30. Antiproliferative effects of imatinib and ABT-737 as single-agents in imatinib-resistant cells.....	105
Figure 31. ABT-737 and imatinib synergistically inhibit the viability of imatinib-resistant GIST cells.....	106

Figure 32. Analysis of synergy between imatinib and ABT-737 in imatinib-resistant GIST cells.....	107
Figure 33. ABT-737 and imatinib induce morphologic apoptosis in imatinib-resistant GIST cells.....	109
Figure 34. Western blot detection of Bcl-2 proteins and apoptotic markers in GIST48IM cells.....	110

LIST OF TABLES

Table 1. Basal expression of Bcl-2, Bcl-xL, and Mcl-1 and apoptosis.	59
Table 2. Autophagosome formation and imatinib-induced alterations in the Bcl-2 family.....	62
Table 3. PET response and imatinib-induced alterations in the Bcl-2 family.....	63
Table 4. Clinical and Pathologic Characteristics: MDACC ID03-0023 Study.....	66
Table 5. Association of clinicopathologic factors with post-imatinib BIM, Bcl-2, Bcl-xL and Mcl-1 mRNA.....	67
Table 6. Association of clinicopathologic factors with overall survival.....	69
Table 7. Association of clinicopathologic factors with disease-free survival.....	72
Table 8. Association of Bcl-2 family gene expression with disease-free survival.....	73
Table 9. Overall results from isobologram (synergy) analyses of imatinib/ABT-737 combinations in GIST cells.....	111

LIST OF ABBREVIATIONS

ABL1	V-abl Abelson murine leukemia viral oncogene homolog 1 gene
ABT	ABT-737 (Abbott Pharmaceuticals)
A1	Bcl-2-related protein encoded by the BCL2A1 gene
Apaf-1	Apaf-1 Apoptotic protease activating factor 1
ATP	Adenosine triphosphate
BAK	Bcl-2 homologous antagonist killer
BAX	Bcl-2-associated X protein
Bcl-2	B-cell lymphoma 2 protein
Bcl-w	Bcl-2-like protein 2 encoded by the BCL2L2 gene
Bcl-xL	B-cell lymphoma-extra large
BCR	"breakpoint cluster region" gene
BCR-ABL	fusion of genes ABL1 and BCR caused by the Philadelphia chromosome translocation [t(9;22)(q34;q11)]
BID	BH3 interacting domain death agonist
BIM	Bcl-2 interacting mediator of apoptosis, also known as BCL2L11
CML	chronic myelogenous leukemia
CR	complete response
DFS	disease-free survival
DNA/RNA	deoxyribonucleic acid / ribonucleic acid
EB/AO	ethidium bromide/acridine orange
FASL	CD95L; death ligand belonging to tumor necrosis factor (TNF) family
ICC	interstitial cells of Cajal

IC ₅₀	half-maximal inhibitory concentration
IM	Imatinib mesylate (Gleevec®; Novartis Pharmaceuticals)
GIST	gastrointestinal stromal tumor
KIT	c-KIT; cellular homolog of <i>v-KIT</i> oncogene (HZ4 feline sarcoma virus)
Mcl-1	Induced myeloid leukemia cell differentiation protein 1
MOMP	mitochondrial outer membrane permeabilization
MTS	3-(4,5-dimethylthiazol-2-yl)-5-(3-carboxymethoxyphenyl)-2-(4-sulfophenyl)-2H-tetrazolium inner salt
NI	Nilotinib (Tasigna®; Novartis)
OS	overall survival
PARP	poly-ADP-Ribose polymerase
PDGFR- α/β	platelet-derived growth factor receptors –alpha and beta
PI	propidium iodide
PMS	phenazine methosulfate
PR	partial response
PUMA	p53 upregulated modulator of apoptosis
RTK	receptor tyrosine kinase
SCF	stem cell factor
SD	stable disease
SO	Sorafenib (Nexavar®; Onyx/Bayer)
SU	Sunitinib (Sutent®; Pfizer)
TKI	tyrosine kinase inhibitor
TUNEL	TdT-Mediated dUTP Nick-End Labeling

Chapter 1: Introduction

Gastrointestinal stromal tumors

Gastrointestinal stromal tumors (GISTs) are soft-tissue sarcomas, cancers of mesenchymal origin, which can arise anywhere along the alimentary tract but occur primarily in the stomach (60%) and small bowel (35%), and rarely in the esophagus, large bowel, rectum, or mesentery (<5%). The median age at diagnosis is between 55 and 65 years, with a minority of tumors (3%) arising in patients younger than 21 years of age [1-5]. Although patients with GIST comprise less than one percent of all patients with gastrointestinal cancers, GIST is the most common sarcoma of the digestive tract, with an incidence of 10 to 20 cases per million people, or approximately 5000 patients per year in the United States. For comparison, new cases of colorectal carcinoma exceeded 140,000 in 2011 [1-3].

Patients with GIST may present with symptoms such as abdominal pain, early satiety, distention, GI bleeding (melena or hematochezia), or weight loss, and physical examination may reveal signs suggestive of a gastrointestinal lesion, including a palpable mass, GI obstruction, or anemia [1]. However, given their tendency for indolent growth and extraluminal location, it is common for GISTs to enlarge and spread in the absence symptoms. Consequently, a significant number of tumors are discovered incidentally (12-18%) or emergently (40%), and many patients are diagnosed with metastatic or inoperable GIST (40-50%) at the time of presentation [2-4].

For many years, GISTs were categorized on morphologic appearance and incorrectly grouped with smooth muscle sarcomas, or leiomyosarcomas [2]. In 1983, Mazur and Clark recognized that many sarcomas of the GI wall were not derived from smooth muscle but exhibited mixed neural and smooth muscle elements [3]. Following

this observation, it became apparent that these GI “stromal” tumors heralded distinctly unfavorable prognoses in comparison with other sarcomas. Specifically, less than 5% of patients with advanced GIST respond to cytotoxic chemotherapies, including doxorubicin- or ifosfamide-based regimens, which are standard-of-care for other advanced sarcomas [4]. Consequently, the median disease-specific survival (DSS) was determined to be between 9 and 19 months for patients with recurrent, metastatic or unresectable GIST [5]. The outcome of patients with localized GIST treated with complete surgical resection was only marginally better, with approximately 50% of patients experiencing tumor recurrence within five years [5]. With long-term follow up, some investigators have found that up to 90% of patients with localized GIST eventually experience tumor recurrence after surgical resection [5, 6].

Two discoveries in 1998 revolutionized the prognosis of patients with GIST. Kindblom and colleagues found that GISTs share ultrastructural and immunophenotypic features with interstitial cells of Cajal (ICC), the pacemaker cells responsible for gastrointestinal peristalsis, and suggested that GISTs may be derived from ICCs or from a common lineage. Specifically, these investigators found that the majority of GISTs express the receptor tyrosine kinase KIT (c-KIT), named after its viral homolog v-KIT from the Hardy-Zuckerman 4 feline sarcoma virus [6, 7]. In parallel, Hirota and colleagues discovered gain-of-function mutations in the *KIT* gene, and demonstrated that transfection of mutant *KIT* constructs caused neoplastic transformation of Ba/F3 murine lymphoid cells [8]. These seminal findings shed light on the tumorigenic mechanism of GIST and provided a target for therapeutic intervention, beginning its transformation

from a chemotherapy-resistant orphan disease into an exemplar of molecular-targeted therapy.

KIT and platelet-derived growth factor receptor–alpha (PDGFR- α)

We now know that greater than 95% of GISTs exhibit strong expression of KIT by immunohistochemistry. Mutually-exclusive activating mutations in the genes encoding KIT, or the receptor for platelet-derived growth factor-alpha (PDGFR- α), occur in approximately 80-85% and 5-7% of tumors, respectively. The remaining 10% of tumors lack mutations in either gene, and are termed ‘wild-type’ GIST [9-11].

The *KIT* and *PDGFRA* genes are located in adjacent loci on chromosome 4q12, and encode transmembrane glycoproteins which belong to the Type III family of receptor tyrosine kinases (RTKs). KIT and PDGFR- α are the cell-surface receptors for stem cell factor (SCF) and platelet-derived growth factor (PDGF), respectively. Members of this family, which also includes the colony-stimulating factor-1 receptor (CSF-1R), Fms-like tyrosine kinase 3 (Flt-3), and PDGFR- β , are characterized by a ligand-binding extracellular domain consisting of five immunoglobulin (Ig) regions, an autoinhibitory intracellular juxtamembrane domain, and a ‘split’ kinase domain consisting of an amino-terminal ATP-binding region and a carboxy-terminal phosphotransferase region (Figure 1) [12].

Upon binding to their physiologic ligands, type III RTKs homodimerize and undergo transphosphorylation at tyrosine residues within the juxtamembrane domain, initiating signal transduction cascades that promote cellular growth, proliferation, and survival by inhibition of apoptosis [13-16]. In humans, KIT is expressed by, and required

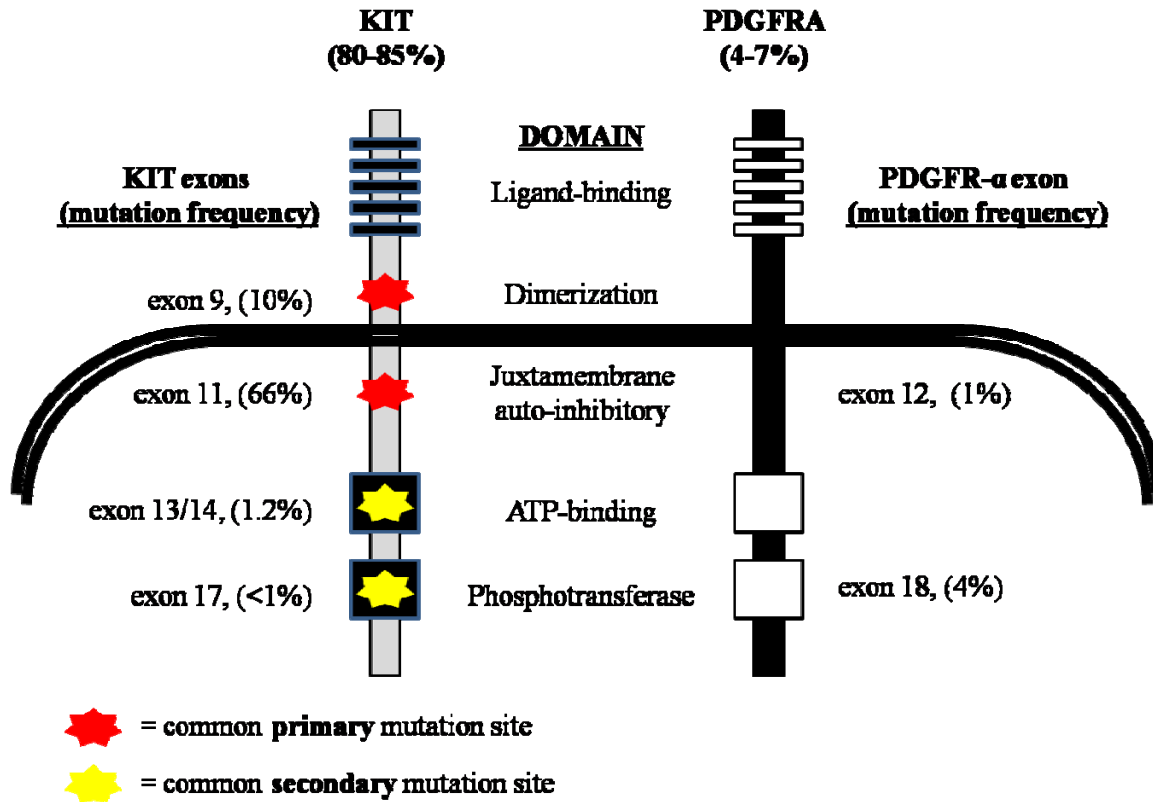
for development of, melanocytes, germ cells, hematopoietic stem cells, mast cells, and interstitial cells of Cajal [17]. In these normal cells, signaling cascades are limited by auto-regulatory mechanisms, including the inhibitory juxtamembrane domain, which sterically hinders the kinase domain in the absence of ligand [18], dephosphorylation of active KIT by the phosphatase SHP-1 [19], and activation-induced receptor endocytosis coupled with proteasomal degradation [20].

Gain-of-function mutations in the *KIT* or *PDGFRA* genes abrogate the regulatory mechanisms of their respective proteins, and cause constitutive, ligand-independent signaling that drives the neoplastic proliferation and survival of GIST. Importantly, mutations in *KIT* or *PDGFRA* are thought to be tumor-initiating events in the development of GIST, as evidenced by their occurrence in ICC hyperplasia and very small, incidentally-discovered GIST, by their ability to induce malignant transformation in non-neoplastic cells, and by the causative role of germline *KIT/PDGFRA* mutations in familial GIST syndromes [8, 21, 22].

In GIST, most mutations are found in *KIT* exon 11 (70-80%), and cause disruption of the autoinhibitory function of the juxtamembrane domain [18]. *KIT* exon 9 mutations are found in approximately 12-15% of tumors and are thought to permit KIT activation in the absence of homodimerization [23]. A minority of primary mutations (<2%) occur in the kinase domains encoded by *KIT* exons 13 and 17; these mutations cause kinase hyperactivity, rather than escape autoinhibition [10, 24]. Although rare at clinical presentation, kinase domain mutations are responsible for the majority of acquired imatinib-resistance found in patients with GIST (Figure 1) [24-27].

While somatic *KIT* and *PDGFRA* mutations are necessary and sufficient to initiate and maintain tumorigenesis in GIST, other molecular and genetic aberrations contribute to its progression [28]. In particular, deletion or loss of heterozygosity of chromosome regions 14q and 22q are common features, observed in 40-67% of advanced GIST [29, 30]. Moreover, loss of the gene encoding tumor suppressor p16^{Ink4A}, known as cyclin-dependent kinase inhibitor 2A (*CDKN2A*) on chromosome 9p, has been found to associate with highly-malignant behavior in GIST [31]. Additional cytogenetic aberrations associated with GIST include deletions of 1p, 13q, and 15q, although the mechanism by which these contribute to the pathogenesis of GIST is unclear [32].

Figure 1. KIT/PDGFR- α Structure and Mutation Frequencies



KIT and PDGFR- α are members of the Type III family of receptor tyrosine kinases, characterized by ligand-binding extracellular domains consisting of five Ig regions, autoinhibitory intracellular juxtamembrane domains (*KIT* exon 11; *PDGFRA* exon 12), and kinase domains separated into ATP-binding region (*KIT* exon 13; *PDGFRA* exon 14) and phosphotransferase region (*KIT* exon 17; *PDGFRA* exon 18). *KIT* exon 11 mutations are the most common primary mutations encountered in GIST patients, whereas *KIT* exons 13 or 17 are the most common secondary mutations responsible for imatinib-resistance.

Targeted therapy with imatinib mesylate

Discovery of *KIT/PDGFR*A mutations as the primary oncogenic mechanism driving GIST facilitated therapy with imatinib mesylate (Gleevec; Novartis Pharmaceuticals), a small-molecule tyrosine kinase inhibitor (TKI) specific for KIT, PDGFR- α , and the fusion kinase BCR-ABL, which is caused by the Philadelphia chromosome translocation t(9;22)(q34;q11) in patients with chronic myelogenous leukemia (CML). Imatinib is an orally-bioavailable derivative of 2-phenylaminopyrimidine that binds with high affinity ($K_i < 0.01 \mu\text{M}$) to the structurally-related ATP-binding pockets of these kinases and competitively inhibits substrate phosphorylation. Importantly, imatinib binds to the kinase domain of KIT in its inactive conformation, explaining why *KIT* exon 13 and 17 (kinase) mutations exhibit resistance to imatinib.

Imatinib was first used for the treatment of patients with CML, yielding complete hematologic responses in 98% of patients [33]. Following the extraordinary clinical response of a patient with widely metastatic GIST who was treated compassionately [34], a series of phase I, II, and III clinical trials confirmed the efficacy and safety of imatinib [35-37]. In 2002, imatinib (400-800 mg daily) was approved by the FDA for treatment of patients with metastatic and unresectable GIST, and has since been shown to benefit 80-90% of patients and extend median overall survival (OS) from 9 to 57 months [38]. Furthermore, in the adjuvant (post-surgical) setting, imatinib effectively delays tumor recurrence in patients at high risk [39], and is increasingly used in the neoadjuvant (pre-surgical) setting to reduce tumor volume and facilitate resection of bulky and borderline-inoperable tumors [40].

Despite its overwhelming success in comparison to cytotoxic chemotherapies, the long-term efficacy of imatinib is limited by resistance, cytostatic effects, and the heterogeneous resistance of GISTs. Collectively, these factors subvert the curative potential of imatinib and facilitate tumor progression, causing immeasurable physical and emotional suffering among our patients.

Imatinib delays progression but does not cure advanced GIST

Approximately 80-90% of patients with advanced GIST treated with imatinib achieve objective clinical benefit (disease control), defined as complete or partial decreases in tumor size, or stabilization of tumor growth, for greater than six months. The remaining 10-20% of patients experience disease progression (tumor growth or metastasis) within six months. Tumors that progress immediately are said to exhibit primary (inherent) resistance to imatinib, a phenotype commonly attributed to ‘wild-type’ *KIT/PDGFR*A status, to *PDGFR*A exon 18 mutations, or to *KIT* exon 13/17 mutations. A minority of patients (4%) are non-compliant with therapy or incapable of tolerating the adverse effects of imatinib, which include periorbital edema (25-40%), nausea and vomiting (33-61%), diarrhea (17-54%), fatigue (12-45%), and low-grade anemia (up to 90%) [35-37].

Among patients whose tumors initially respond by decreasing in size, complete responses (disappearance of all lesions) are observed in only 1-3% of patients [35-37]. More often, tumor shrinkage eventually ceases and 50% of patients experience progression at approximately two years after initiating imatinib (Figure 2). When GIST progression occurs after initial response to imatinib, it is typified by the outgrowth of

isolated tumor nodules within a stable or partially-responding tumor mass. Such ‘limited progression’ reflects the selection of imatinib-resistant GIST subclones, in contrast to the ‘generalized progression’ that occurs with primary resistance.

Acquired (secondary) resistance to imatinib is the most common cause of treatment failure and tumor progression, and various mechanisms of imatinib-resistance have been characterized in GIST. In 70% of patients with progressing tumors, secondary *cis*-mutations (in the same allele as the primary mutation) develop in the kinase domains of KIT, disrupting imatinib-binding and restoring oncogenic signaling to tumors [25, 26]. Importantly, a vast number of distinct drug-resistant secondary mutations have been described in GIST patients. These may occur in separate metastatic lesions and even in different regions within the same tumor [41]. A minor proportion of acquired resistance occurs by amplification of the *KIT* locus, by adoption of alternative oncogenes, or by rhabdomyoblastic differentiation [41-44].

Acquired resistance to targeted therapy is not unique to GIST, but is commonly observed in other oncogene-addicted hematologic and solid malignancies, including BCR-ABL⁺ CML, and non-small cell lung cancers (NSCLC) driven by mutations in the epidermal growth factor receptor (EGFR). In CML, primary resistance is observed in 15-25% of patients, while secondary resistance develops in 7-15% at 24 months [45]. Overall, approximately 60% of patients with CML continue to sustain complete cytogenetic responses (CCyR) five years after treatment initiation [45]. Analogous to GIST, acquired imatinib-resistance in CML mainly occurs through secondary mutations within the kinase domain, and the BCR-ABL T315I mutation is responsible for the majority [46]. Similarly, 50% of progressing lung tumors from patients with resistance to

erlotinib (Tarceva; Astellas Pharma.) or gefitinib (Iressa; AstraZeneca), harbor T790M secondary *cis*-mutations in the kinase domain of EGFR [47]. Mechanisms of resistance independent of secondary oncogene mutations have also been observed, particularly in CML, and include increased expression of the drug efflux pump P-glycoprotein (Pgp) [48], and decreased expression of the organic cation transporter (hOCT1) responsible for cellular uptake of imatinib [49].

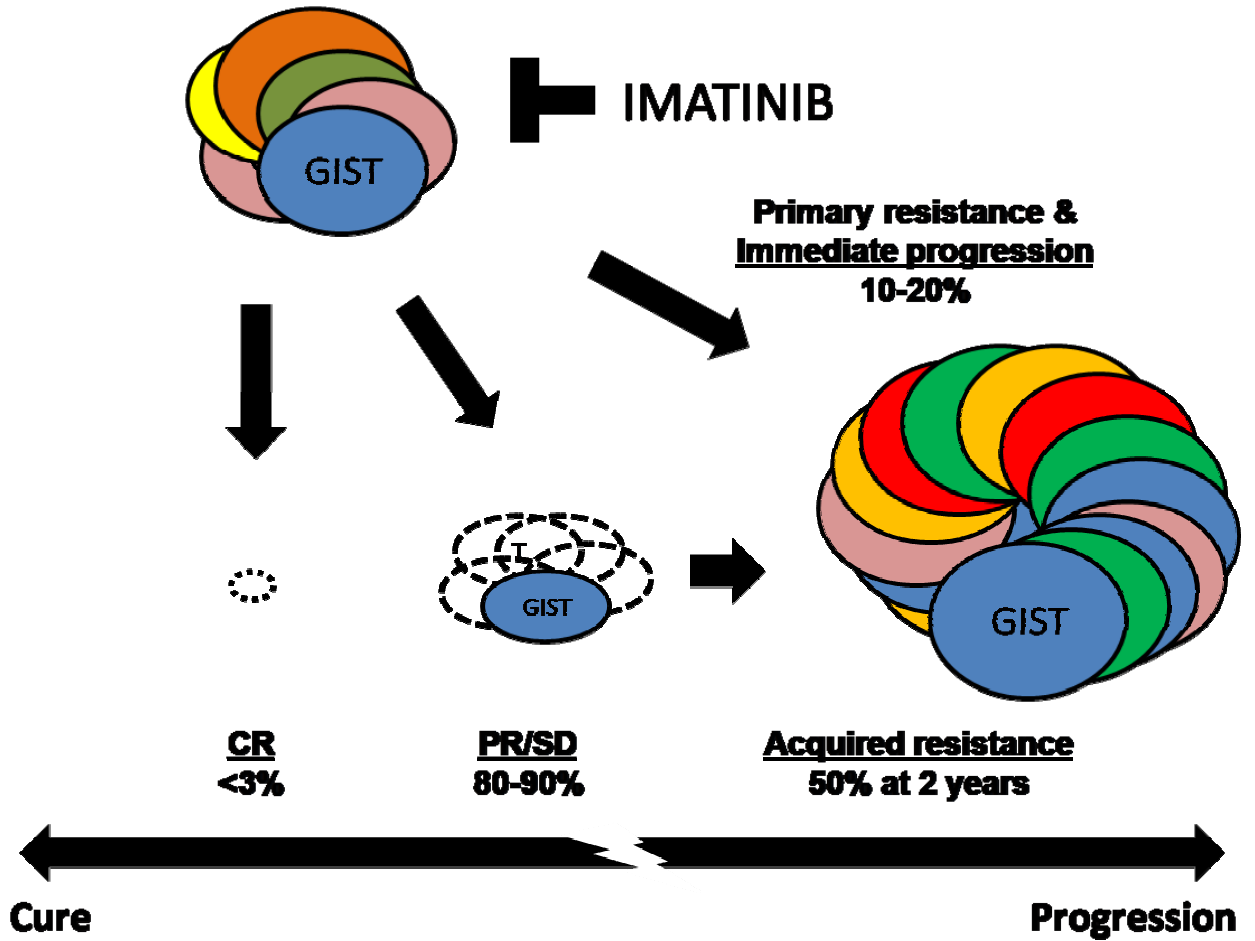
In addition to acquired resistance, GIST cells survive imatinib monotherapy via adaptive cellular responses, such as quiescence and autophagy. Several investigators have observed viable tumor nodules containing autophagic or quiescent GIST cells on histopathologic examination of imatinib-treated tumors, *in vitro* and *in vivo* [25, 50, 51]. These findings are consistent with the clinical observation that imatinib-discontinuation often leads to resumption of tumor progression [52]. It is not certain how the ability to remain metabolically dormant contributes to the development of imatinib-resistant mutations, or vice-versa. What is clear is that resistance and cytostatic effects prevent cure, and cause patients to remain on therapy indefinitely. This is not trivial, given the burden of impending progression, and the cost of imatinib (\$50,000 to \$80,000 per year) [53].

Sunitinib malate (Sutent; Pfizer), a TKI whose molecular targets include KIT, PDGFR- α , and vascular endothelial growth factor receptor (VEGFR), is the only FDA-approved agent for patients with imatinib-refractory GIST, but it postpones progression by only 21 weeks in comparison with placebo, and achieves responses in only 7% of patients [54]. Other TKIs, such as nilotinib (Tasigna; Novartis), pazopanib (Votrient, Glaxo-Smith-Kline), dasatinib (Sprycel, Bristol-Meyer-Squibb), or sorafenib (Nexavar;

Onyx/Bayer), are used in clinical trials or off-label, as third-line agents for patients with imatinib- and sunitinib-resistant GIST, but these provide limited benefit, with eventual disease progression [55]. Furthermore, given that progressing GISTs are composed of heterogeneous cells undergoing adaptive selection, it is unlikely that KIT inhibition as a sole therapeutic strategy will achieve cure.

In sum, although it was previously thought that tumor cell death was the predominant effect of imatinib in GIST, the lack of cures, emergence of resistance, and eventual progression of disease imply that inhibition of KIT signaling, even when complete, is not equivalent to cell death. Mixed cytostatic and cytotoxic effects at the cellular level partially explain the variability of clinical responses to imatinib, and underscore the need for therapeutic targets other than KIT. Thus, to augment the cytotoxicity of imatinib and overcome resistance, it is necessary to understand how GIST cells succumb to therapy. To that end, the studies described in this dissertation focus on the mechanism of imatinib-induced apoptosis in GIST, and define its translational (therapeutic and prognostic) relevance.

Figure 2. Imatinib delays progression but does not cure patients with GIST.



Clinically, GIST responses to imatinib lie on a continuum between cure (CR, complete response) and progression (continued tumor growth or metastasis). Most tumors initially respond by shrinking (PR, partial response) or ceasing to grow (SD, stable disease), while a minority progress immediately after initiation of therapy. Acquired imatinib-resistance eventually leads to disease progression in most patients whose tumors initially respond. Progressing GISTs are composed of heterogeneous clones, harboring diverse imatinib-resistant mutations, which preclude the efficacy of further therapy with imatinib or second-generation tyrosine kinase (KIT/ PDGFR- α) inhibitors.

Imatinib-induced apoptosis in GIST

Apoptosis is a conserved mechanism of programmed cell death that mediates turnover of damaged or unwanted cells within multicellular organisms. Thus, the ability to evade apoptosis is a defining feature of cancer cells, one which promotes their survival in the face of normal homeostatic mechanisms, but also in the presence of cytotoxic agents such as radiotherapy and chemotherapy [56].

Apoptosis is distinguishable from necrotic cell death by the stereotypic manner in which it proceeds. Unlike necrotic cells, apoptotic cells do not swell, lyse, or induce inflammation. Morphologically, apoptotic cells compact and degrade their cytoplasmic and nuclear (DNA and RNA) contents, form plasma membrane blebs, and externalize phosphatidyl serine to attract phagocytes [57]. Biochemically, these cellular changes are mediated by caspases, a family of cysteine-dependent **aspartate-directed proteases** that are activated by two distinct mechanisms [58]. The ‘extrinsic pathway of apoptosis’ triggers cell death in response to external stimuli, including binding to death-ligands such as FAS-L, whereas the ‘intrinsic (mitochondrial) pathway’ responds to intracellular stresses, such as irreparable DNA damage or oncogenic signaling. As its name suggests, the intrinsic pathway culminates with mitochondrial outer membrane permeabilization (MOMP), which releases cytochrome c into the cytoplasm. Cytochrome c then binds to the cytosolic protein Apaf-1 to form a multimeric complex, known as the apoptosome, which activates initiator caspase 9 by proteolysis (pro-caspase to caspase cleavage). In turn, caspase 9 cleaves effector caspases 3, 6, and 7, which activate the proteases and nucleases that ultimately degrade the vital macromolecules of the cell [57].

Although cell death resulting from inhibition of KIT is moderate across GIST study models, imatinib has been shown to induce apoptosis in patient and murine tumors, as well as cell lines [59-62]. For example, in 19 patients with GIST who received imatinib (600 mg daily) for 3, 5, or 7 days, McAuliffe and colleagues demonstrated that GIST cell apoptosis increased by a mean of 12% (range 0-33%), and correlated significantly with duration of therapy [60]. Similarly, in a mouse model of GIST, Rossi and colleagues showed that apoptosis is not an immediate effect, but requires prolonged exposure to imatinib. These investigators observed few histologic changes consistent with apoptosis in mice treated for 6, 12, 24, or 48 hours (45 mg/kg imatinib twice daily), but found significant decreases in cellularity, increases in myxoid stroma, and caspase 3 cleavage after 7 days of treatment [62]. In contrast, Miselli and colleagues examined 11 imatinib-treated specimens from patients with GIST and found no cleaved caspase 3 or 7 by immunohistochemistry. Instead, they reported finding LC3-II by western blot, and suggested that autophagy, rather than apoptosis, mediated cell death in GIST [63]. Albeit interesting, these findings are inconclusive, as they were not corroborated via electron microscopic visualization of autophagosomes, which is the gold standard method for detection of autophagy. Additionally, these samples were evaluated after prolonged imatinib exposure, raising the question as to whether autophagy may be a marker of resistance rather than apoptosis.

In patient-derived GIST cell lines, apoptosis induction by imatinib is equally controversial. While Tuveson found that the proportion of apoptotic GIST882 cells, by Annexin V staining, increased 2-3-fold upon treatment with 1 μ M imatinib for 4 and 7 days [59], Sambol and colleagues reported that exposure to 0.1-10 μ M imatinib was

insufficient to increase apoptosis of GIST882 cells above baseline (<10%) [64]. This discrepancy may be explained by the fact that the latter study did not treat GIST cells beyond 72 hours, and the finding by Liu and colleagues that some GIST882 cells do not undergo apoptosis, but enter p27(Kip1)-mediated quiescence in response to imatinib [50]. Similarly, most investigators have reported induction of apoptosis by imatinib in the imatinib-sensitive cell line GIST-T1 [65-67], whereas Gupta and colleagues reported that imatinib induces autophagy as a survival pathway, in lieu of apoptosis, in these cells [51].

In light of the paradoxical observations regarding imatinib-induced apoptosis, our laboratory and others' have focused on identifying the molecular mediators of imatinib-induced cytotoxicity. Importantly, prior work from our laboratory demonstrated that early molecular alterations, including upregulation of insulin-like growth factor binding protein 3 (IGFBP3) and VEGF downregulation, correlate with apoptosis induction *in vivo* [68, 69]. In addition, studies by Duensing, Bauer and colleagues clearly identified the phosphatidylinositol 3-kinase (PI3K) and mitogen-activated protein kinase (MEK1/2, also known as MAPKK1/2) signaling pathways as the primary mediators of survival downstream of KIT, and excluded SRC, JAK/STAT or PLC- γ signaling pathways in this regard [61, 70]. These investigators subsequently implicated the intracellular stresses, γ -H2AX-mediated transcriptional arrest and endoplasmic reticulum (ER) stress, in the mechanism of imatinib-induced apoptosis in GIST [65, 71].

Despite an abundance of molecular culprits and imatinib-induced intracellular stresses, the mechanism by which cytotoxic and cytostatic stimuli are integrated to determine the fate of GIST cells remained unclear until recently. In the latter part of 2007, evidence from seemingly dissimilar “oncogene-addicted” cancers began to

coalesce, and suggested that imatinib-induced apoptosis in GIST involved the Bcl-2 (B-cell lymphoma-2) family of proteins, given their role as regulators of the intrinsic pathway of apoptosis at the level of the mitochondria [72].

The Bcl-2 family of proteins

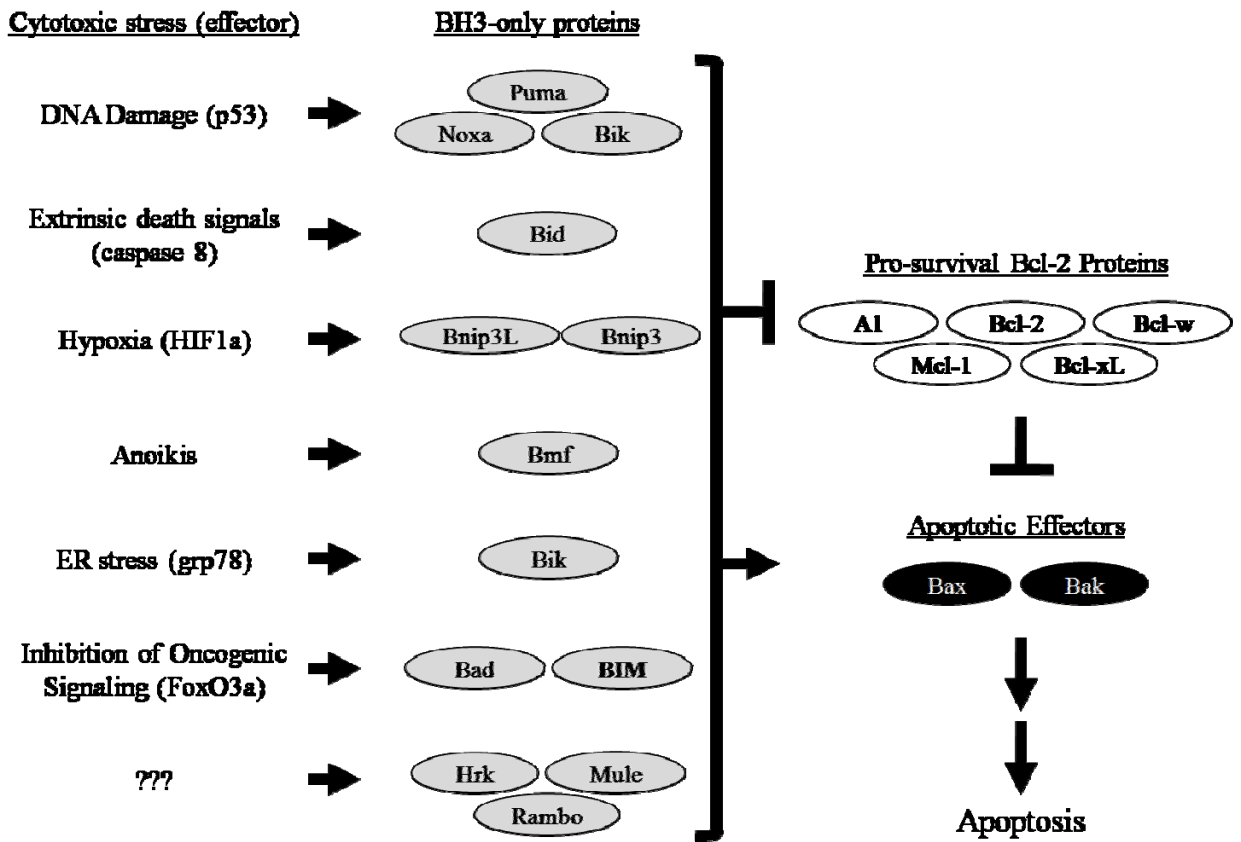
The Bcl-2 family of proteins controls the intrinsic pathway of apoptosis by modulating the permeability of the mitochondria (Figure 3). Three subgroups with unique regulatory mechanisms and roles make up this family. The first group, consisting of pro-survival members Bcl-2, Bcl-xL, Bcl-w, A1, and Mcl-1, prevent apoptosis by inhibiting the second subgroup, consisting of apoptotic effectors BAX and BAK, from forming a pore on the mitochondrial outer membrane [73, 74]. The namesake of the family, Bcl-2, was the first human cancer protein found to enhance cell survival under cytotoxic stress [75, 76], followed by Bcl-xL, Bcl-w, A1, and Mcl-1 [77, 78]. It was later noted that homologues BAX and BAK interact intimately with pro-survival proteins, but antagonize them to induce apoptosis [79, 80].

The third subgroup function as molecular sensors of intracellular stress [81]. These BH3-only proteins, so called because they share only **Bcl-2** homology domain **3** with the rest of the family, include BIM, BAD, PUMA, NOXA, BMF, and BIK. These proteins are kept suppressed during normal cell cycling by growth and survival signaling, and become activated by specific intracellular stresses. For example, PUMA and NOXA are activated by DNA damage through p53 transcriptional activation, whereas BIK and BMF are activated by ER stress and anoikis, respectively [81]. Once activated, BH3-only

proteins promote apoptosis by antagonizing the pro-survival Bcl-2 proteins, or by directly activating BAX and BAK [82].

While there is considerable debate as to exactly how BH3-only proteins promote apoptosis, the current model proposes that they disrupt the equilibrium between pro- and anti-apoptotic members, which otherwise titrate one another by forming heterodimers [83]. Under this model, the relative concentrations of opposing members partly determines whether cells will live or die in response to cytotoxic stress, but the BH3-only proteins actually sense those stresses and trigger mitochondrial permeabilization [82].

Figure 3. The Bcl-2 Family



Members of the Bcl-2 family of proteins regulate the intrinsic pathway of apoptosis, upstream of caspase activation, by modulating the permeability of the mitochondrial outer membrane. BH3-only proteins (gray) are pro-apoptotic members of this family, which sense a variety of intracellular cytotoxic stresses, and become activated by transcriptional and post-translational mechanisms. Upon activation, BH3-only proteins antagonize pro-survival Bcl-2 proteins (white) and/or directly activate pro-apoptotic Bcl-2 proteins BAX and BAK to form a pore to permeabilize the mitochondria [81].

Oncogene-addiction and BIM

“Oncogene addiction” refers to an absolute dependence of tumor cells on specific oncogenic pathways for proliferation or survival [84, 85]. This phenomenon is exhibited by certain types of cancers, and contrasts with the model of tumorigenesis in cancers that lack oncogene addiction, in which the multi-step accumulation of scores of genetic and epigenetic alterations results in the gradual progression from the normal to the malignant phenotype [86, 87].

The phenomenon of oncogene addiction was first illustrated by studies in transgenic mouse models and human cancer cell lines [88-93]. In a transgenic model of T-cell and myeloid leukemias, Felsher and Bishop demonstrated that inducible overexpression of Myc caused proliferation and survival of leukemia cells, whereas "switching off" Myc invariably resulted in growth arrest and apoptosis [88]. Similarly, in a model of BCR-ABL⁺ myeloid leukemias, blocking BCR-ABL expression caused apoptosis and differentiation of leukemic cells [89]. Subsequently, oncogene addiction was found to extend to some solid tumors, including B-RAF- or H-RAS-induced melanomas and EGFR-mutant NSCLC transgenic models, where inhibiting activated oncogenes was also found to trigger apoptotic tumor cell death [93].

Perhaps the most convincing evidence in support of oncogene addiction comes from clinical studies in which the dependence on specific oncogenes has been exploited therapeutically. Examples of extraordinary clinical responses to targeted therapies can be found among patients with BCR-ABL⁺ CML treated with imatinib [94], patients with EGFR-mutant or -amplified NSCLCs treated with gefitinib/erlotinib [95], and patients with advanced GIST treated with imatinib [38].

One model to explain the dependence of tumor cells on specific signaling pathways suggests that pro-apoptotic and pro-survival signals have different rates of attenuation upon oncogene inactivation [96]. That is, because survival signals are generally short-lived whereas apoptotic signals generally persist, an unbalanced accumulation of pro-apoptotic effectors occurs upon oncogene inhibition [96].

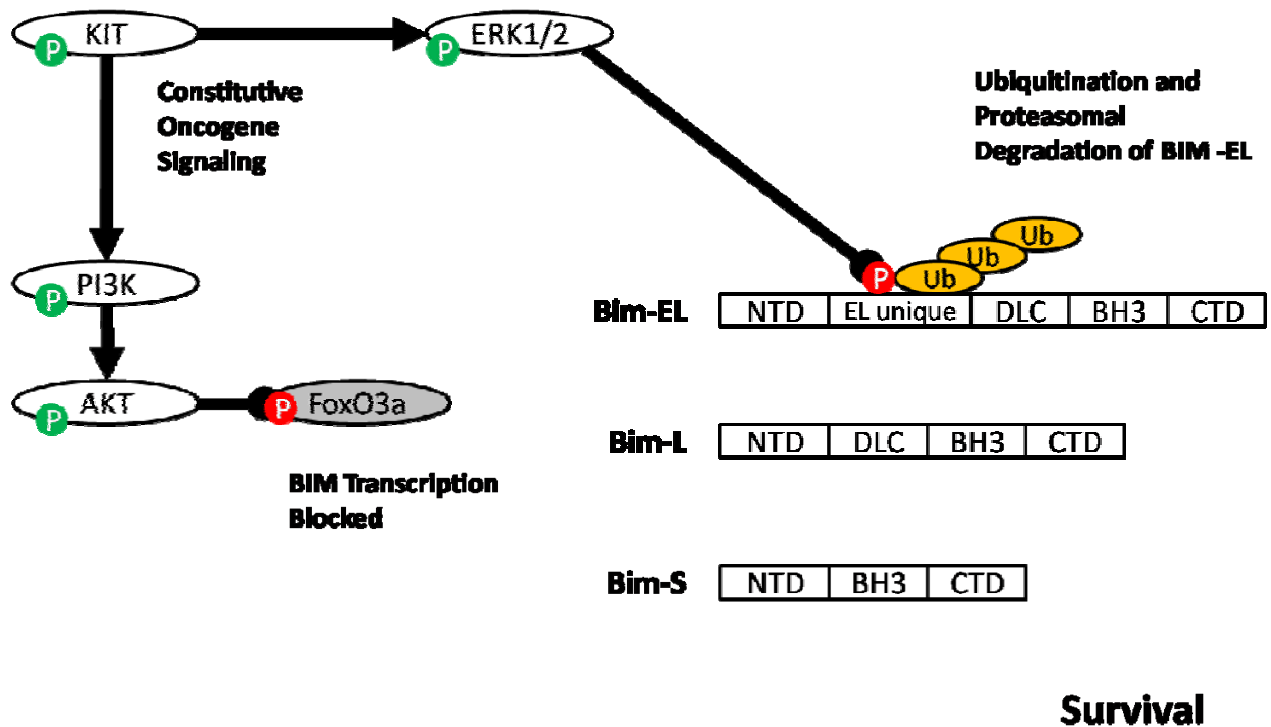
In this context, the BH3-only protein BIM (**B**cl-2 interacting **m**ediator of apoptosis) has emerged as a universal mediator of apoptosis in oncogene-addicted malignancies treated with targeted therapies [97, 98]. In untreated oncogene-addicted tumors, the PI3K/AKT and MEK/ERK survival pathways are constitutively activated and suppress the expression and activity of BIM (Figure 4). Consequently, targeted therapy with their respective oncogene inhibitors causes upregulation of BIM and activation of apoptosis (Figure 5). For example, in patient-derived BCR-ABL⁺ cells, Kuroda and others have demonstrated that BIM plays an effector role in imatinib- and nilotinib-induced apoptosis, and that siRNA silencing of BIM abrogates the apoptotic effect of these BCR-ABL inhibitors [99-101]. Similarly, KIT-driven systemic mastocytosis treated with KIT inhibitor PKC412 offer analogous evidence in support of the pro-apoptotic role of BIM in oncogene-addicted cancers [102].

The role of BIM as mediator of TKI-induced apoptosis extends to oncogene-addicted solid-tumors. For instance, human melanoma cells harboring the B-RAF V600E mutation are dependent on MEK1/2 signaling for survival, and inhibition of BRAF or MEK1/2 with the TKIs PLX4720 or CI-1040, respectively, results in BIM upregulation and apoptosis [98, 103]. Similarly, Costa and colleagues demonstrated that upregulation of BIM is required for apoptosis in EGFR-mutant lung cancer cells treated with gefitinib

or erlotinib [104]. In addition, these investigators showed that the T790M secondary mutations that cause resistance to gefitinib/erlotinib prevent apoptosis by blocking upregulation of BIM [104].

Against this background, Gordon and Fisher recently demonstrated that BIM contributes functionally to imatinib-induced apoptosis in a GIST cell culture model [105]. Specifically, inhibition of KIT, PI3K/AKT and MEK/ERK signaling in imatinib-sensitive GIST882 cells causes transcriptional and post-translational upregulation of BIM, which results in activation of apoptosis. Inhibition of PI3K enables transcription of BIM by FOXO3A (a transcription factor inhibited by AKT-mediated phosphorylation), whereas inhibition of MEK leads to dephosphorylation of BIM on serine 69, preventing its proteasomal degradation [105].

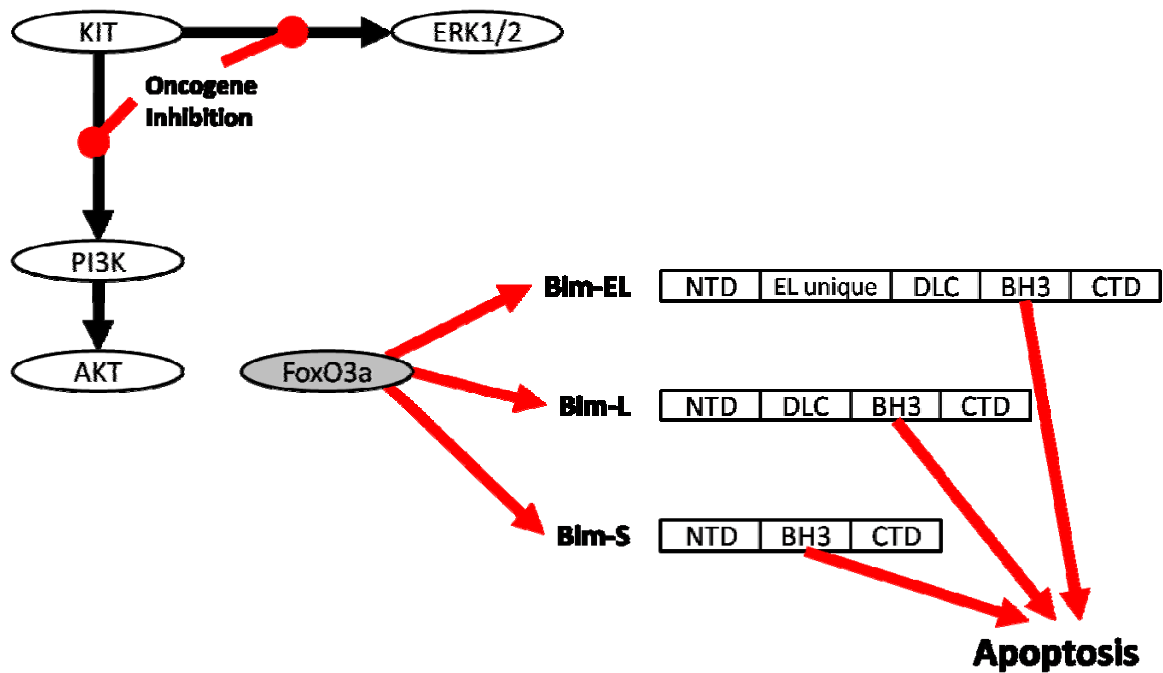
Figure 4. BIM is suppressed by constitutive oncogene signaling.



Oncogene-driven Suppression of BIM

Constitutive oncogene-signaling suppresses BIM expression and function via the PI3K/AKT and MEK/ERK signaling pathways. BIM-EL, the largest BIM isoform, is suppressed by ERK1/2-mediated phosphorylation on serine 69, which targets it for poly-ubiquitination and proteasomal degradation. BIM-L and BIM-S lack this “EL unique” domain and are not regulated by ERK1/2-mediated phosphorylation. All three isoforms are regulated at the transcriptional level by AKT-mediated inhibitory phosphorylation of transcription factor FoxO3a (S253). NTD, Amino-terminal domain; “EL unique,” protein domain unique to BIM-EL, containing serine 69; DLC, dynein light-chain binding domain possessed by BIM-EL and BIM-L to allow these isoforms to activate apoptosis in response to cytoskeletal perturbations; BH3, BH3-only domain that permits inhibition of pro-survival Bcl-2 proteins; CTD, carboxy-terminal domain. Green “P,” activating phosphorylation. Red “P,” inhibitory phosphorylation. Ub, ubiquitin.

Figure 5. Inhibition of oncogene signaling upregulates BIM to induce apoptosis.



Activation of BIM by Oncogene Inhibition

Withdrawal of oncogene signaling resulting from tyrosine kinase inhibition (i.e. imatinib therapy), disrupts survival signaling via PI3K/AKT and MEK/ERK pathways, and causes upregulation of BIM by two mechanisms: First, BIM-EL is relieved of ERK1/2-mediated phosphorylation on serine 69, allowing it to escape poly-ubiquitination and proteasomal degradation. Second, transcription factor FoxO3a is relieved of AKT-mediated inhibitory phosphorylations, particularly on serine 253, enabling FoxO3a to transcribe all isoforms of BIM. Active BIM isoforms inhibit pro-survival Bcl-2 proteins to induce mitochondrial apoptosis.

Specific aims and significance of study

While the aforementioned studies clarified our understanding of the mechanism by which KIT inhibition induces apoptosis, the role of BIM in GIST is of uncertain clinical relevance. Imatinib-sensitive GIST882 cells harbor homozygous *KIT* exon 13 activating mutations (K642E) in the ATP-binding region of the split tyrosine kinase domain, which are rarely found in GIST patients (1%) [59]. Thus, it is necessary to ascertain whether BIM mediates apoptosis in GIST cells harboring *KIT* exon 11 mutations, which are found in approximately 70% of patients [11]. Secondly, while BIM may be important for imatinib-induced apoptosis *in vitro*, the role of the BIM/Bcl-2 axis in tumor cell apoptosis has not been evaluated in GIST patient samples.

No studies have examined whether BIM is upregulated in patients with GIST treated with imatinib, or whether its expression is related to response or survival. Further, given that imatinib monotherapy appears to achieve inadequate neutralization of pro-survival Bcl-2 proteins, a rational drug combination that inhibits both KIT signaling and Bcl-2 proteins may achieve greater apoptotic cell death. Therapeutic inhibition of pro-survival Bcl-2 molecules in GIST has not been attempted. To address these issues and characterize the translational implications of BIM-mediated apoptosis in GIST, I carried out the following research aims:

1. **To validate the role of BIM as a mediator of imatinib-induced apoptosis in clinically-representative GIST cells, and examine the clinical significance of BIM in patients with GIST treated with imatinib (Chapter 2).**
2. **To enhance the apoptotic effect of imatinib in GIST by targeting the pro-survival Bcl-2 proteins with inhibitor ABT-737 (Chapter 3).**

This dissertation details efforts to understand the role of BIM in imatinib-induced apoptosis in GIST, as well as to evaluate the potential of Bcl-2 proteins as biomarkers and/or therapeutic targets. In Chapter 2, the expression and function of BIM in clinically-representative GIST cells is examined. The mechanism of BIM upregulation was studied by treating cells with imatinib and inhibitors specific of downstream pathways. To examine the cytotoxic function of BIM, three known functional isoforms of BIM were transfected and expressed in GIST cells, and their ability to induce caspase activation was assessed. Given the role of BIM in imatinib-induced apoptosis *in vitro*, I hypothesized that its function extends to patients with GIST. To test this hypothesis, mRNA expression levels of BIM and pro-survival Bcl-2 proteins (Bcl-2, Bcl-xL, and Mcl-1) were quantified, before and after imatinib, in tumor specimens from patients with GIST, and gene expression alterations were correlated to tumor cell apoptosis, autophagy, FDG-PET response and disease-free survival.

In chapter 3, therapeutic inhibition of Bcl-2 as an approach to enhance the cytotoxicity of imatinib was examined in GIST. Given the current understanding of imatinib-induced apoptosis, I targeted the pro-survival Bcl-2 proteins therapeutically, using a novel pro-apoptotic BH3-mimetic, ABT-737. I hypothesized that inhibition of pro-survival Bcl-2 proteins enhanced the cytotoxicity of imatinib to overcome imatinib-resistance in GIST. The antiproliferative and apoptotic effects of ABT-737 were assessed in imatinib-sensitive and -resistant GIST cells, and synergy with imatinib was quantified.

Chapter 2: Defining the role of BIM in imatinib-induced apoptosis in GIST cells and patient tumors

Introduction

As discussed previously, current evidence suggests that imatinib lacks sufficient cytotoxicity to eradicate GIST cells and achieve cure. Thus, it is necessary to understand the molecular mechanisms that underlie its cytotoxicity, with the hope that this can result in the formulation of rational combination therapies in GIST. Importantly in this regard, BIM mediates the apoptotic effect of targeted therapies in multiple analogous oncogene-addicted malignancies [97, 98], and has been shown to contribute functionally to imatinib-induced apoptosis in the imatinib-sensitive cell line GIST882 [105].

Although we have a better understanding of the regulatory role of BIM and the Bcl-2 family in the intrinsic pathway of apoptosis in GIST, it is necessary to validate the clinical and translational significance of the current evidence. In particular, current understanding of the role of BIM in imatinib-induced apoptosis was derived from evidence obtained in a single study in GIST882 cells, which harbor *KIT* exon 13 mutations (K642E) [59]. As this genotype is found in less than one percent of patients with GIST, current findings are of uncertain, and potentially limited, clinical relevance.

Before concluding that BIM mediates imatinib-induced apoptosis in all GIST, it is necessary to ascertain whether BIM mediates apoptosis in GISTs harboring *KIT* exon 11 mutations, which are found in approximately 70% of patients [11]. This is necessary, as genotype-specific distinctions are common among GIST [70], and observations in *KIT* exon 13 mutant GIST do not always extend to tumors harboring exon 11 mutations. Indeed, Dupart and colleagues recently showed that imatinib-responsive cell lines, GIST-T1 and GIST882, exhibit opposing effects upon overexpression of the pro-apoptotic insulin-like growth factor binding protein 3 (IGFBP3), which was previously thought to

mediate imatinib-induced apoptosis in GIST [68, 106]. Similarly, whereas GIST-T1 cells undergo apoptosis by induction of ER stress, and GIST882 cells undergo apoptosis by transcriptional arrest, these mechanisms are exclusive to the cell lines in which they were described, and are not been extended to other GIST cells, or to patients treated with imatinib [65, 71].

Further, three functional BIM isoforms, BIM-S (small), BIM-L (large), and BIM-EL (extra large), derived from alternative splicing of the *BCL2L1* gene, are known to differ in regulation and propensity to induce apoptosis [107]. Specifically, O'Connor and colleagues, who discovered BIM through a bacteriophage screen for proteins that interact with Bcl-2, also found that while each of the BIM isoforms clearly bound to Bcl-2, BIM-S antagonized Bcl-2 and suppressed FDC-P1 and L929 fibroblast colony formation more effectively than BIM-L or BIM-EL. Other than BIM-EL, the activation of BIM isoforms by imatinib, and their individual cytotoxicity, has not been evaluated in GIST. Most importantly, while BIM may be important for imatinib-induced apoptosis in cell culture, the role of the BIM/Bcl-2 axis in has not been evaluated in GIST patient samples.

In keeping with the translational goals of this study, both *in vitro* and patient-based approaches were employed to accomplish the specific aims. Specifically, patient-derived GIST cell lines harboring clinically-representative *KIT* exon 11 mutations were used to study the regulation, expression, and function of BIM in apoptosis. To validate cell culture findings and evaluate the clinical relevance of BIM-mediated apoptosis, specimens from patients with GIST were examined *ex vivo*.

For logical flow, this study was divided into two experimental objectives: First, I examined whether imatinib causes upregulation and activation of BIM in clinically-

representative GIST cell lines and evaluated the ability of three BIM isoforms to activate caspases. Second, I examined imatinib-induced expression of BIM and pro-survival Bcl-2 proteins in patient specimens, before and after imatinib treatment, and studied their association with therapeutic responses at the level of the cell (apoptosis and autophagy), the tumor (response by FDG-PET imaging), and the patient (disease-free survival).

The studies in GIST cells demonstrate that three functional isoforms of BIM (BIM-S, BIM-L, and BIM-EL) are upregulated by imatinib treatment. Upregulation of BIM at the mRNA and protein level was caused by inhibition of KIT and the PI3K pathway, but not by inhibition of MEK signaling. Although both untreated imatinib-sensitive and imatinib resistant GIST cells express BIM at baseline and after imatinib, only imatinib-sensitive cells activate apoptosis significantly with treatment. Further, BIM-S, BIM-L, and BIM-EL are equally capable of activating effector caspases 3 and 7 and apoptosis when overexpressed in GIST cells.

In specimens from GIST patients, BIM and Mcl-1 are upregulated by imatinib, while Bcl-2 is downregulated, and these gene expression alterations were greater in tumors exposed to longer durations of imatinib therapy. Additionally, BIM upregulation is associated with tumor apoptosis and prolonged disease-free survival, with trends toward decreased autophagosome formation and early response by PET.

Materials and Methods

Cell lines and Culture Conditions

GIST-T1 cells harbor a heterozygous imatinib-sensitive *KIT* exon 11 deletion of 20 amino acids (V560-Y579del), within the cytoplasmic juxtamembrane domain of KIT,

which disrupts its autoinhibitory function [108] and causes constitutive KIT signaling. GIST-T1 cells were established from a patient with metastatic GIST by Dr. Takahiro Taguchi (Kochi Medical School, Japan), and are sensitive to imatinib and other TKIs.

GIST48IM cells were established from a metastatic GIST after progression during imatinib therapy. These cells were derived from imatinib-refractory GIST48 cells [109, 110], harboring primary *KIT* exon 11 mutation (V560D), and secondary *KIT* exon 17 mutation (D820A). The latter mutation, in the phosphotransferase region of the KIT kinase domain, confers imatinib-resistance and is encountered commonly in patients who progress after initial response to imatinib [61, 109-111]. GIST48IM cells were generated by Dr. Jonathan Fletcher (Brigham and Women's Hospital; Boston, MA), and provided by Dr. Anette Duensing (University of Pittsburgh Cancer Institute; Pittsburgh, PA).

All cells were maintained at 37°C in a humidified incubator containing 95% atmospheric air and 5% CO₂. GIST-T1 cells were cultured in Dulbecco's Modified Eagle's Medium (DMEM), supplemented with penicillin/streptomycin (1%), and fetal bovine serum (FBS; 10%). GIST48IM cells were maintained in Ham's media (F-10), supplemented with FBS (15%), L-glutamine (2 mM), penicillin/streptomycin (1%), amphotericin (0.1%), gentamycin (10 µg/ml), MITO+ serum extender (0.5%), and bovine pituitary extract (1%), purchased from VWR International (Roden, Netherlands). All cell lines were validated by STR DNA fingerprinting, and STR profiles were compared to known fingerprints.

Chemicals, antibodies, and plasmids

Imatinib mesylate was procured from M. D. Anderson Cancer Center. PI3K inhibitor LY294002 (#9901) and MEK1/2 inhibitor U0126 (#9903) were purchased from Cell signaling Technology (Danvers, MA). Drugs were dissolved in dimethyl sulfoxide (DMSO) (Fisher Bioreagents, Fair Lawn, NJ) to a stock concentration of 10 mM, sterile-filtered through a 0.22 micron low protein binding filter (Millipore, Bedford, MA), and stored at -20°C prior to use.

Primary antibodies specific for BIM (#2819), phospho-BIM (S69) (#4581), total FoxO3a (#2497), and phospho-FoxO3a (S253) (#9466), were procured from Cell Signaling Technology. Primary β -actin antibody (sc-8432), and horseradish peroxidase (HRP)-conjugated anti-mouse (sc-2031) and anti-rabbit (sc-2305) secondary antibodies were purchased from Santa Cruz Biotechnology (Santa Cruz, CA).

Plasmid vectors [pEGFP-(C2)] encoding enhanced green fluorescent protein (EGFP), and containing BIM-S, BIM-L, or BIM-EL insert sequences were generated as previously described [107]. Empty pEGFP-(C3) plasmid (Clontech, Mountain View, CA), lacking BIM inserts, was used as a control to determine the cytotoxicity of EGFP expression alone.

Western Blotting

Cells were harvested by trypsinization (adherent cells) and centrifugation (non-adherent cells), washed twice with phosphate-buffered saline (PBS), and lysed on ice for 5 min in Cell Extraction Buffer (#FNN0011, Invitrogen, Eugene, Oregon), containing commercial protease inhibitor cocktail (Complete, Mini tablets; Roche, Mannheim,

Germany) and 1 μ M phenylmethane sulfonylfluoride (PMSF; a serine protease inhibitor). Protein concentration was measured with the bicinchoninic acid (BCA) Protein Assay kit (Fisher Scientific, Pittsburgh, PA). Lysates were diluted with NuPAGE LDS (lithium dodecyl sulfate) sample buffer/reducing agent, and heated to 70°C for 10 min; 30 μ g protein per lane were then resolved by denaturing electrophoresis at 100V for 35 min on pre-cast 4-12% gels (NuPAGE System, Invitrogen, Carlsbad, CA). Resolved proteins were blotted onto methanol-activated polyvinylidene fluoride (PVDF) membranes (Millipore, Bedford, MA) by wet electrophoretic transfer (Bio-Rad Laboratories, Hercules, CA) for 1 hr at 100V. Membranes were blocked with 5% (w/v) dry, non-fat milk dissolved in 0.05% Tween-20 in PBS (PBS-T) for one hour, and washed thrice with 0.05% PBS-T for 10 minutes. The membranes were incubated for one hour with primary antibodies diluted at 1:1000 in 5% milk-PBS-T, per the manufacturers' recommendations. Membranes were washed with 0.05% PBS-T thrice for 10 minutes before incubation with horseradish peroxidase-conjugated secondary antibodies at 1:5000 for an hour at room temperature. Membranes were washed as above, incubated 1 minute in chemiluminescence solution (Amersham Life Science, Piscataway, NJ), and subjected to autoradiography.

Quantitative reverse transcriptase-polymerase chain reaction (RT-PCR) assay

The mirVana miRNA Isolation Kit (Applied Biosystems, Foster City, CA), was used to extract total RNA from cultured GIST cells, frozen pre-imatinib core-needle biopsies (n=20) and frozen post-imatinib surgical specimens (n=26). To determine changes in gene expression, 1 μ g of total RNA from cell lines, and 400 ng from patient

samples, were reverse transcribed as follows: To each sample, 0.4 μg of pd(N)6 random hexamers (Amersham Biosciences, Piscataway, NJ) were first added in 11 μL , and the solution was heated at 70°C for 10 min, followed by 10 min incubation at room temperature (RT). SuperScript II RT buffer (Invitrogen), 10 mM dithiothreitol (Invitrogen), 0.5 mM deoxynucleotide triphosphate (dNTPs) (Bioexpress, Kaysville, UT), 20 U of RNase inhibitor (Applied Biosystems), and 200 U of SuperScript II RT (Invitrogen) were added to 20 μL , and the reaction was incubated for 10 min at RT to allow primer annealing, held at 37°C for 1 hr, then incubated at 42°C for 90 min followed by 50°C for 30 min.

Real-time PCR was performed on the ABI Prism 7700, using pre-validated Assays-on-Demand specific for BCL2L11 (BIM; Hs00197982_m1), MCL1 (Hs03043899_m1), BCL2L1 (Bcl-xL; Hs00236329_m1), BCL2 (Hs00608023_m1), and endogenous control genes cyclophilin or β -Actin Vic-labeled PreDeveloped Assay Reagent (Applied Biosystems). Initial experiments were performed to determine the valid range of RNA concentrations and to determine PCR efficiencies for BCL2L11, MCL1, BCL2L1 and BCL2 compared to endogenous control genes. A 15 μL final reaction volume containing 1X TaqMan Universal PCR Master Mix (Applied Biosystems) and 1X Assay-on-Demand was used to amplify 80 ng cDNA with the following cycling conditions: 10 min at 95°C, followed by 40 cycles of 95°C for 15 sec and 60°C for 1 min. Cycle threshold values (Ct) were used to determine relative mRNA abundance using the $\Delta\Delta\text{CT}$ method [112].

Apoptosis assays

GIST-T1 and GIST48IM cells were cultured to 80% confluence in 100-mm plates (BD Falcon, Franklin Lakes, NJ), then left untreated or treated for 24 or 72 hr with DMSO (vehicle), 1 or 10 μ M imatinib, 30 μ M LY294002, or 10 μ M U0126. As methods to detect apoptosis may yield different results depending on apoptotic stimulus and time, I examined two characteristic features of apoptosis: For quantification of phosphatidyl serine externalization (early apoptosis), adherent cells were harvested by trypsin treatment, and non-adherent cells were harvested by centrifugation at 100xg for 5 min. These were combined, washed twice with cold PBS, and incubated with 5% (v/v) Alexa-488- conjugated Annexin V containing 1 μ g/ml of the DNA-intercalating dye propidium iodide (PI) in 100 μ l total volume of 1X Annexin V binding buffer, using the Vybrant Apoptosis Assay Kit #2 (Invitrogen, Eugene, Oregon). Early-stage apoptotic cells, defined as positive for Annexin-V Alexa 488 (green fluorescence), and negative for PI (red fluorescence), were quantified by flow-cytometry on a BD FACSCanto II (BD Biosciences, San Jose, CA). For quantification of DNA fragmentation (late apoptosis), cells were harvested as above, washed twice in PBS, and permeabilized in ice-cold 70% ethanol overnight. Apoptotic cells with hypodiploid DNA content (sub-G1 phase) were quantified as described [113, 114].

Transfection and caspase activity assay

To study the effect of BIM expression in GIST cells, I transfected plasmid vectors (pEGFP, pEGFP-BIM-S, pEGFP-BIM-L, or pEGFP-BIM-EL) using the FuGENE 6 Transfection Reagent (Roche, Mannheim, Germany). Controls were as follows:

untransfected cells, mock transfected cells (only transfection reagent), and empty pEGFP vector. Briefly, 3×10^3 cells/well were seeded in 100 μ l in 96-well plates, and allowed to reach 50% confluence. FuGENE 6 reagent (μ l) and plasmid DNA (μ g) were combined at a 6:1 ratio in 94 μ l of serum-free medium, and incubated for 30 minutes at RT to form DNA:transfection reagent complexes; 5 μ l of this mixture was added to triplicate wells. Caspase activity was assessed at 12, 24 or 48 hr post-transfection, using the Apo-ONE Homogeneous Caspase-3/7 Assay (Promega, Madison, WI). At each time point, 3 ml of ApoOne reagent and 30 μ l of substrate were combined, and 100 μ l was added to each well; plates were incubated for 10 hr at RT, on an orbital shaker at 300 revolutions per minute, protected from light. Each condition was assayed with and without 20 μ M of caspase inhibitor Z-VAD-FMK (Promega). Fluorescence was normalized to untransfected cells.

Patients and Tumor Specimens

With IRB-approval and informed consent, two sets of clinically-annotated specimens were examined. The first set of tumor specimens were acquired through a prospective, randomized phase II study of preoperative and postoperative imatinib (MDACC ID03-0023) [60]. From August 2003 to October 2008, 28 patients were diagnosed with resectable, KIT-positive GIST at M. D. Anderson Cancer Center, and asked to enroll in a study of preoperative (neoadjuvant) and postoperative (adjuvant) imatinib. The objectives of this study were (1) to assess the safety of preoperative imatinib, (2) to understand the mechanisms of action of imatinib *in vivo* by procuring correlative molecular, cellular, radiographic, and survival data, and (3) to evaluate the

efficacy of two years of adjuvant imatinib in preventing or delaying tumor recurrence after surgery.

To accomplish these objectives, patients underwent pre-imatinib baseline studies (core-needle tumor biopsy, FDG-PET, CT, and routine blood work), randomized to receive neoadjuvant imatinib (600 mg daily) for 3, 5, or 7 days prior to surgical resection, and underwent post-imatinib studies immediately before surgery. To assess early response to imatinib in the preoperative period, patients underwent [18F]-fluorodeoxyglucose-positron emission tomography (FDG-PET) scans, before and after preoperative imatinib therapy. Where possible, surgical specimens were stored frozen in optimal cutting temperature (OCT) tissue matrix, or embedded in paraffin after fixation in formalin. After surgery, patients received adjuvant imatinib (600 mg daily) for up to two years, and followed up prospectively every three months by the Department of Sarcoma Medical Oncology.

Comprehensive patient (age, sex, race, and presentation status) and tumor (size, histologic subtype, *KIT/PDFRA* genotype) variables were recorded and updated into a database until September 2011. Presentation status, including extent of disease and history of prior treatment, was categorized as primary, metastatic, or locally recurrent. Histologic diagnosis of GIST, as well as histologic subtype, were assessed by the pathology department at MDACC. Tumor size was considered the greatest primary tumor diameter in any dimension by CT, and stratified as ≤ 5 cm, 5 to 10 cm, or >10 cm. All clinicopathologic data were obtained from patient records.

The second set of clinically-annotated specimens consists of 53 surgical specimens from patients diagnosed with KIT-positive GIST who underwent surgical

resection without preoperative imatinib. A tissue microarray (TMA) was constructed and validated from these specimens by our group [69]. I used this TMA to determine the level of apoptosis in imatinib-naïve GIST at the time of resection, for comparison with imatinib-treated GIST.

Immunohistochemical Detection of Apoptosis and Autophagy

Immunohistochemical detection of autophagosome formation in human GIST specimens was performed by immunohistochemical detection of α -LC3 [51]. Degree of punctate α -LC3 staining was defined as negative (0% cells positive), focal (< 25% cells positive), or moderate (\geq 25% cells positive). To evaluate imatinib-induced apoptosis in patient tumors, I performed TdT-Mediated dUTP Nick-End Labeling (TUNEL) on formalin-fixed paraffin-embedded surgical specimens (n=25), using the ApopTag In Situ Apoptosis Detection Kit (Millipore, Billerica, MA). Briefly, slides were deparaffinized with serial washes in xylene (3 x 5 min), 100% ethanol (2 x 5 min), 95% ethanol (once), and 70% ethanol (once), treated with 20 μ g/ml proteinase K for 15 min (followed by two 5 min washes with dH₂O), and quenched with 3% H₂O₂ (followed by 2 x 5 min washes with dH₂O). After 5 min incubation in equilibration buffer, a solution of 30% TdT enzyme/70% reaction buffer was applied for 1 hr in a humidified chamber at 37°C, and the reaction was stopped by PBS wash (3 x 1 min). Slides were incubated with anti-digoxigenin conjugate for 30 min, washed with PBS (3 x 2 min), and incubated with peroxidase substrate 3,3'-diaminobenzidine (DAB). Color development was stopped by washing in dH₂O (3 x 5 min), and slides were counterstained with 0.5% (w/v) methyl

green. Results were visualized by brightfield microscopy and apoptotic cells per five high-powered fields (200x) were quantified using the open-source software ImageJ [115].

Statistics

Computations were performed using GraphPad Prism 5 software (GraphPad Software, La Jolla, CA), with significance set at P-value ≤ 0.05 . Cell lines were examined separately, and in vitro assays were repeated at least twice; means \pm standard deviations (SD) were calculated. For parametric measurements, two-sample t-tests were used to assess the differences between two groups, whereas analysis of variance (ANOVA) was used to assess differences in outcomes among multiple (>3) groups or time points. For nonparametric, two-sample and multiple-sample comparisons the Mann-Whitney and Kruskal-Wallis tests were used, respectively. To evaluate associations between gene expression and apoptosis, I used linear regression analyses and Pearson correlation.

Patient and tumor variables were analyzed in relation to disease-free and overall survival (DFS/OS), determined by Kaplan–Meier analysis. Local recurrence was defined as tumor growth at the primary site, whereas metastasis involved distant tumor spread to liver or non-primary sites. DFS was defined as the time from surgical resection to recurrence or death, whereas OS was calculated from diagnosis to date of death. Associations between clinicopathologic characteristics and outcome were tested by univariate analysis using log-rank tests, with $P < 0.05$ considered statistically significant.

Results

Inhibition of KIT and PI3K signaling upregulates BIM and activates apoptosis in GIST cells

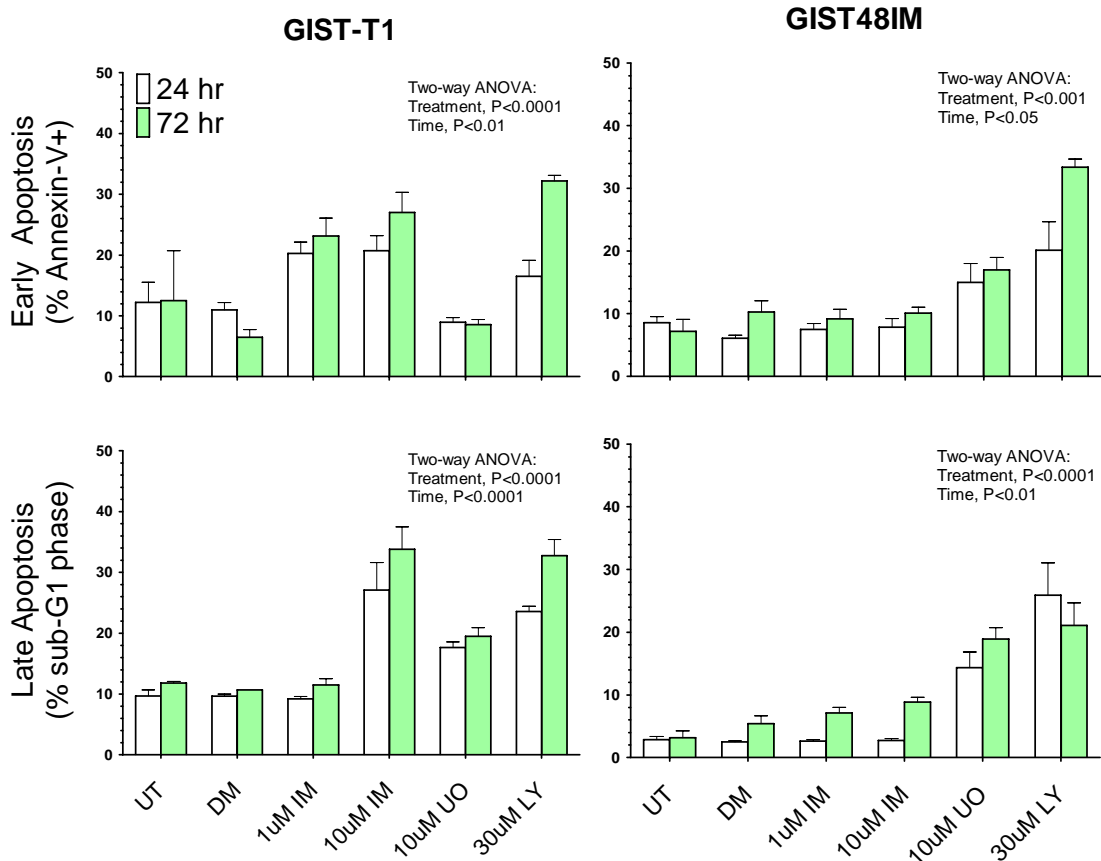
The bimodal (transcriptional and post-translational) mechanism controlling BIM expression and function in oncogene-addicted cancers is well-characterized (Figures 4 and 5). Briefly, PI3K signaling suppresses BIM mRNA expression through inhibitory AKT-mediated phosphorylation of transcription factor FoxO3a at serine 253 (S253), which translocates FoxO3a to the cytoplasm and prevents transcription. Phosphorylation of BIM by ERK1/2, leads to ubiquitination and proteasomal degradation of BIM. In GIST882 cells, a FRE-Luciferase Reporter Vector assay was used by Gordon and Fisher to demonstrate that imatinib treatment increases the transcriptional activity of FoxO3a at the FoxO3a response element (FRE) in the promoter region of the *BCL2L1* (BIM) gene. Likewise, these investigators showed that imatinib treatment inhibits the S69 phosphorylation of BIM by ERK1/2, causing decreased ubiquitination and halting the proteasomal degradation of BIM [105].

To determine whether a BIM-mediated mechanism of apoptosis extends to GIST cells with *KIT* exon 11 mutations, GIST-T1 and GIST48IM cells were first treated with DMSO, 1 or 10 μ M imatinib, 30 μ M LY294002, or 10 μ M U0126, and early apoptosis (phosphatidyl serine externalization by Annexin V staining) and late apoptosis (DNA fragmentation) were quantified. These drug concentrations have been shown to completely inhibit signaling by their respective targets (KIT, PI3K, or MEK1/2) in GIST cells [67].

Consistent with published data [59, 67], the overall apoptotic effect resulting from KIT inhibition was moderate (<40% with 10 μ M imatinib at 72 hrs), and demonstrated significant time- and dose-dependence by two-way ANOVA. Apoptosis was most increased in GIST-T1 cells treated with 10 μ M imatinib and 30 μ M LY294002 at 24 and 72 hrs, as compared to untreated and DMSO-treated controls (Figure 6). Whereas both 1 μ M and 10 μ M imatinib induced significant early apoptosis, the apoptotic effect of 1 μ M imatinib appeared to subside after 24 hours, whereas late apoptosis was sustained at 72 hours in GIST-T1 cells treated with 10 μ M imatinib.

Importantly, the apoptotic effect of imatinib in GIST-T1 cells was recapitulated by PI3K inhibition with 30 μ M LY294002 (20-30%), but not MEK1/2 inhibition with 10 μ M U0126 (19%). In contrast to GIST-T1 cells, GIST48IM cells were largely resistant to imatinib, but underwent apoptosis upon inhibition of PI3K signaling (26%), and to a lesser extent MEK1/2 inhibition (14%).

Figure 6. Inhibition of KIT and PI3K activates apoptosis in GIST cells.



Annexin V positivity, evidence of early apoptosis (top), and DNA fragmentation, evidence of late apoptosis (bottom), results from inhibition of KIT, PI3K, and, to a lesser extent, MEK1/2 signaling in GIST-T1 cells (left), whereas inhibition of PI3K and MEK1/2, but not KIT, causes apoptosis in GIST48IM cells (right). Bars represent the mean of triplicate experiments; error bars represent standard deviation (SD). Abbreviations: (UT), untreated; (DM), DMSO-treated; (IM), imatinib; (UO), UO126; (LY), LY294002

Next, I examined the expression of BIM mRNA and protein levels, by RT-PCR and western blot, respectively. As early as 24 hrs, BIM mRNA was increased 4-fold and 5-fold in GIST-T1 cells treated with 1 μ M and 10 μ M imatinib, respectively, compared with untreated cells (Figure 7, top left). PI3K inhibition, but not MEK1/2 inhibition, induced a 3-fold increase in BIM mRNA at 24 hrs. At 72 hrs, BIM mRNA levels increased by greater than 5-fold in cells treated with 1 μ M and 10 μ M imatinib and 30 μ M LY294002. In contrast, BIM mRNA was minimally upregulated in GIST48IM cells treated with 10 μ M imatinib and 30 μ M LY294002 at 72 hrs, with a 2-fold increase in BIM mRNA in cells compared with untreated and DMSO-treated GIST48IM cells (Figure 7, top right).

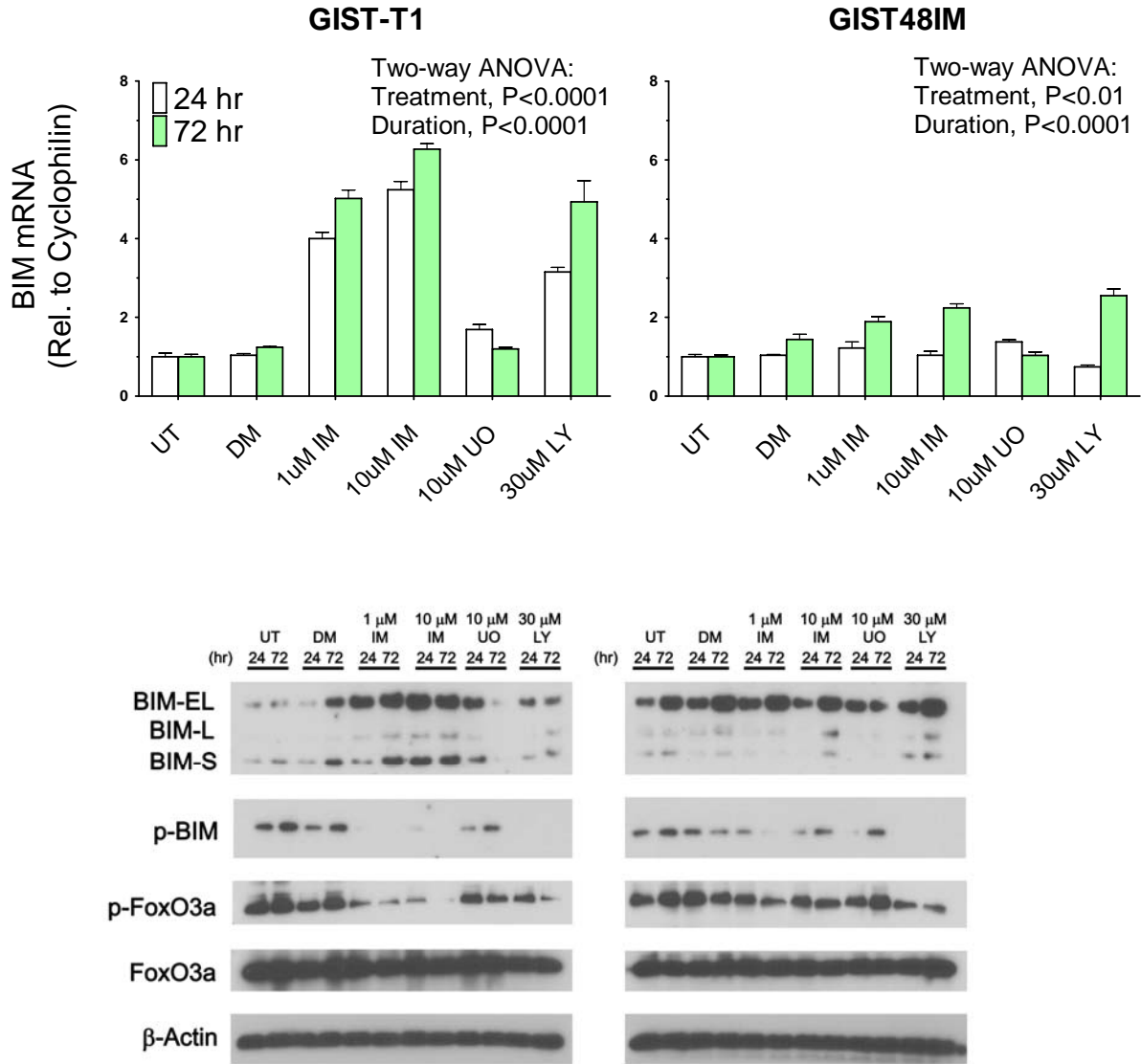
At the protein level, BIM-EL and BIM-S, but not BIM-L, were expressed at low levels in untreated GIST-T1 cells (Figure 7, bottom left), but increased considerably after treatment with 1 μ M and 10 μ M imatinib and 30 μ M LY294002, consistent with upregulation of BIM mRNA. In contrast, moderate-to-high basal BIM-EL protein levels were detectable in untreated GIST48IM cells, and only treatment with 10 μ M imatinib and 30 μ M LY294002 increased expression above this baseline.

To better understand the mechanism of BIM activation in GIST cells, the phosphorylation status of BIM and its transcription factor, FoxO3a, were examined by western blotting. BIM-EL phosphorylation at serine 69 (S69) is known to negatively regulate BIM function by promoting its proteasomal degradation [116], whereas AKT-mediated phosphorylation of FoxO3a at serine 253 (S253) contributes to its translocation from the nucleus, and blocks transcription of BIM [105, 117].

In accordance with this model, BIM-EL was constitutively phosphorylated at S69 in untreated and DMSO-treated in GIST-T1 cells, and phosphorylation was abolished by incubation with 1 and 10 μ M imatinib for 24 and 72 hrs, in parallel with increased unphosphorylated (native) BIM-EL. Decreased S69-phosphorylation of BIM-EL was similarly achieved by treatment with 30 μ M LY294002, but not by treatment with U0126. Similarly, S253-phosphorylated FoxO3a was decreased at 24 and 72 hrs with imatinib, and at 72 hrs with LY294002, but not with U0126. Importantly, dephosphorylation of transcription factor FoxO3a correlated with increased BIM mRNA and protein levels, particularly BIM-S and BIM-EL.

In GIST48IM cells, dephosphorylation of BIM-EL was inconsistently achieved with imatinib (1 or 10 μ M) or 10 μ M U0126, but phosphorylation was abolished completely by treatment with LY294002. Likewise, only PI3K inhibition achieved significant S253-dephosphorylation of FoxO3a in GIST48IM cells. Collectively, these findings suggest that in clinically-representative GIST cells, BIM is regulated transcriptionally and post-translationally by KIT and PI3K signaling, and that upregulation of BIM accompanies apoptosis.

Figure 7. Inhibition of KIT and PI3K upregulates BIM in GIST cells.



TOP PANEL: BIM mRNA levels are increased by inhibition of KIT and PI3K in GIST-T1 (left) and GIST48IM (right) cells, in a time- and dose-dependent manner. Columns represent the mean of triplicate experiments; error bars represent standard deviation (SD).

BOTTOM PANEL: Representative western blots demonstrating upregulation of BIM-EL, BIM-L (minor), and BIM-S in protein extracts of imatinib-treated GIST-T1 cells, compared to untreated (UT) and DMSO-treated cells (DM). KIT and PI3K inhibition abolish phosphorylation of BIM (S69) and FoxO3a (S253). High basal level of BIM-EL was noted in untreated and DMSO-treated GIST48IM cells.

Isoforms BIM-EL, BIM-L, and BIM-S activate apoptosis equally in GIST cells

Having observed that three known functional isoforms of BIM are upregulated in GIST cells by KIT and PI3K inhibition, and that BIM upregulation parallels induction of apoptosis, I asked whether BIM mediates apoptosis functionally, and whether the individual isoforms of BIM differ with regard to cytotoxicity in GIST. To examine whether BIM causes activation of apoptosis in GIST cells, the ability of three distinct BIM isoforms to activate effector caspases 3 and 7 was evaluated.

For this, GIST-T1 and GIST48IM cells were transfected with pEGFP-(C2) expression vectors containing BIM-EL, BIM-L, or BIM-S inserts, or empty pEGFP vector, and quantified the activity of caspases 3 and 7, which are irreversibly activated by apoptosis. I anticipated that BIM over-expression would cause increased apoptosis, as compared to control cells transfected with empty pEGFP-vector, mock-transfected cells, and untransfected cells.

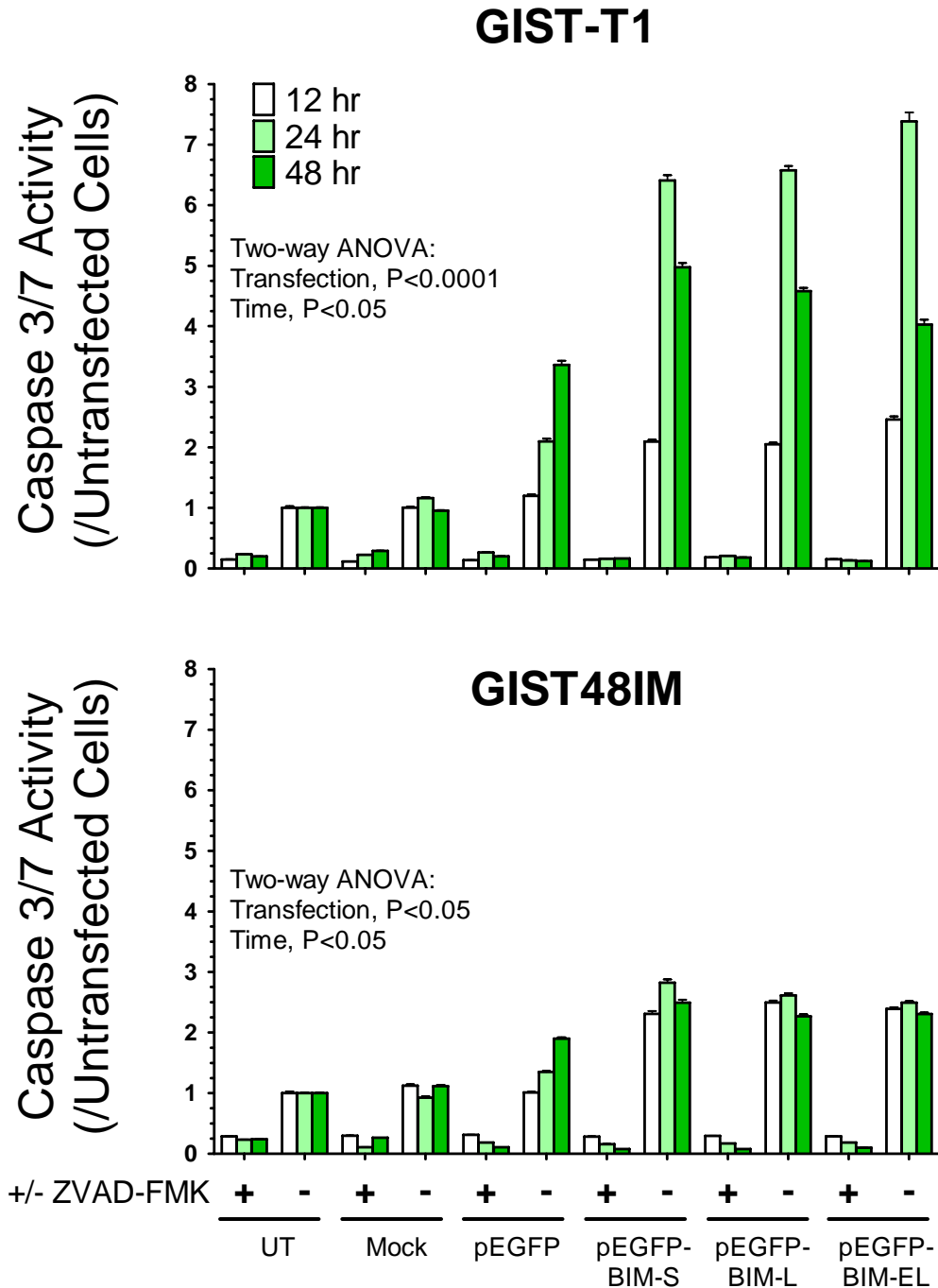
In both cell lines, transfection with pEGFP-BIM-EL, pEGFP-BIM-L, and pEGFP-BIM-S significantly increased caspase activation in a time-dependent manner, in comparison to untransfected, mock-transfected, and pEGFP-transfected cells (Figure 8). In GIST-T1 cells, a 2-fold increase in caspase activity was observed as early as 12 hrs post-transfection with all three isoforms, and peaked at 24 hrs (>6-fold increase) before returning to 4-fold at 48 hrs.

GIST48IM cells transfected with pEGFP-BIM-EL, pEGFP-BIM-L, or pEGFP-BIM-S similarly demonstrated increased caspase 3/7 activation, compared to untransfected, mock-transfected, and pEGFP-transfected cells. However, the magnitude

of caspase 3/7 activation relative to untransfected cells did not surpass 2-fold with any of the BIM isoforms in GIST48IM.

Importantly, there were no significant differences in caspase 3/7 activation among the individual BIM isoforms, suggesting that they are equally cytotoxic when expressed in GIST cells. In all cases, caspase activation and cytotoxicity were abolished by co-treatment with the pan-caspase inhibitor Z-VAD-FMK (20 μ μ M), confirming that the cytotoxic effect of BIM expression is mediated by caspase activation, and therefore by apoptosis.

Figure 8. BIM-EL, BIM-L, and BIM-S activate effector caspases in GIST cells.

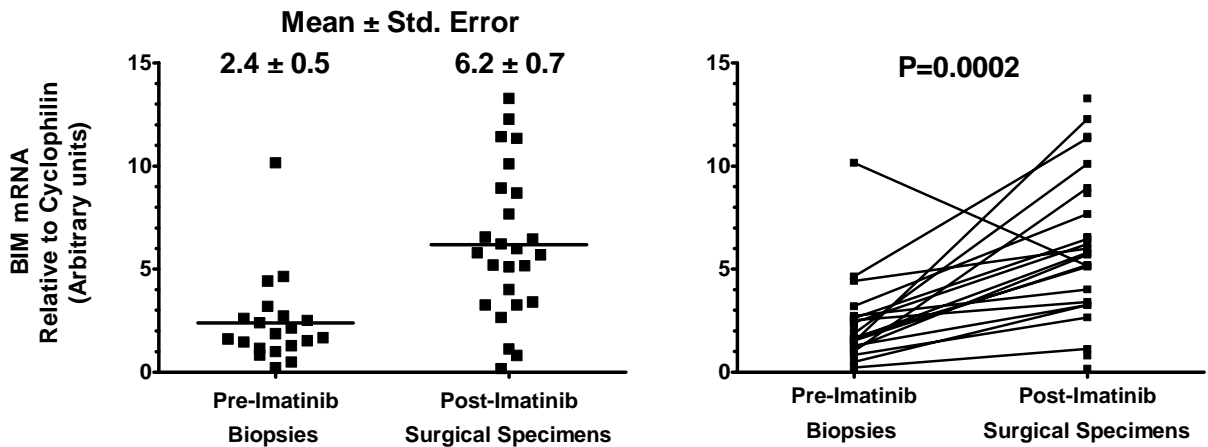


Isoforms BIM-EL, BIM-L, and BIM-S activate apoptosis equally in GIST cells. A. Significant, time-dependent activity of caspases 3 and 7 was observed after transfection of GIST-T1 cells (top) and GIST48IM cells (bottom) with expression vectors encoding isoforms BIM-EL, BIM-L, and BIM-S. Bars, mean of triplicate experiments; error bars, standard deviation (SD).

Imatinib treatment causes BIM mRNA upregulation in GIST patients

To determine whether a BIM-mediated mechanism of imatinib-induced apoptosis extends to patient GISTs, I investigated whether BIM mRNA was upregulated in tumors from patients with GIST who were treated with 600 mg imatinib daily for 3, 5, or 7 days before undergoing surgical resection of their tumor [60]. I performed quantitative RT-PCR to evaluate BIM mRNA levels in 20 pre-imatinib and 26 post-imatinib specimens. Where paired specimens were available (n=20), I determined the magnitude of BIM upregulation (fold-change in BIM mRNA in post-imatinib surgical specimen normalized to pre-imatinib biopsy), as well as its relation with temporal exposure to imatinib.

Figure 9. Imatinib upregulates BIM mRNA in GIST patients.

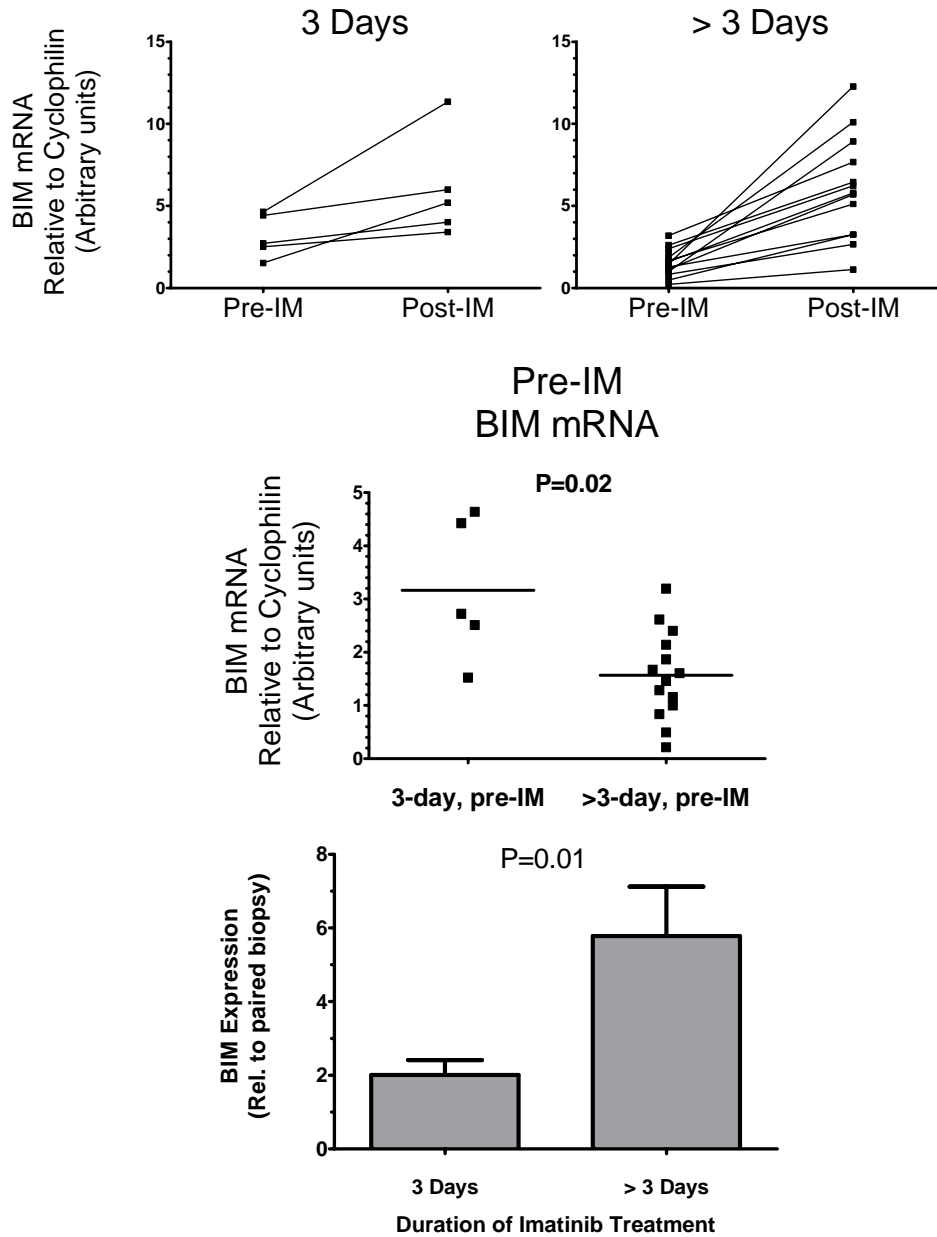


BIM mRNA levels were quantified by RT-PCR ($\Delta\Delta\text{CT}$ method) in pre-imatinib biopsies and post-imatinib surgical specimens from patients with GIST treated preoperatively. Statistics: Paired t-test.

As shown in Figure 9 (left panel), mean BIM mRNA was significantly higher in post-imatinib surgical specimens (Mean \pm Std. Error, 6.2 ± 0.7), as compared with pre-imatinib biopsies (2.4 ± 0.5 ; Paired t-test, $P=0.0002$). Moreover, 19 out of 20 paired specimens demonstrated upregulation of BIM mRNA after treatment with imatinib, and only one patient demonstrated downregulation of BIM (Figure 9, right).

In addition, as shown in Figure 10 (bottom), patients treated beyond three days exhibited a mean 5-fold increase in BIM expression, as compared to a 2-fold increase in patients who received imatinib for only three days (Mann Whitney test, $P=0.03$). However, the pre-imatinib (basal) levels of BIM mRNA were significantly greater in tumors treated for 3 days, making it impossible to conclude that the increases in BIM mRNA were directly proportional to the length of exposure to imatinib (Figure 10, middle).

Figure 10. Comparison of BIM upregulation in GISTs treated with imatinib for 3 days and GISTs treated for >3 days.



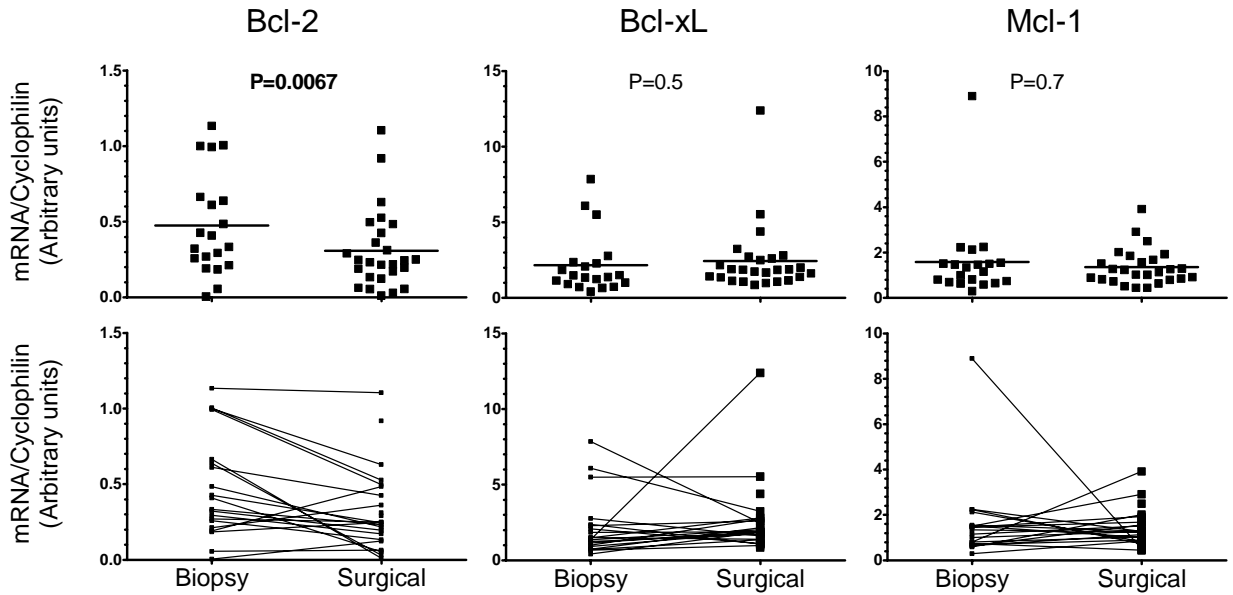
Fold-changes in BIM expression (mRNA levels in surgical specimens normalized to paired biopsy samples) were greater in tumors exposed to longer durations of imatinib therapy, with GISTs treated for >3 days exhibiting a mean BIM increase of 5.78 ± 1.3 , as compared to GISTs treated for only 3 days (mean BIM increase of 2.0 ± 0.4). Statistics: Mann-Whitney test.

Imatinib downregulates Bcl-2, and upregulates Mcl-1 in GIST patients

Given that BIM functions in direct opposition to the pro-survival Bcl-2 family members, I evaluated the expression of Bcl-2, Bcl-xL, and Mcl-1 mRNA by RT-PCR in GIST patients treated with imatinib (Figure 11). Overall, the mean levels of Bcl-2 mRNA in post-imatinib tumor specimens (0.31 ± 0.05) were significantly lower in comparison with pre-treatment biopsy samples (0.47 ± 0.08 ; Paired t-test, $P=0.007$). In contrast, I observed mixed upregulation and downregulation of Bcl-xL and Mcl-1 mRNA, such that mean Bcl-xL and Mcl-1 levels were statistically equivalent between pre-imatinib biopsies and post-imatinib surgical specimens.

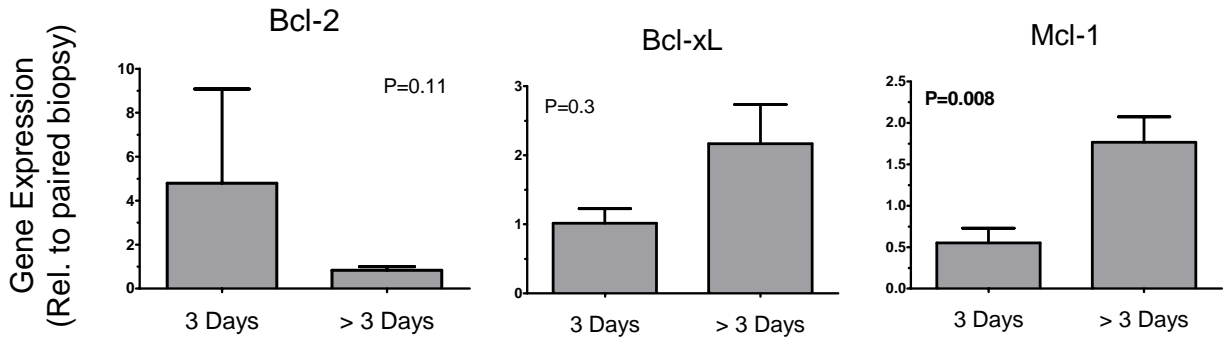
As with BIM, post-imatinib mRNA levels of pro-survival Bcl-2 proteins in surgical specimens were also normalized to their corresponding pre-imatinib biopsies. I noted a trend toward time-dependent Bcl-2 downregulation, although this was not statistically significant, given the high variability of Bcl-2 expression in tumors from patients treated for three days (Figure 12). Similarly, there was no association between Bcl-xL mRNA and temporal exposure to imatinib. Notably, upon normalizing post-imatinib Mcl-1 mRNA to matched pre-imatinib biopsies, it became evident that Mcl-1 was downregulated in tumors treated for 3 days (Mean fold-change = 0.55 ± 0.18), but upregulated in tumors treated for >3 days (Mean fold-change = 1.77 ± 0.31 ; Mann-Whitney test, $P=0.009$).

Figure 11. Imatinib-induced alterations in pro-survival Bcl-2 genes in GIST patients.



Bcl-2 mRNA levels were significantly lower in post-imatinib surgical specimens, as compared with pre-imatinib biopsies. Bcl-xL and Mcl-1 mRNA levels were comparable in GIST specimens before and after treatment.

Figure 12. Imatinib-induced alterations in pro-survival Bcl-2 genes in GISTs treated with imatinib for 3 days and >3 days.



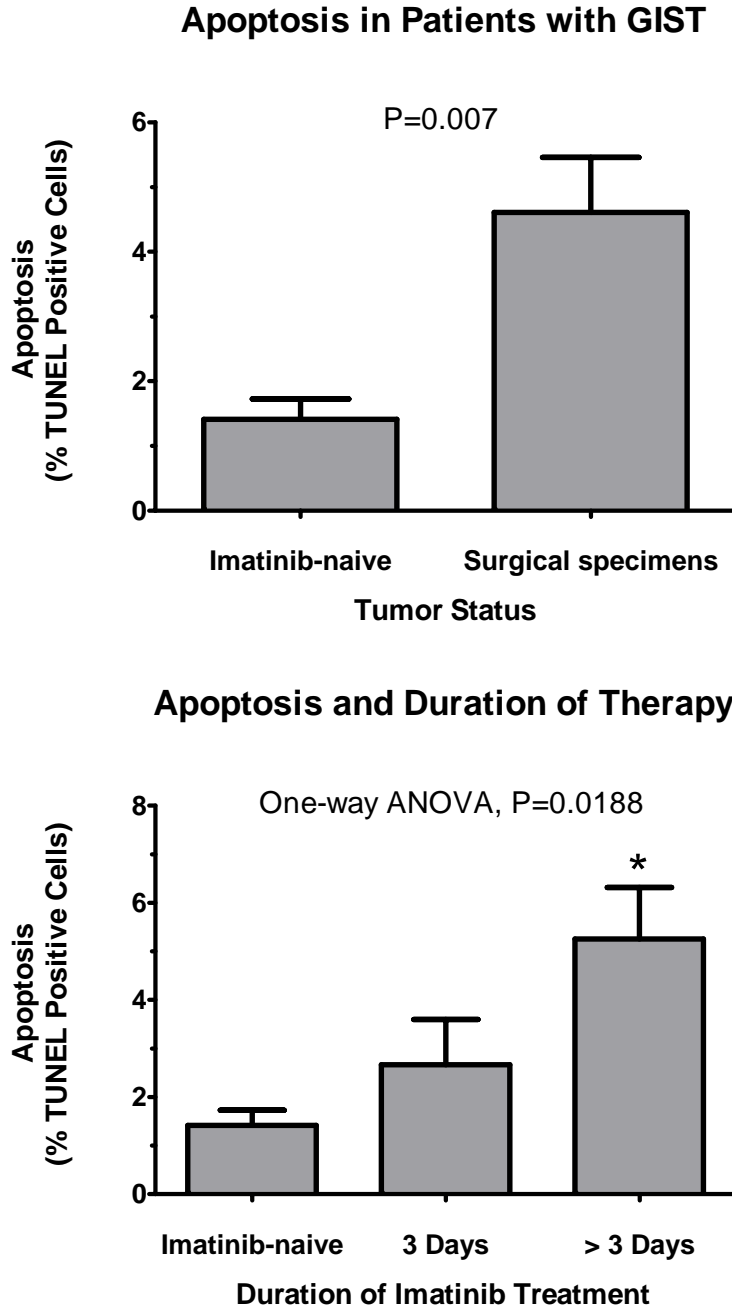
Fold-changes in Mcl-1 expression (mRNA levels in surgical specimens normalized to paired biopsy samples) differ with shorter and longer treatment, with GISTs treated for >3 days exhibiting a mean Mcl-1 increase of 1.77 ± 0.31 , as compared to GISTs treated for only 3 days (0.55 ± 0.18 ; $P=0.008$). Statistics: Mann-Whitney test.

Imatinib therapy induces tumor cell apoptosis in patients with GIST

Our laboratory previously reported that imatinib activates tumor cell apoptosis *in vivo*, and that the rate of apoptosis is dependent on the duration of therapy [60]. Importantly, results of the previous study were reported prior to completion of accrual by the clinical trial MDACC ID03-0023, and consisted of 10 pre-imatinib biopsies and 17 surgical specimens, obtained from 19 patients with GIST; in the interim, nine more patients were accrued onto the study, yielding eight more post-imatinib surgical specimens and one more biopsy. I assessed activation of apoptosis by TUNEL on 25 post-imatinib formalin-fixed paraffin-embedded surgical specimens. For comparison, I used a GIST tissue microarray, consisting of 53 imatinib-naïve surgical specimens [69].

Consistent with the previous report, tumors treated preoperatively with imatinib exhibited significantly higher, albeit moderate, rates of apoptosis ($4.6 \pm 0.9\%$), than untreated tumors (Figure 13, top; $1.4 \pm 0.3\%$; Mann Whitney test, $P=0.007$). Moreover, tumor cell apoptosis (%) was significantly higher in tumors treated for greater than three days with imatinib therapy, as compared with tumors treated for 3 days, or untreated tumors (Figure 13, bottom; One-way analysis of variance, $P=0.01$).

Figure 13. Imatinib therapy induces tumor cell apoptosis in patients with GIST.



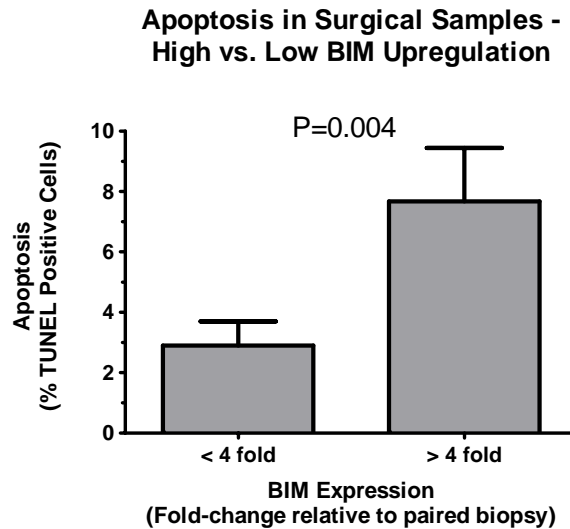
TOP: GISTs treated preoperatively with imatinib (n=25) exhibited significantly higher, albeit moderate, rates of apoptosis as compared with untreated tumors (n=53; Mann-Whitney test, P=0.007).

BOTTOM: Tumor cell apoptosis is greater with longer exposure to imatinib. (*) denotes p<0.05 by Bonferroni's Multiple Comparison Test.

Upregulation of BIM correlates with tumor cell apoptosis in GIST patients

Given that tumor cell apoptosis and BIM upregulation were found to be concurrent and time-dependent in GIST patients treated with imatinib, I determined whether there was an association between upregulation of BIM and activation of apoptosis in patient tumors. Tumors that exhibited upregulation of BIM by greater than 4-fold demonstrated considerably higher levels of apoptosis ($7.7 \pm 1.8\%$), than tumors which downregulated BIM, or increased its expression by less than 4-fold (Figure 14; $2.9 \pm 0.8\%$; Mann Whitney test, $P=0.004$). Moreover, linear regression and Pearson correlation of BIM expression and apoptosis in surgical specimens revealed that BIM upregulation trended toward an association with apoptosis (Figure 15; Pearson correlation, $P=0.06$).

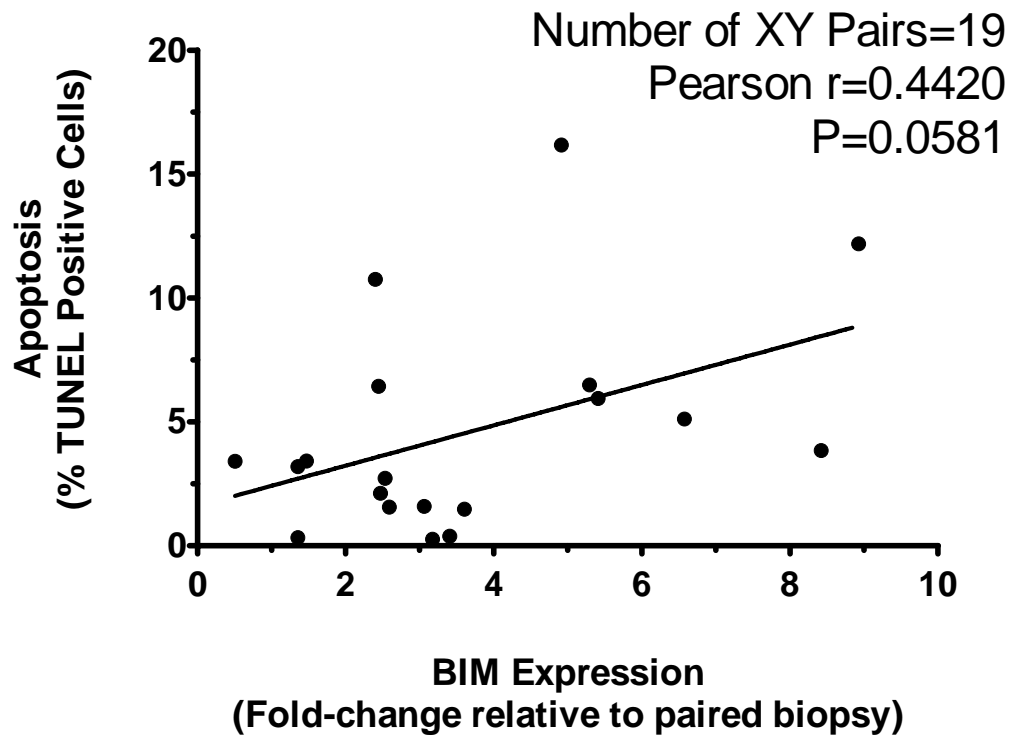
Figure 14. Upregulation of BIM correlates with tumor cell apoptosis in GIST patients.



Patients whose tumors upregulated BIM by greater than 4-fold demonstrated higher levels of apoptosis than patients whose tumors downregulated, or increased BIM expression by less than 4-fold (Mann-Whitney test, $P=0.004$).

Figure 15. Linear regression analysis of BIM expression and apoptosis.

Apoptosis and BIM Expression in Patients



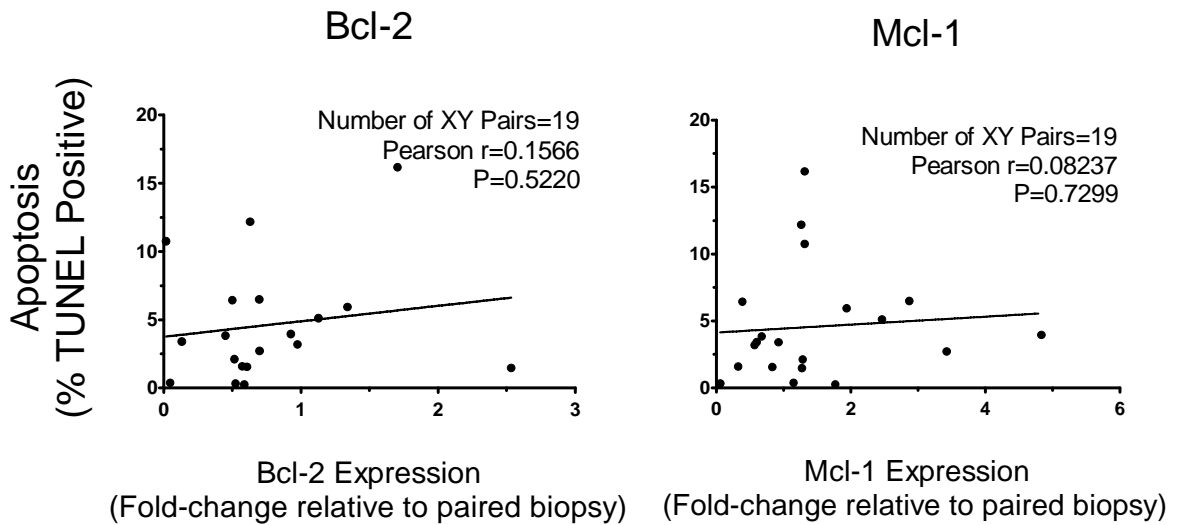
Linear regression analysis and Pearson correlation of BIM expression and apoptosis in surgical specimens revealed that BIM upregulation trended toward a linear association with apoptosis (P=0.06).

Imatinib-induced alterations in pro-survival Bcl-2 proteins and apoptosis

Having observed significant imatinib-induced alterations in expression of Bcl-2 and Mcl-1, I asked whether these changes in pro-survival proteins were associated with apoptosis in patient tumors. Specifically, I hypothesized that tumors which downregulated Bcl-2 mRNA would exhibit higher rates of apoptosis than those which upregulated it. Similarly, I postulated that tumors which upregulated Mcl-1 would exhibit lower rates of apoptosis, in accordance with its pro-survival function.

Contrary to my hypotheses, no association between imatinib-induced alterations in pro-survival Bcl-2 proteins and apoptosis were found in patient tumors by linear regression analysis (Figure 16).

Figure 16. Imatinib-induced alterations in pro-survival Bcl-2 proteins and GIST apoptosis.



Basal expression of Bcl-2, Bcl-xL, and Mcl-1 and apoptosis

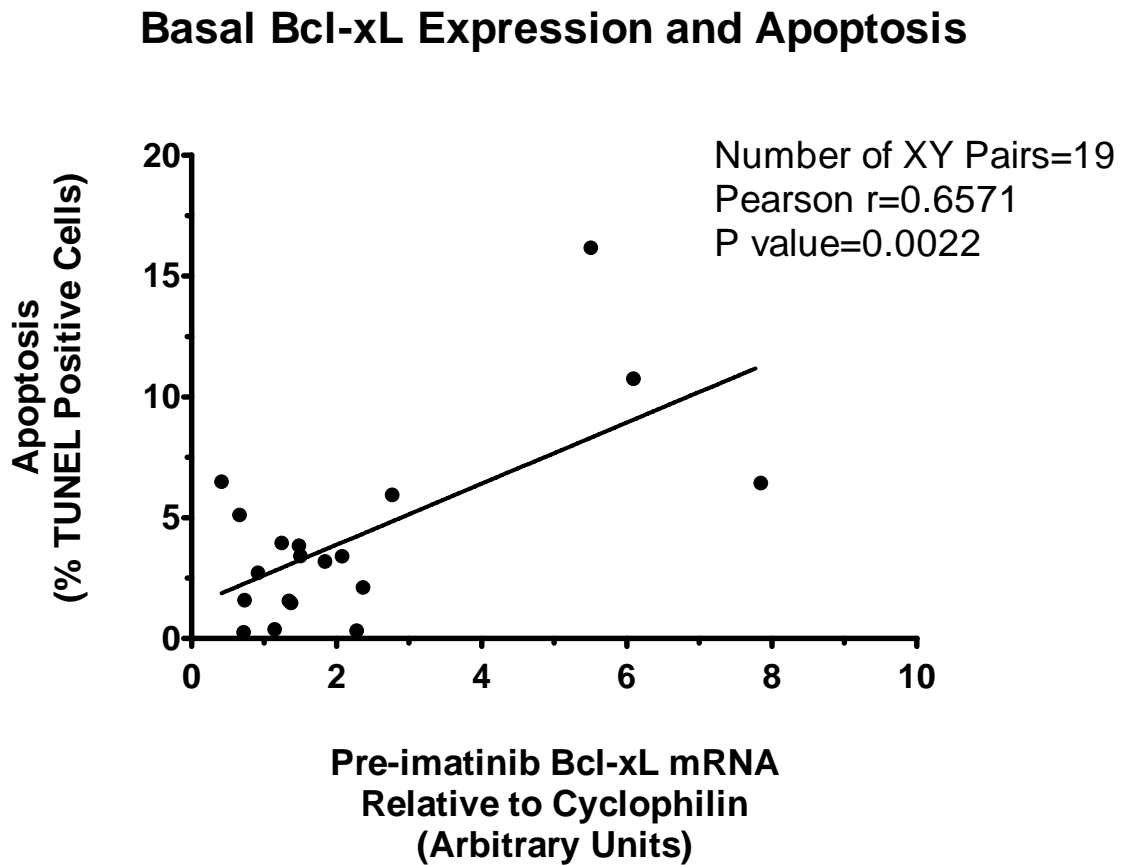
As post-imatinib expression changes in pro-survival Bcl-2 proteins did not appear to associate with tumor cell apoptosis, I examined whether basal, or pre-treatment, expression, as opposed to imatinib-induced alterations, influenced BIM-mediated apoptosis in GIST. For this analysis, I quantified mRNA in pre-imatinib biopsy samples and divided the group into quartiles, hypothesizing that tumors in the upper quartile of pre-treatment Bcl-2, Bcl-xL, or Mcl-1 expression would correlate with lower rates of apoptosis. Paradoxically, tumors in the upper quartile of pre-treatment Bcl-xL mRNA exhibited higher rates of post-treatment apoptosis (n=5; $8.3 \pm 2.4\%$) as compared with tumors in the lowest three quartiles (n=15; $3.3 \pm 0.8\%$; Unpaired t test, P=0.02). (Table 1). This was confirmed by Pearson correlation (Figure 17), suggesting an association between high pre-treatment Bcl-xL expression and post-treatment apoptosis (P=0.002; r =0.66).

Table 1. Basal expression of Bcl-2, Bcl-xL, and Mcl-1 and apoptosis.

	Bcl-2		Bcl-xL		Mcl-1	
Apoptosis (%TUNEL Positive Cells)	Mean \pm SEM	p-value	Mean \pm SEM	p-value	Mean \pm SEM	p-value
Upper Quartile (N=5)	6.6 \pm 2.2	0.23	8.3 \pm 2.3	0.02	2.6 \pm 1.0	0.24
Lower 3Q (N=15)	3.9 \pm 1.0		3.3 \pm 0.8		5.2 \pm 1.2	

Tumors in the upper quartile of pre-treatment Bcl-xL expression exhibited significantly higher rates of apoptosis than patients in the lowest three quartiles. Statistics: Two-tailed, unpaired t-test.

Figure 17. High basal (pre-imatinib) Bcl-xL mRNA correlates with apoptosis.



Pearson correlation of basal Bcl-xL expression and tumor apoptosis, depicting a significant association between high pre-treatment Bcl-xL expression and post-treatment apoptosis.

Autophagy in imatinib-treated GIST patient samples

Although imatinib caused significant pro-apoptotic gene expression alterations (i.e. upregulation of BIM and downregulation of Bcl-2) in GIST specimens from patients treated with imatinib, these pro-apoptotic gene expression changes did not account fully for the apoptotic response, suggesting that alternative mechanisms may modulate BIM-

mediated apoptosis in GIST. Depending on cellular context, autophagy may promote cell death, or serve as an adaptive mechanism that allows cancer cells to survive cytotoxic stress [118]. In GIST cells, autophagy was previously shown to function as an adaptive response to imatinib, and therapeutic inhibition of autophagy synergized with imatinib to activate apoptosis. By detection of punctate α -LC3, Gupta and colleagues previously demonstrated that imatinib induces autophagosome formation in human GIST specimens, and that autophagosome formation correlates inversely with apoptosis [51].

Given that BH3-only proteins and pro-survival Bcl-2 proteins are known to play opposing roles in autophagy [119], I hypothesized that autophagosome formation might be related to sub-apoptotic BIM upregulation, or conversely, to upregulation of Bcl-2, Bcl-xL, or Mcl-1. I thus examined imatinib-induced alterations in Bcl-2 family genes in relation to autophagosome formation by punctate α -LC3 immunohistochemical staining. Specifically, BIM, Bcl-2, Bcl-xL, and Mcl-1 mRNA levels were quantified relative to endogenous cyclophilin, and post-imatinib levels were normalized to corresponding pre-imatinib mRNA levels. I then compared average fold-changes in gene expression between autophagosome-positive (focal or moderate) and -negative GISTs (Table 2).

BIM was upregulated 6-fold in autophagosome-negative specimens compared with a 3-fold increase in autophagosome-positive specimens ($P=0.17$). In accordance with its pro-survival function in promoting autophagy, Bcl-2 was upregulated 3-fold in autophagosome-positive tumors and unchanged in autophagosome-negative tumors ($P=0.37$). Although neither of these associations reached statistical significance, they stood in agreement with the previous observation that tumors with high BIM upregulation tended to activate apoptosis rather than autophagy. In contrast, expression changes in

Mcl-1 and Bcl-xL did not demonstrate notable trends in relation to autophagosome formation in patient GISTs.

Table 2. Autophagosome formation and imatinib-induced alterations in the Bcl-2 family.

Autophagosome Formation	BIM		Bcl-2		Bcl-xL		Mcl-1	
	Mean ± SEM	p-value	Mean ± SEM	p-value	Mean ± SEM	p-value	Mean ± SEM	p-value
LC3-negative (N=9)	6.2 ± 2.2	0.17	2.9 ± 2.4	0.37	1.3 ± 0.3	0.24	1.6 ± 0.5	0.70
LC3-positive (N=11)	3.3 ± 0.4		0.9 ± 0.2		2.4 ± 0.8		1.4 ± 0.3	

Mean fold-changes in gene expression between autophagosome-positive and autophagosome-negative tumors were compared. Statistics: Two-tailed, unpaired t-test.

Bcl-xL upregulation is associated with imatinib-resistance by PET

FDG-PET is a sensitive method to evaluate early tumor responses in GIST, and PET response has been found to be predictive of prolonged disease-free survival in patients with GIST treated with imatinib [120]. Having observed an association between BIM upregulation and apoptosis in patient tumors, I asked whether gene expression alterations at the cellular level correlated with radiographic tumor responses. Specifically, I asked whether imatinib-induced expression changes in the Bcl-2 family of proteins were associated with early responses by PET, which were defined as a relative decrease greater than 70% in maximum standard uptake value (SUV_{max}) of the tumor, or residual $SUV_{max} \leq 3.9$ [60].

To test the hypotheses that BIM expression correlates with response to imatinib, whereas Bcl-2, Bcl-xL, and Mcl-1 correlate with resistance, I examined the associations between imatinib-induced expression changes and intratumoral glucose metabolism by FDG-PET. I anticipated that patients whose tumors upregulated BIM in response to imatinib also exhibit decreased glucose uptake. Conversely, I anticipated that imatinib-treated patients whose tumors exhibit upregulation of Bcl-2, Bcl-xL and Mcl-1, or downregulation of BIM experienced inferior responses.

Bcl-xL was upregulated 3-fold in non-responders ($P < 0.05$), compared to PET responders (Table 3). Conversely, PET responders, on average, upregulated BIM by 5-fold compared to a 2-fold increase in non-responders, a tendency which failed to reach statistical significance ($P = 0.09$), but which nonetheless was consistent with the putative role of BIM in mediating imatinib-induced apoptosis.

Table 3. PET response and imatinib-induced alterations in the Bcl-2 family.

Radiographic Response	BIM		Bcl-2		Bcl-xL		Mcl-1	
	Mean \pm SEM	p-value	Mean \pm SEM	p-value	Mean \pm SEM	p-value	Mean \pm SEM	p-value
PET Responder (N=14)	5.1 \pm 1.4	0.09	2.2 \pm 1.5	0.63	1.4 \pm 0.3	0.01	1.5 \pm 0.3	0.8
Non-responder (N=5)	2.3 \pm 0.4		0.9 \pm 0.4		3.5 \pm 0.5		1.3 \pm 0.6	

Mean fold-changes in gene expression between PET responders and non-responders were compared. Statistics: Two-tailed, unpaired t-test.

Survival of patients with GIST and the Bcl-2 family

Having found that imatinib causes early gene expression alterations in the Bcl-2 family that correlate with tumor cell apoptosis and early response by PET, I asked whether these changes associated with clinical outcome, particularly disease-free survival time. Before undertaking this analysis, I updated the clinical outcomes of patients enrolled in the MDACC ID03-0023 study, as the previous report was published before completion of patient accrual into the study [60].

Patient and tumor characteristics: MDACC Study ID03-0023

The clinicopathologic variables for the cohort of 28 patients with GIST are summarized in Table 4. The group consisted of 16 men and 12 women, with median age of 59 years (range 29 to 84). Race distribution was: 17 (61%) white, 6 (21%) black, and 5 (18%) Asian. Clinical presentation was primary in 22 patients (79%), and recurrent or metastatic in 6 (21%).

The most common site of tumor origin was the stomach, occurring in 21 patients (75%), followed by the small intestine in 7 (25%). Median tumor size was 7 cm (range 0.9 to 22 cm). Seven patients (25%) presented with tumors less than 5 cm, 11 patients (39%) presented with tumors between 5 and 10 cm, and 10 patients (36%) presented with tumors > 10 cm. Twenty-three tumors (82%) were described as having spindle morphology, two (7%) were epithelioid, and three were undetermined. The vast majority of tumors in this cohort, 23 (82%), were found to harbor *KIT* exon 11 mutations, and one tumor harbored a *KIT* exon 9 mutation. Interestingly, two tumors were found to harbor *PDGFRA* exon 12 mutations, and two were found to be wild-type for *KIT* and *PDGFRA*.

Complete surgery (R_0) was achieved in 27 of 28 patients (96%), whereas a single patient (with a 22 cm gastric GIST) was found to have evidence of gross and microscopic residual disease after resection. Nineteen patients (68%) went on to complete two years of adjuvant imatinib, while 9 patients (32%) discontinued therapy. Three patients removed themselves from the study after surgical resection, deciding not to participate in further treatment or follow-up.

Associations between post-imatinib BIM, Bcl-2, Bcl-xL, and Mcl-1 mRNA levels and clinicopathologic factors were examined, including *KIT/PDGFRA* genotype, tumor size, and primary tumor location (Table 5). Albeit not statistically-significant, post-imatinib BIM mRNA levels were considerably higher in gastric GISTs (8.7 ± 2.3), as compared with small bowel tumors (5.1 ± 0.9). Similarly, tumors ≤ 10 cm were found to have higher BIM mRNA levels than tumors > 10 cm after treatment with imatinib (9.3 ± 2.7 and 5.2 ± 0.7 , respectively). Notably, *KIT* exon 11 mutant GISTs expressed lower levels of BIM mRNA after treatment with imatinib (7.4 ± 2.0), than tumors harboring other *KIT/PDGFRA* genotypes (9.4 ± 2.2). There were no notable associations between clinicopathologic variables and post-imatinib expression of Bcl-2, Bcl-xL, and Mcl-1.

Table 4. Clinical and Pathologic Characteristics: MDACC ID03-0023 Study

	n	% of Total
Age		
≤ 50	7	25
> 50	21	75
Sex		
Male	16	57
Female	12	43
Race		
White	17	61
Asian	5	18
Black	6	21
Tumor Size		
≤ 5 cm	7	25
>5 cm, ≤ 10 cm	11	39
> 10 cm	10	36
Presentation Status		
Primary	22	79
Recurrent/Metastatic	6	21
Primary Site		
Stomach	21	75
Sm. Intestine	7	25
Histology		
Epithelioid	2	7
Spindled	23	82
Other/unknown	3	11
Genotype		
KIT exon 11	23	82
KIT exon 9	1	4
PDGFRA	2	7
Wild type	2	7
Surgical Margins		
R0, complete resection	27	96
R1 or R2, incomplete	1	4
Adjuvant Imatinib		
Completed 2 years	19	68
Discontinued	9	32

Table 5. Association of clinicopathologic factors with post-imatinib BIM, Bcl-2, Bcl-xL and Mcl-1 mRNA.

	n	BIM	Bcl-2	Bcl-xL	Mcl-1
		Mean ± SEM	Mean ± SEM	Mean ± SEM	Mean ± SEM
Tumor Size					
≤ 10 cm	16	9.3±2.7	0.3±0.1	2.0±0.2	1.5±0.2
> 10 cm	10	5.2±0.7	0.4±0.1	3.1±1.1	1.2±0.1
Primary Site					
Stomach	19	8.7±2.3	0.3±0.1	2.3±0.6	1.4±0.2
Sm. Intestine	7	5.1±0.9	0.3±0.1	2.7±0.5	1.2±0.2
Genotype					
<i>KIT</i> exon 11	22	7.4±2.0	0.3±0.1	2.5±0.5	1.4±0.2
Other	4	9.4±2.2	0.3±0.1	1.9±0.5	1.2±0.4

Mean fold-changes in gene expression were compared according to clinicopathologic characteristics with prognostic value: Tumor size, primary tumor location, and *KIT/PDGFR*A genotype. Statistics: Two-tailed, unpaired t-test.

Long-term Overall Survival

Overall survival of the entire ID03-0023 cohort is depicted graphically in Figure 18. With median follow-up of 53 months (range 29-91), OS was 100% for the first four years, 92% at 5 years, 84% at 6 years, and 72% at 7 years. As of September 2011, only three of the original 28 patients have died as a result of GIST progression (recurrence or metastasis), and none have died of other causes. Of the 25 living patients, 19 (76%) are alive and free of disease recurrence and six (24%) are alive with recurrent or metastatic disease. Given that all three deceased patients had small bowel GIST greater than 10 cm at primary presentation, tumor size and primary tumor site were significant predictors of overall survival by univariate analysis (Figure 19 and Table 6).

Figure 18. Overall survival of patients enrolled in MDACC ID03-0023 study

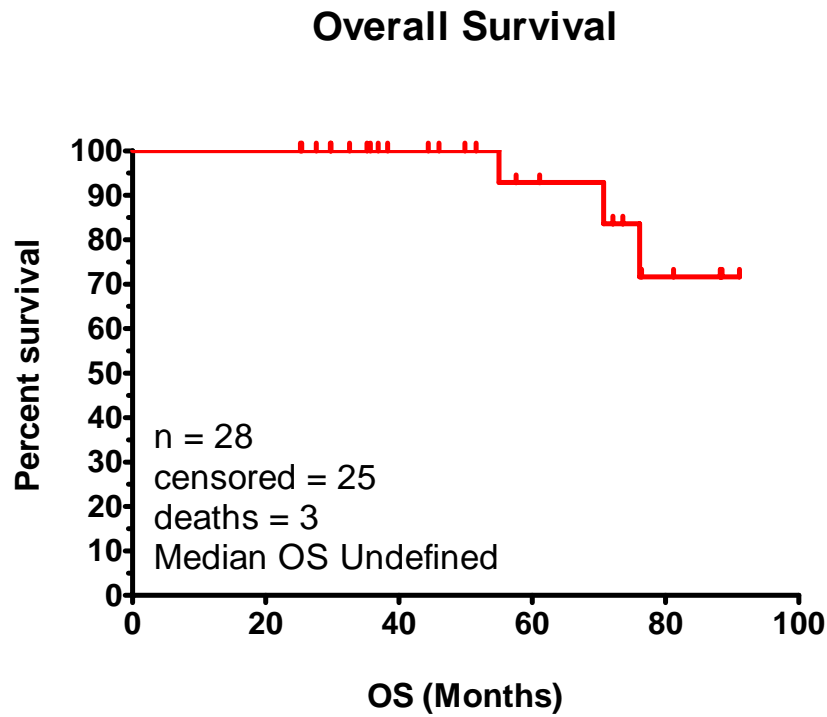


Figure 19. Overall survival by tumor size and primary tumor site in patients enrolled in MDACC ID03-0023 study

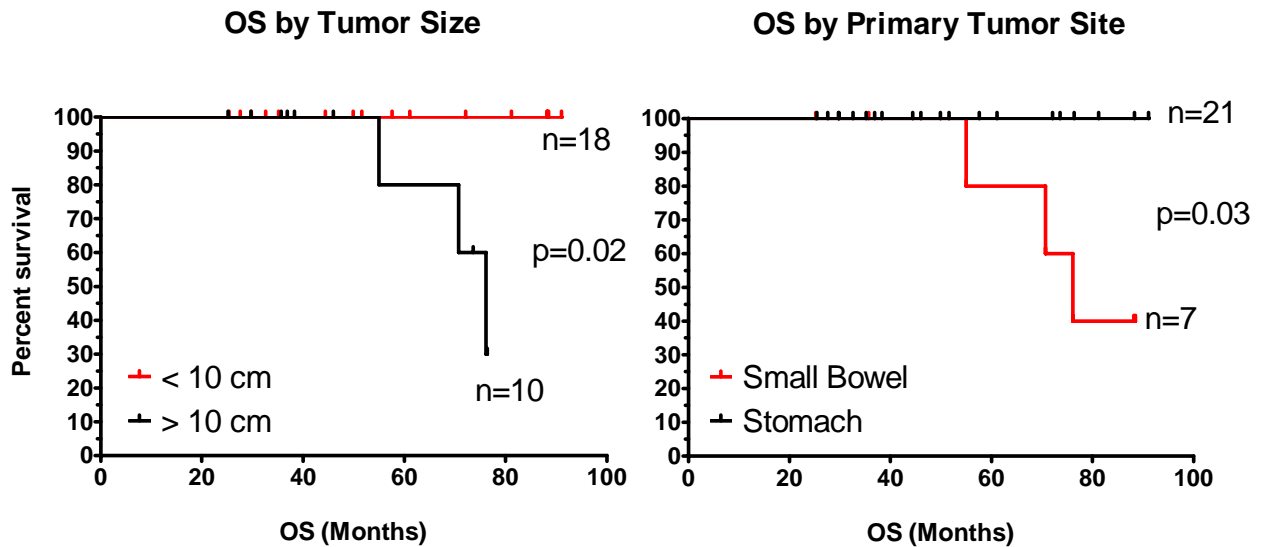


Table 6. Association of clinicopathologic factors with overall survival

	Patients (n)	Deaths (n)	Median OS (months)	Univariate p-value
All Patients	28	3	Undefined	
Age				
≤ 50	7	1	Undefined	0.986
> 50	21	2	Undefined	
Sex				
Male	16	2	Undefined	0.3284
Female	12	1	Undefined	
Race				
White	17	2	Undefined	0.6146
Other	11	1	Undefined	
Tumor Size				
≤ 10 cm	18	0	Undefined	0.0171
> 10 cm	10	3	76.10	
Primary Site				
Stomach	21	0	Undefined	0.0318
Sm. Intestine	7	3	76.10	
Genotype				
KIT exon 11	23	2	Undefined	0.3790
Other	5	1	Undefined	
Adjuvant Imatinib Two years				
Completed	19	2	Undefined	0.8261
Discontinued	9	1	Undefined	

Long-term Disease-Free Survival

With median follow-up of 53 months, tumor recurrence or metastasis has occurred in nine of 28 patients after surgical resection, 3 of whom have died of disease. Two of nine patients (22%) experienced local recurrence alone, two patients (22%) experienced both local and metastatic progression, and four patients (44%) experienced metastasis alone (three to liver, one to peritoneum). One patient had extra-abdominal recurrence to the lung, in addition to liver metastasis. Disease-free survival rates for the

entire cohort were: 96% at 1 year, 92% at 2 years, 80% at 3 years, 55% at 4 through 7 years (Figure 20, top left).

As with overall survival, only tumor size and primary tumor site were significantly associated with recurrence (Table 7 and Figure 20, bottom panel). In accordance with established risk-stratification criteria, six of seven patients (86%) patients with small bowel tumors and five of 10 patients (50%) with GIST > 10 cm experienced disease progression.

Importantly, among patients who actually completed the study protocol, there were no instances of progression during the two years of therapy with adjuvant imatinib, whereas two of nine patients (22%) who discontinued adjuvant therapy progressed within the first two years. Accordingly, DFS rates for patients who completed two years of adjuvant imatinib were 100% at 1 and 2 years, but fell to 80% at 3 years. These data are consistent with the results of a published clinical study reporting that adjuvant imatinib effectively delays tumor recurrence in patients with high-risk GIST [39].

Figure 20. Disease-free survival, MDACC ID03-0023.

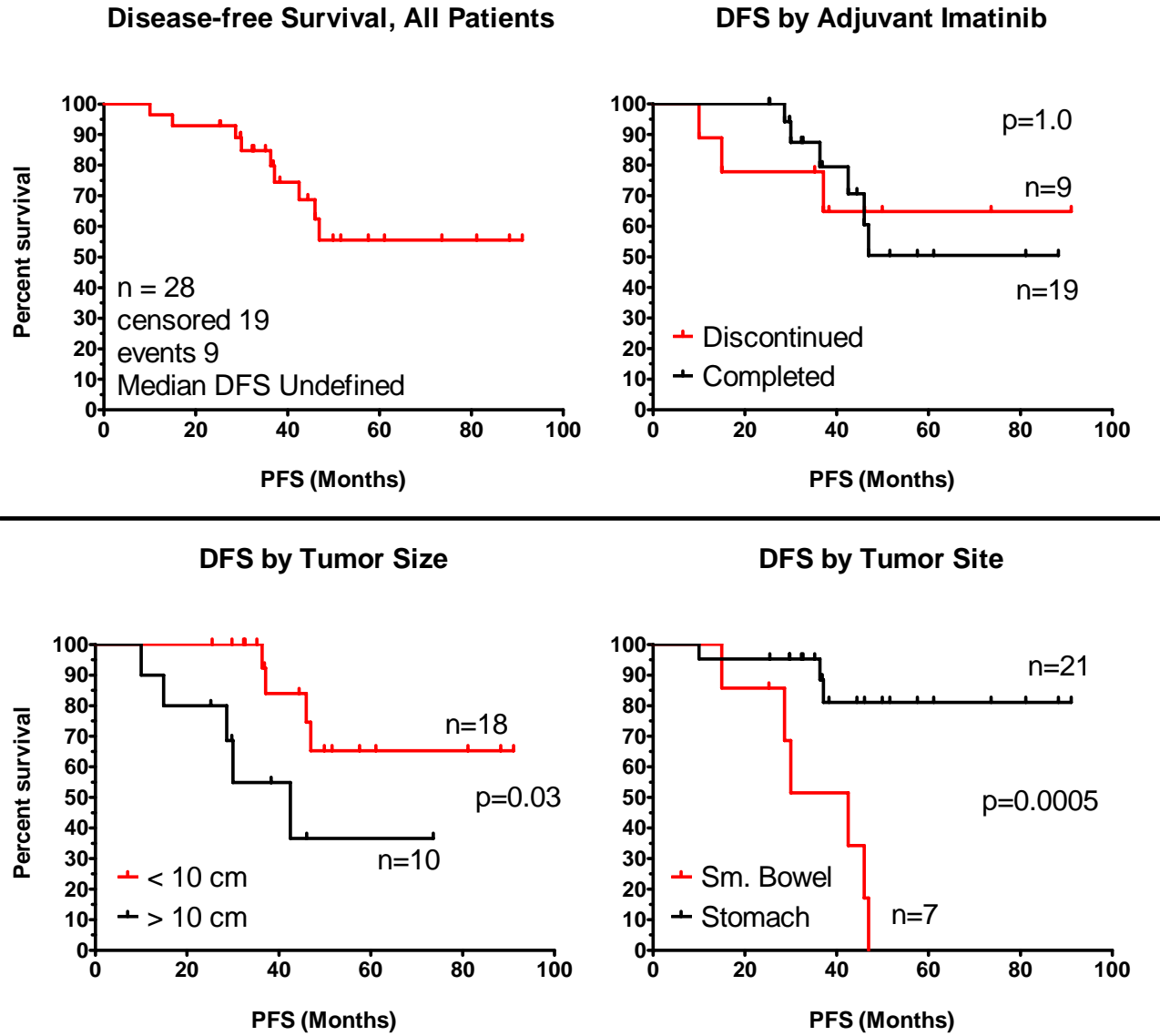


Table 7. Association of clinicopathologic factors with disease-free survival

	Patients (n)	Recurrent	Median DFS (months)	Univariate p-value
All Patients	28	9	Undefined	
Age				
≤ 50	7	4	46.00	0.2259
> 50	21	5	Undefined	
Sex				
Male	16	4	Undefined	0.4444
Female	12	5	46.90	
Race				
White	17	6	46.90	0.7485
Other	11	3	Undefined	
Tumor Size				
≤ 10 cm	18	4	Undefined	0.0315
> 10 cm	10	5	42.47	
Primary Site				
Stomach	21	3	Undefined	0.0005
Sm. Intestine	7	6	42.47	
Genotype				
KIT exon 11	23	8	46.90	0.4758
Other	5	1	Undefined	
Adjuvant Imatinib				
Two years				
Completed	19	6	Undefined	0.9998
Discontinued	9	3	Undefined	

Upregulation of BIM is associated with improved DFS in patients with GIST treated with adjuvant imatinib

Having found that two years of adjuvant imatinib effectively delays GIST progression, I hypothesized that imatinib-induced alterations which promote tumor apoptosis, such as BIM upregulation and Bcl-2 downregulation, associated with improved DFS. In other words, I asked whether those patients who benefited longest from delays in tumor progression did so because their GIST exhibited higher BIM

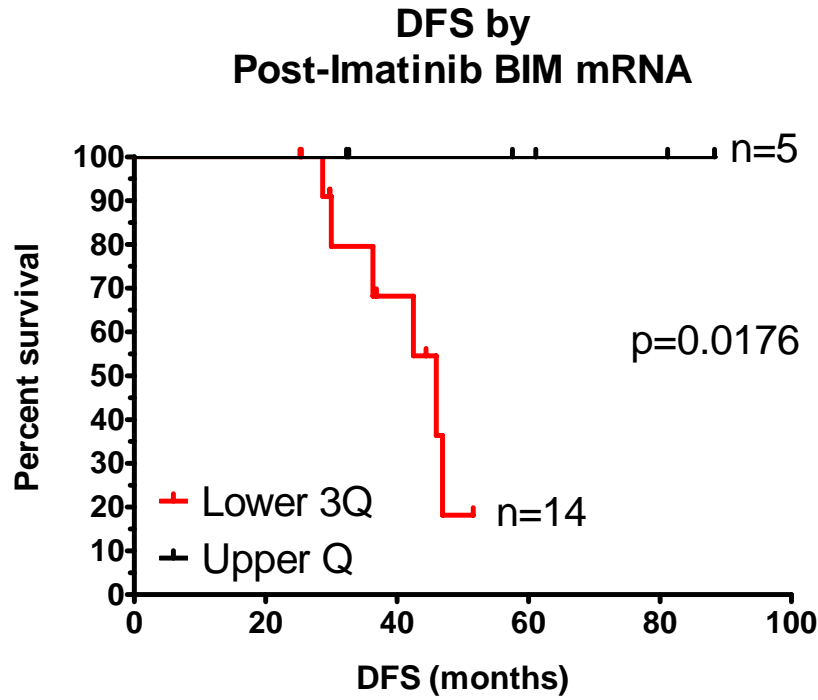
upregulation (and presumably apoptosis) while receiving imatinib post-operatively. Conversely, I postulated that alterations which promoted the survival of tumors, such as Mcl-1 upregulation, associated with inferior DFS. By univariate analysis, I evaluated DFS according to post-imatinib gene expression, comparing tumors in the upper quartile of BIM, Bcl-2, Bcl-xL, or Mcl-1 mRNA with those in the lower three quartiles (Table 8). To avoid the confounding effect of noncompliance or interruptions, I excluded the nine patients who did not complete the 2-year period of adjuvant imatinib from this survival analysis.

Importantly, no tumor recurrences were observed among patients whose tumors were in the upper quartile of post-imatinib BIM mRNA, as compared with 6 recurrences in 14 patients whose tumors were in the lower three quartiles of BIM mRNA expression (Figure 21).

Table 8. Association of Bcl-2 family gene expression with disease-free survival.

	Patients (n)	Recurrence	Median DFS (months)	Univariate p-value
Patients treated with Adjuvant IM	19	6	Undefined	
BIM mRNA (post-IM)				
Lower 3Q	14	6	45.97	0.0176
Upper Quartile	5	0	Undefined	
Bcl-2 mRNA (post-IM)				
Lower 3Q	14	4	46.9	0.6963
Upper Quartile	5	2	Undefined	
Bcl-xL mRNA (post-IM)				
Lower 3Q	14	3	Undefined	0.4050
Upper Quartile	5	3	45.97	
Mcl-1 mRNA (post-IM)				
Lower 3Q	14	6	46.9	0.1366
Upper Quartile	5	0	Undefined	

Figure 21. Post-imatinib BIM mRNA level is associated with prolonged DFS in patients with GIST treated with adjuvant imatinib.



By univariate survival analysis, post-imatinib BIM mRNA (upper quartile expression) was significantly associated with prolonged disease-free survival ($P=0.02$), as compared with lower levels of BIM mRNA.

Discussion

The purpose of this study was to determine whether a BIM-mediated mechanism of apoptosis, as previously-reported in GIST cells with *KIT* exon 13 mutations, extends to GIST cells with clinically-relevant *KIT* exon 11 mutations and/or patient tumors. Further, I examined whether imatinib-induced alterations in expression of Bcl-2 family members were associated with tumor apoptosis, autophagy, FDG-PET response, or disease-free survival.

In GIST cells with *KIT* exon 11 mutation, inhibition of KIT with imatinib upregulated three functional variants of BIM at the mRNA and protein levels. Further, BIM upregulation accompanied activation of apoptosis, and both effects were recapitulated by PI3K inhibition, but not by MEK1/2 inhibition. Accordingly, two post-translational modifications known to inhibit BIM expression and activation are reversed by KIT or PI3K inhibition, namely S253-phosphorylation of transcription factor FoxO3a and S69-phosphorylation of BIM-EL. Collectively, these findings confirm that BIM is suppressed downstream of KIT in GIST-T1 and GIST48IM cells.

In contrast to GIST cells with *KIT* exon 13 mutations, however, BIM is regulated exclusively by PI3K signaling in GIST cells with exon 11 mutations. This is not unprecedented, as other investigators have reported genotype-specific distinctions in signaling pathways among GIST cells and primary tumors with different mutations, and between tumors with similar genotypes [70]. GIST-T1 cells appear to preferentially depend on the PI3K survival pathway, perhaps owing to deletion of 20 amino acids from the juxtamembrane domain of KIT, as opposed to GIST882 cells, which are driven by missense mutation in exon 13 in the KIT kinase domain. I speculate that the deletion may alter the conformation of the juxtamembrane domain, limiting the potential docking partners and downstream signal transducers available to effect the survival of GIST-T1 cells.

While other investigators have reported differences in cytotoxicity among isoforms BIM-EL, BIM-L, or BIM-S [107, 121], I found no such variability. When transfected into GIST cells, all three isoforms exhibited equivalent time-dependent caspase activation that peaked 24 hours post-transfection. Interestingly, I observed

differences between GIST-T1 and GIST48IM cells with regards to baseline expression and cytotoxic potential of BIM. Whereas minimal BIM expression was observed in untreated GIST-T1 cells, moderate amounts of BIM-S and BIM-EL were detected by western blot in untreated GIST48IM cells, in the absence of demonstrable cytotoxicity. Moreover, BIM protein levels were higher in 72 hr GIST48IM cultures compared to corresponding 24 hr cultures, irrespective of treatment, and only supraphysiologic concentrations of imatinib (10 μ M) and LY294002 (30 μ M) induced expression of BIM above this baseline. Indeed, GIST48IM cells transfected with BIM-EL, BIM-L, or BIM-S demonstrated significant caspase activation, compared to untransfected cells, but maximum caspase activity (2-fold) was far below GIST-T1 cells (>5-fold). These findings suggest that BIM does not activate apoptosis in an absolute (all-or-nothing) manner when expressed in GIST cells, and imply that imatinib-resistant cell lines may possess additional mechanisms and molecules that may suppress, or counteract, the pro-apoptotic function of BIM.

The aforementioned *in vitro* findings confirmed that imatinib-induced apoptosis in GIST was mediated by BIM activation, and suggested a similar role in GIST patients. To corroborate this, I examined imatinib-induced alterations in BIM and pro-survival Bcl-2 molecules at the mRNA level, and evaluated their association with tumor apoptosis, PET response, and clinical outcome. These studies found that BIM is upregulated in patient tumors in proportion to the duration of exposure to imatinib, and BIM upregulation was associated with apoptosis. However, while there was a general tendency for higher rates of apoptosis in tumors with large BIM increases, the Pearson correlation coefficient (r) of the interaction was calculated as 0.44, indicating a weak

linear relationship. This was not unexpected, and suggests that factors other than BIM contribute to, or dampen, GIST apoptosis.

I suspected that BIM-antagonists (Bcl-2, Bcl-xL, or Mcl-1) or adaptive responses, including autophagy, modulate cell death of GIST cells. In this context, it was intriguing to observe that tumors with demonstrable autophagosome formation exhibited lower BIM induction than autophagosome-negative tumors. These observations suggest that BIM upregulation above an effective threshold may lead to GIST cell apoptosis, whereas insufficient BIM up-regulation may lead to autophagosome formation and diminished apoptotic response to imatinib. Future studies are necessary to determine whether apoptosis and autophagy are mutually exclusive responses to imatinib in GIST, and to clarify the role of the pro-survival Bcl-2 proteins in this decision point.

Interestingly, I suspect that there is an inverse relation between autophagosome formation and apoptosis in imatinib-treated GIST patient samples, suggesting that a threshold of BIM may determine whether GISTs induce apoptosis or tumor adaptation. Notably, tumors with low-BIM (≤ 4 -fold) upregulation post-treatment had lower rates of apoptosis and tended to exhibit positive autophagosome formation, whereas tumors with high-BIM (> 4 -fold) upregulation had higher rates of apoptosis, and tended to be negative for autophagosome formation.

Previous published data on the expression of Bcl-2 family members in GIST patients was limited to immunohistochemistry studies of Bcl-2, and no patient-based information on mRNA levels of BIM, Bcl-xL or Mcl-1 was available [122]. Whereas Bcl-2, Bcl-xL and Mcl-1 have previously been found to be KIT-independent in GIST cells [64, 105, 114], I observed significant imatinib-induced alterations in their

expression in patient tumors.

Importantly, prior to the era of targeted therapy with imatinib, immunohistochemical studies found that Bcl-2 expression was a negative, or neutral, prognostic factor for disease-free survival [123-125] [122], whereas high Bcl-2 expression in the imatinib-era was found to correlate with improved outcome [126]. These paradoxical observations are reconciled by the finding that Bcl-2 is downregulated by imatinib, suggesting that Bcl-2 expression is KIT-dependent in patient tumors, and its downregulation may be viewed as a surrogate marker of response.

To our knowledge, this is the first study to evaluate the expression of Mcl-1 and Bcl-xL in specimens from GIST patients. These studies found that Mcl-1 was significantly upregulated in tumors treated with imatinib for longer than three days. I speculate that Mcl-1 upregulation may neutralize the pro-apoptotic function of BIM in some tumor cells, and contribute to short-term imatinib-resistance. Future studies must determine whether Mcl-1 upregulation is a transient or sustained response, and whether it is part of a global tumor response that mitigates the cytotoxicity of imatinib. Lastly, these studies found that high pre-treatment Bcl-xL correlates with increased apoptosis after imatinib treatment, and that Bcl-xL upregulation was associated with imatinib-resistance by PET. Given the established function of Bcl-xL as an anti-apoptotic protein, the finding that high pre-treatment Bcl-xL expression associates with imatinib-induced apoptosis appears paradoxical. I speculate that this may reflect a predisposition, by a subset of GIST, on KIT-dependent, Bcl-xL-mediated survival. Consequently, treatment with imatinib in these tumors results in Bcl-xL downregulation and apoptosis. The small sample size available for this study limits interpretation of this finding, and further

functional studies are necessary to fully characterize the function of Bcl-xL in GIST.

Taken together, imatinib-induced expression changes in the Bcl-2 family in GIST have important therapeutic and prognostic implications. In Chapter 3, I demonstrate that inhibition of pro-survival Bcl-2 proteins *in vitro* synergistically augments the cytotoxicity of imatinib, and is capable of overcoming imatinib-resistance in GIST cells [114]. Given that imatinib-induced apoptosis *in vivo* similarly appears to be mediated by BIM upregulation, it is possible that rational drug combinations that converge on the intrinsic pathway of apoptosis may also be effective in patients.

Furthermore, identification of mechanism-based prognostic factors, both favorable and adverse, is necessary to optimize the management of patients with GIST. Given the variability of clinical responses to imatinib, knowledge of individual BIM/Bcl-2 expression profiles may improve prediction of treatment efficacy, assessment of prognosis, risk-stratification, and selection of patients for alternative therapies.

One corollary result of the patient-based studies was independent of apoptosis: To study the association of BIM and the Bcl-2 family of proteins with clinicopathologic variables, FDG-PET response, and disease-free survival, I updated the patient database for the MDACC ID03-0023 study. Notably, patients who completed two-years of adjuvant imatinib were free of recurrence during the treatment period, supporting the efficacy of imatinib at preventing recurrence after resection. In addition, this long-term survival and recurrence data supports the established risk factors for recurrence in GIST, confirming the negative prognostic significance of tumor size and primary tumor site.

Chapter 3: Synergistic activation of apoptosis by the Bcl-2 Inhibitor ABT-737 and imatinib in GIST cells

Introduction

Most pre-clinical research conducted after the initial discovery of the oncogenic mechanism in GIST has focused on inhibition of KIT signaling as a therapeutic goal, with the assumption that this would invariably achieve cell death. To date, the consensus approach is exemplified by *in vitro* studies targeting KIT function (with imatinib, sunitinib, dasatinib, and sorafenib), KIT expression (flavopiridol and siRNA-KIT), KIT stability (inhibition of chaperone protein HSP90), inhibition of downstream signaling pathways PI3K/AKT and MEK/ERK (LY294002, UO126), and inhibition of pathways parallel to KIT, including PKC- θ , IGF-1R, and FAK [61, 64, 109, 127-134]. Collectively, these studies have established that inhibition of oncogenic KIT signaling, even when complete, is not equivalent to tumor apoptosis [50, 61, 70].

Importantly, while failing to demonstrate that apoptosis is the predominant effect resulting from inhibition of KIT, these studies have shown that GISTs, in general, do not impair the apoptotic pathway to acquire resistance, and suggest that the molecular components of the apoptotic pathway in GIST are intact, and may be therapeutic targets [111, 135].

As discussed previously, the immense diversity of primary and secondary *KIT* and *PDGFRA* mutations that have been observed imply that kinase inhibition as monotherapy may not be sufficient to achieve cure in GIST [136, 137]. Therefore, new approaches must be sought to enhance the therapeutic efficacy of imatinib and overcome imatinib-resistance. In this context, combining imatinib with a pro-apoptotic drug may augment imatinib-induced cytotoxicity and prevent resistant cells from emerging *a priori*.

The studies described in Chapter 2 demonstrated that BIM is upregulated by imatinib, and that it effects apoptosis in GIST cells with clinically-representative genotypes, confirming and extending the findings in a previous published report. However, while BIM appears to mediate imatinib-induced apoptosis, adequate inhibition of pro-survival Bcl-2 proteins is not realized with imatinib monotherapy [64]. This suggests that the efficacy of imatinib might be improved by increasing BIM expression or by activating complementary effectors of apoptosis. One promising strategy involves inhibiting KIT with imatinib while concurrently engaging the intrinsic pathway of apoptosis. Herein, I aimed to modulate the BIM/Bcl-2 axis toward apoptosis by inhibiting pro-survival Bcl-2 proteins, an approach that is a practical application of current understanding of imatinib-induced apoptosis in GIST.

ABT-737 is a small-molecule inhibitor of pro-survival Bcl-2 proteins that was developed by Abbott laboratories with the objective of mimicking the pro-apoptotic function of BH3-only proteins, which is mediated through interaction of their BH3 α -helix with a hydrophobic pocket on anti-apoptotic Bcl-2 family proteins [138]. Specifically, Oltsdorf and colleagues employed a nuclear magnetic resonance (NMR)-based method to screen a chemical library for molecules that bind to the hydrophobic groove of Bcl-xL. They then modified lead compounds (minimizing binding to human serum albumin) to obtain ABT-737, which exhibits high affinity (inhibitory constant $K_i < 1\text{nM}$) for Bcl-xL, Bcl-2 and Bcl-w, but not for Mcl-1 or A1 ($K_i > 1\ \mu\text{M}$) [139]. In contrast to other putative Bcl-2 inhibitors (chelerythrine, obatoclax, EM20-25, gossypol, and apogossypol), ABT-737 is the only compound proven to target Bcl-2 proteins

specifically, and induce death strictly by BAX/BAK- and caspase-9-mediated apoptosis [140].

With regards to anti-tumor effects, ABT-737 exhibits remarkable single-agent efficacy against human B lymphoma cells, primary follicular lymphoma cells, and chronic lymphocytic leukemias [139]. In studies of mice implanted with human follicular lymphomas and studies of small cell lung cancer (SCLC) xenografts, daily injections of ABT-737 were well-tolerated, and morbidity was delayed. Most importantly, ABT-737 induced complete regression in the majority (>75%) of SCLC xenografts. Notably, although solid tumor cells (with the exception of SCLC) were generally resistant to single-agent ABT-737, their responses to radiation and cytotoxic chemotherapies was enhanced up to 20-fold with ABT-737 [139]. These pre-clinical findings motivated the use of ABT-737 in combination with cytotoxic and targeted therapies, where it has been shown to act downstream, and independently, of TKIs, etoposide, doxorubicin, cisplatin, and paclitaxel to effect BAX/BAK-dependent apoptosis in a time- and dose-dependent manner in multiple tumor models [141-143].

The studies in the following sections demonstrate that ABT-737 acts in synergy with imatinib to arrest proliferation and induce apoptosis in GIST cells. Importantly, the antitumor effects of ABT-737 in GIST cells are independent of initial imatinib-sensitivity or -resistance, and these are evident at physiologically-relevant concentrations of ABT-737.

Materials and Methods

Chemicals and Antibodies

ABT-737 and its inactive stereoisomer (Compound A793844) were obtained through a Materials Transfer Agreement with Abbott Pharmaceuticals (Abbott Park, IL). These were dissolved to 10 mM stock concentration in DMSO (Fisher-Scientific, Fair Lawn, NJ), sterile-filtered with 0.22 µm pore-size syringe microfilters, and stored in the dark at -20°C. I used primary rabbit antibodies against poly-ADP-Ribose polymerase (PARP) (#9542; 1:1000), Bcl-2 (#2870; 1:1000), Bcl-xL (#2764; 1:1000), and Mcl-1 (#4572; 1:1000), as well as mouse monoclonal antibodies specific for caspase 3 (#9668; 1:1000), (Cell Signaling Technology; Danvers, MA). Mouse monoclonal primary antibodies specific for β-actin (sc-8432; 1:5000) and HRP-conjugated anti-mouse and anti-rabbit secondary antibodies, (sc-2031; 1:2000) and (sc-2305; 1:2000), respectively, were purchased from Santa Cruz Biotechnology (Santa Cruz, CA).

Cell Culture

The origin, genotype, and culture methodology relevant to GIST-T1 and GIST48IM cells was detailed in Chapter 2 Materials and Methods.

The GIST882 cell line was established from a primary, untreated GIST, and harbor homozygous missense *KIT* exon 13 mutations (K642E) [59]. Being homozygous mutant, GIST882 cell do not express wild type KIT and are dependent on constitutive KIT signaling for survival [65, 67, 70, 129, 144]. This imatinib-sensitive GIST cell line was kindly provided by Jonathan Fletcher (Dana-Farber Cancer Institute; Boston, MA),

and cultured in DMEM, containing 1% (w/v) streptomycin/penicillin as well as 10% (v/v) heat-inactivated FBS.

As in the previous study, cells were maintained at 37°C, in a humidified incubator, with 5% CO₂, subjected to STR DNA fingerprinting for validation, and STR profiles compared to known fingerprints.

Western blot analysis

Treated and untreated cells were harvested by centrifugation, and washed twice with ice-cold PBS. Cell pellets were then lysed for 5 min in ice-cold cell lysis buffer consisting of 50 mM Tris-HCl, pH 7.4, supplemented with Nonidet P-40 [1% (v/v)], sodium chloride (150 mM), sodium orthovanadate (1 mM; Na₃VO₄, inhibitor of tyrosine- and alkaline-phosphatases), sodium fluoride (1 mM), and EDTA (1 mM). Immediately prior to use, the following protease inhibitors were added to RIPA buffer: 5 µg/ml aprotinin (basic pancreatic trypsin inhibitors, inhibits trypsin-like proteolytic enzymes), 5 µg/ml pepstatin (inhibitor of aspartyl proteases), and 1 µM PMSF (Sigma-Aldrich, St. Louis, MO). Lysates were sonicated (3 x 3 sec bursts), and cleared by ultracentrifugation at 14,000 x g for 10 min at 4°C. Total protein concentration in whole-cell lysates was quantified by Bradford's colorimetric assay (Bio-Rad; Hercules, CA). Protein lysates were diluted 1:2 by addition of 10 mM dithiothreitol (DTT)-containing sodium dodecyl sulfate-polyacrylamide gel electrophoresis (SDS-PAGE) loading buffer, and denatured at 70°C for 10 min. Whole-cell lysate (30 µg per lane) were then separated by SDS-PAGE for 35 at 100V min on pre-cast 4-12% gels, and transferred to methanol-activated PVDF

membranes for 1 hour at 100V. The remainder of the western blot protocol was as described in Chapter 2 Materials and Methods.

Analysis of Cell Proliferation and Viability

Proliferation of tumor cells was quantified using a commercial cell proliferation assay (CellTiter 96; Promega Corporation, Madison, WI). This assay detects reduction of 3-(4,5-dimethylthiazol-2-yl)-5-(3-carboxymethoxyphenyl)-2-(4-sulfophenyl)-2H-tetrazolium, salt (MTS) into a soluble product (formazan), which occurs in metabolically active cells after the addition of phenazine methosulfate (PMS). The absorbance ABS_{490nm} is directly proportional to the quantity of living cells in culture.

Briefly, 4×10^3 cells/well were seeded onto 96-well plates, and incubated at $37^\circ C$ for 24 hr. DMSO, single-agent ABT-737 or A793844 (0.1, 1, 10, 20 μM), were combined in a checkerboard manner with imatinib (0.1, 1, 10 μM), in a 100 μL volume/well. Following 24 to 72 hr incubation, MTS and PMS were combined (20:1), 20 μL of this mix was added to each well, and plates were further incubated for 4 hr at $37^\circ C$ to allow formation of formazan. ABS_{490nm} was quantified with Bio-Tek microplate reader A3100 (Bio-Tek Instruments, Winooski, VT), and KC Junior software. Percent viability (relative to DMSO-treated cells) was calculated by the following formula $[(\text{mean } ABS_{490nm, \text{ treatment}} - ABS_{490nm, \text{ background}}) / (\text{mean } ABS_{490nm, \text{ DMSO-treated}} - ABS_{490nm, \text{ background}})] \times 100$.

Propidium Iodide Staining and Cell Cycle Analysis

As discussed previously, one of the characteristic features of apoptosis is fragmentation and loss of cellular DNA content. Propidium iodide (PI)-staining, coupled

with flow cytometric analysis, enables measurement of cellular DNA content, which can distinguish apoptotic cell populations, as well as cell cycle phase. Specifically hypodiploid cells are considered apoptotic(sub-G1 phase), cells with diploid DNA in G0- or G1-phase, cells with supra-diploid DNA in S-phase, and cells with tetraploid content in M-phase.

For this assay, GIST cells were seeded in 100 mm culture plates (Corning Life Sciences, Corning, NY), and grown to >80% confluence, whereupon they were treated with single-agent ABT-737 or ABT-737 combined with imatinib. I harvested non-adherent cells by centrifugation at 100xg for 5 min at 4°C, and adherent cells by trypsinization and centrifugation. I then washed cells twice with ice-cold PBS and permeabilized their plasma membrane by overnight incubation in 70% ethanol/PBS (v/v) at -20°C. Permeabilized cells were collected by centrifugation at 300xg for 5 min at 4°C, washed twice with PBS, and incubated for 30 min in PBS containing RNase-A (1µg/ml) and propidium iodide (50 µg /ml), protected from light. Cellular DNA content was acquired by flow cytometry on a non-cell-sorting FACSCanto II cytometer, and results were analyzed using FACS Diva 6.1 software (BD Biosciences, San Jose, CA).

TdT-Mediated dUTP Nick-End Labeling (TUNEL) Assay

To further quantify apoptosis in GIST cells, I used the DeadEnd Fluorometric TUNEL System, available commercially from Promega Corporation (Madison, WI). The TUNEL assay is useful for quantifying apoptosis-induced DNA-fragmentation and cells within cell populations, and is based on the incorporation of fluorescein-conjugated 2'5'-deoxyuridine-triphosphate (F-dUTP) by cells undergoing apoptotic DNA-fragmentation.

For this assay, GIST cells were cultured, treated, and harvested as for cell cycle analysis (previous section). They were then washed twice with ice-cold PBS, and incubated with 1% paraformaldehyde (methanol-free) for 30 min at RT to fix their internal protein contents. Cells were subsequently washed with PBS twice, permeabilized in 70% ethanol/PBS (v/v), and stored at -20°C until ready for use. Immediately before TUNEL, I PBS-washed the cells twice, and resuspended them in equilibration buffer. Finally, 50 µL of recombinant terminal deoxynucleotidyl transferase (TdT) and fluorescein-12-dUTP were added to the fixed/permeabilized cells, and the cell suspension was incubated with for 2 hr at 37°C in the dark. This reaction was terminated with 150 µL 20mM EDTA, washed cells twice in PBS, and incubated them for 30 min in PBS containing RNase A at 1µg/ml and 50 µg/ml PI, protected from light. As above, apoptotic cells were quantified by flow cytometry on a FACSCanto II cytometer, being defined as double-positive for F-dUTP (green FITC fluorescence) and PI (red fluorescence). Results were analyzed using FACS Diva 6.1 software (BD Biosciences, San Jose, CA).

Ethidium Bromide/Acridine Orange (EB/AO) Apoptosis Assay

To assess morphologic changes consistent with apoptosis (plasma membrane blebbing, pyknosis, nuclear fragmentation, chromatin condensation), GIST cells were cultured in 96-well plates, and treated as per MTS assay protocol. Cells were dual-stained with 10µg/ml acridine orange and 5µg/ml ethidium bromide, as described by Ribble and Goldstein [145]. Specifically, at timepoints from 24 to 72 hr, 20 µl of freshly-prepared dual stain was added, and the plates were incubated at RT for 10 minutes on an orbital shaker at 300 RPM, followed by centrifugation at 100xg for 5 min. I defined apoptotic cells as exhibiting nuclear fragmentation and/or chromatin condensation. Early apoptotic cells display these nuclear changes but still exclude the vital dye ethidium bromide (orange stain), and therefore stain green with acridine orange. Late apoptotic cells display loss plasma membrane integrity and therefore stain orange, in addition to exhibiting nuclear fragmentation and/or chromatin condensation. Necrotic cells, which lose integrity of the plasma membrane without undergoing nuclear condensation, incorporate ethidium bromide (orange stain), and appear as orange cells with normal-sized nuclei. Viable cells by definition do not lose plasma membrane integrity nor undergo nuclear condensation, thus appearing as green (acridine-orange stained) normal-sized nuclei. Apoptosis was calculated as the average proportion of pyknotic cells in replicate wells, counting 200 cells/well with ImageJ Software.

Data analysis: Statistics and Synergy

Statistical analysis was undertaken using GraphPad Prism 5 software (San Diego, CA). Experimental results among three or more experimental groups were compared by

analysis of variance (one- and two-way ANOVA), with Bonferroni's multiple comparisons to compare, post-test, two individual groups. To evaluate whether the anti-tumor effects of ABT-737 and imatinib were synergistic I used the combination index (CI) method described by Chou and Talalay [146-148]. Combination indices for cell viability and apoptosis were generated with CalcuSyn (Biosoft Software, Cambridge, UK).

Results

ABT-737, but not stereoisomer A793844, inhibits the growth of GIST cells

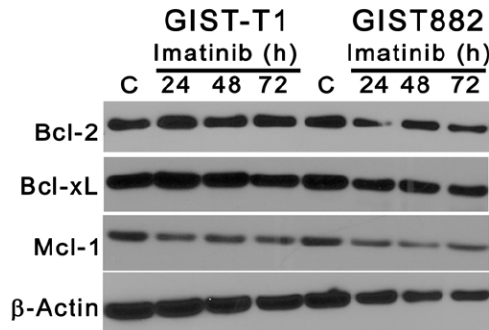
As discussed, ABT-737 was designed to mimic the BH3 domain of the BH3-only protein BAD, and is a highly-specific inhibitor ($K_i < 1$ nM) of Bcl-2, Bcl- x_L , and Bcl-w, while its inactive stereoisomer, a compound known simply as A793844, exhibits limited affinity ($K_i > 100$ nM) or inhibitory effects upon Bcl-2 and Bcl- x_L [139].

Prior to applying ABT-737 in GIST cells, I evaluated whether its protein targets, Bcl-2 and Bcl- x_L , were expressed in imatinib-sensitive GIST-T1 and GIST882 cells, examining protein levels in untreated cells, as well as imatinib-induced alterations, if any, by western blot. In addition, I examined Mcl-1 protein levels, the expression of which has been found to be proportional to ABT-737-resistance in other models. The pro-survival Bcl-2 members A1 and Bcl-w were not queried due to their established tissue-specific distribution in hematopoietic stem cells and testicular germ cells, respectively.

GIST-T1 and GIST882 cells express high levels of Bcl-2 and Bcl- x_L , in addition to Mcl-1 (Figure 22), in accordance with published reports [64, 149]. In contrast to the

studies by Sambol, et al. and Paner, et al., expression of Bcl-2 and Mcl-1 was unaffected by imatinib. The expression of Bcl-xL had not previously been evaluated in GIST cells.

Figure 22. GIST cells express Bcl-2, Bcl-xL and Mcl-1, the targets of ABT-737.



GIST-T1 and GIST882 cells were incubated with DMSO or 1 μ M imatinib for 24, 48, and 72 hrs, and whole-cell lysates were subjected to western blotting for Bcl-2, Bcl-xL, and Mcl-1. β -actin was used to demonstrate equal protein loading. Reprinted from *Molecular Oncology*, Vol 5:1(93-104). Copyright (2010), with permission from Elsevier.

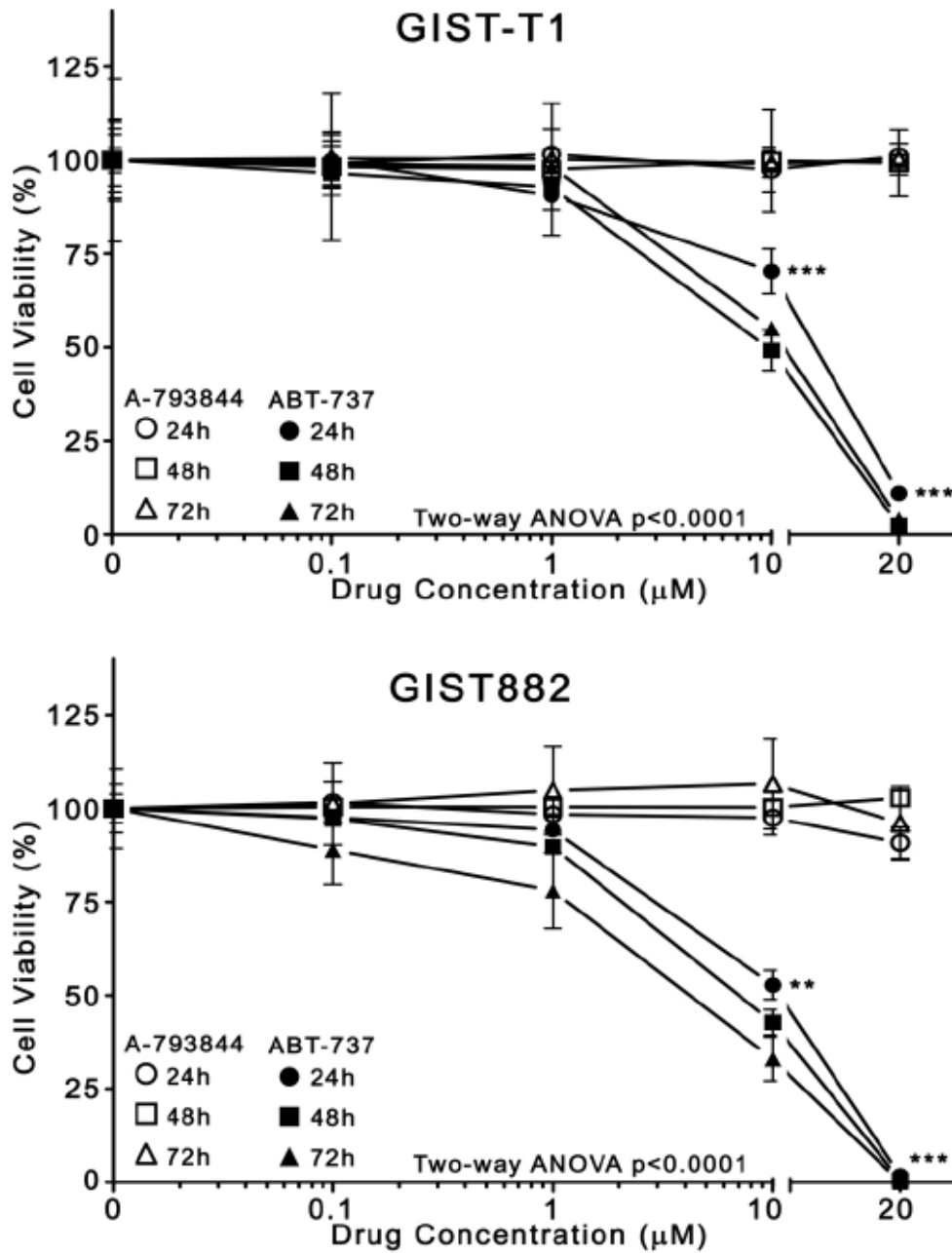
Having found substantial expression of its protein targets in GIST cells, I next evaluated the anti-tumor effects of single-agent ABT-737 in GIST cells. I also determined whether the effect of ABT-737 was due to specific inhibition of its pro-survival targets by comparing its effects with those of A793844, hypothesizing that cell death caused by off-target effects would also be exhibited by its inactive stereoisomer.

To evaluate the antiproliferative activity of ABT-737 and/or A793844, GIST-T1 and GIST882 cell viability was quantified by MTS assay after treatment with incremental concentrations of ABT-737 or A793844 as single agents for 24 to 72 hours (Figure 23).

The concentrations used in this study ranged from 0.1 μM to 20 μM ABT-737, and were comparable to doses used in other preclinical studies of ABT-737 [150].

In GIST-T1 and GIST882 cells, single-agent ABT-737 exhibits limited anti-proliferative activity at concentrations below 1 μM , but effects significant inhibition of viability, in a dose- and time-dependent manner, above this concentration (Two-way ANOVA, $p < 0.0001$). Specifically, the viability of GIST-T1 and GIST882 cells relative to untreated and DMSO-treated controls was reduced by an average of 20% with 1 μM ABT-737, whereas 50% and 95% inhibition were observed with 10 μM and 20 μM ABT-737, respectively. At 72 hours post-treatment, the IC_{50} of ABT-737 for both GIST-T1 and GIST882 cells approximated 10 μM . In contrast, the viability of GIST cells was unaffected by treatment with stereoisomer A793844 at any concentration, consistent with its decreased binding capacity and inhibition of Bcl-2 proteins.

Figure 23. ABT-737, but not its stereoisomer A793844, significantly inhibits the viability of GIST cells.



GIST-T1 and GIST882 cells were treated with DMSO, or incremental concentrations of single-agent ABT-737 or stereoisomer A793844 (0.1, 1, 10, 20 μM) for 24, 48, and 72 hrs. Relative cell viability was quantified by MTS assay. Symbols represent the mean of triplicate experiments; error bars represent standard deviation (SD). Three asterisks (***) represent Bonferroni's multiple post-test comparison, p-value < 0.0001 as compared to A793844 at equal timepoints.

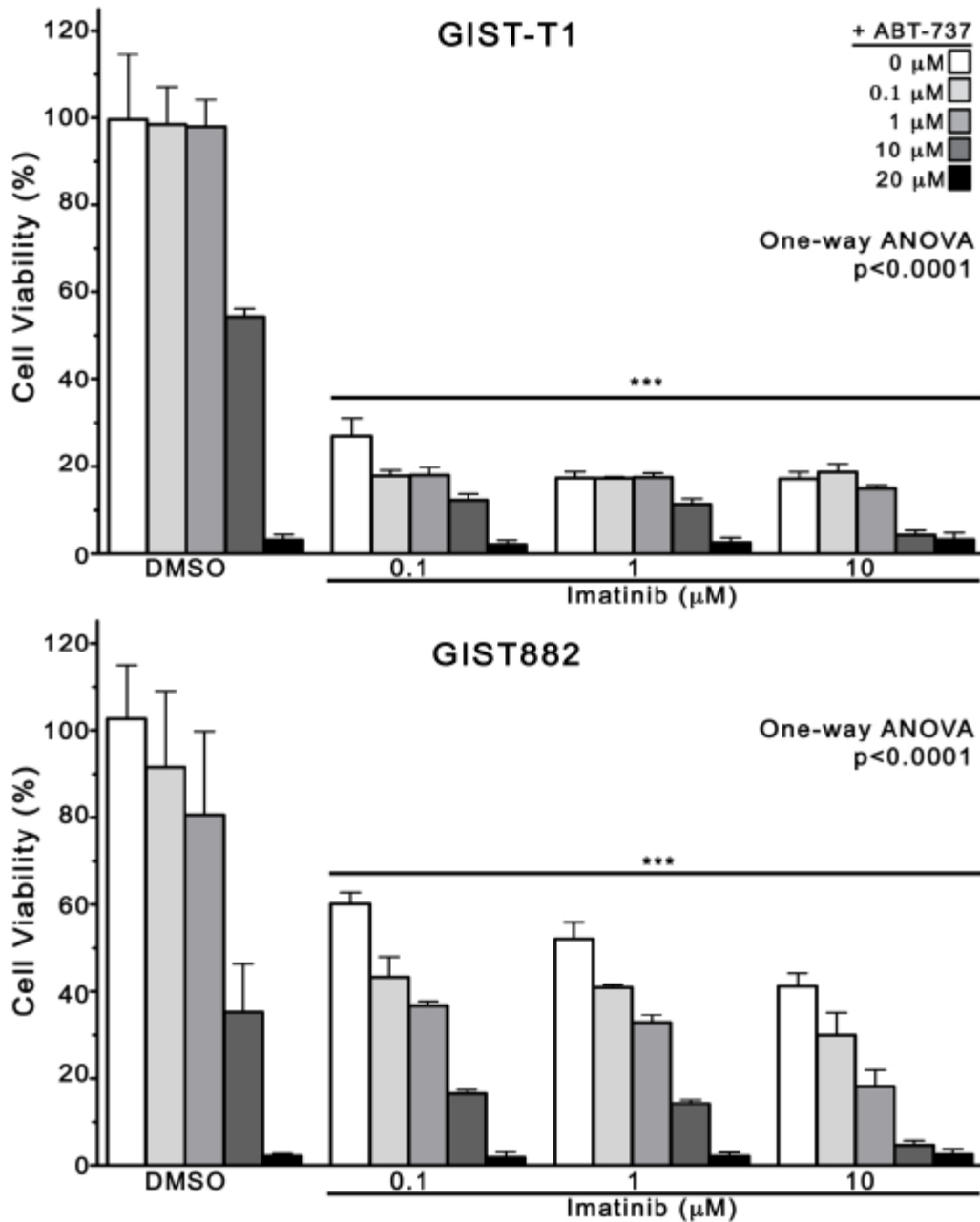
ABT-737 and imatinib inhibit GIST cell viability synergistically

As monotherapy, ABT-737 effectively inhibited the viability of imatinib-sensitive GIST cells, but did so at higher concentrations than has been observed in hematologic tumors models [151, 152]. I thus examined the anti-tumor effects of ABT-737 in combination with imatinib, theorizing that such a rational combination might exhibit superior activity compared with either agent alone. Cells were treated in a standard checkerboard fashion with 0, 0.1, 1, 10, or 20 μM ABT-737 as a single agent and in combination with 0, 0.1, 1, or 10 μM imatinib 72 hours, and quantified cell viability by MTS assay.

Combined treatment causes superior reductions in viability, as compared with either imatinib or ABT-737 as single agents (Figure 24). While maximum growth inhibition with single-agent imatinib (0.1, 1, and 10 μM ; white bars) plateaus at 80% in GIST-T1 cells, and 60% in GIST882 cells, combination with 0.1 to 10 μM ABT-737 results in up to 90% growth inhibition in both cell lines (One-way ANOVA, $p < 0.0001$). Notably, concentrations of ABT-737 that appeared to be ineffective in monotherapy (0.1 and 1 μM ABT-737) potentiated the effect of imatinib in combination.

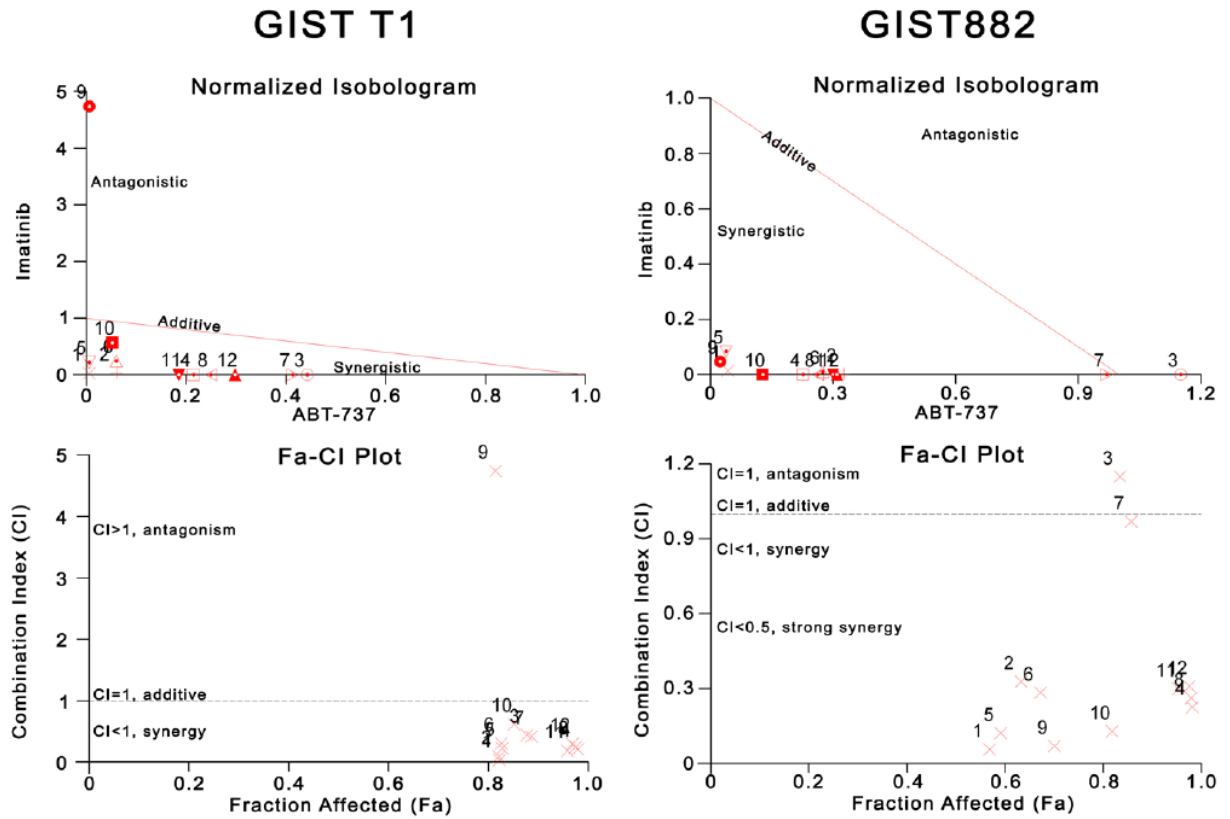
To determine whether the antitumor effects of ABT-737 and imatinib were additive, synergistic, or antagonistic, I conducted isobologram analyses according to the methods of Chou and Talalay. These revealed that reductions in cell viability were strongly synergistic, with $\text{CI} < 0.5$ for most combinations tested (Figure 25). The synergy results are depicted graphically in the Normalized Isobologram, and Fraction affected-Combination Index (Fa-CI) plots generated for GIST-T1 (left panel) and GIST882 (right panel) cells.

Figure 24. ABT-737 and imatinib synergistically inhibit the viability of GIST cells.



GIST-T1 and GIST882 cells were incubated with incremental doses of imatinib (0, 0.1, 1, 10 μM) and ABT-737 (0, 0.1, 1, 10, 20 μM), by checkerboard fashion, and analyzed by MTS assay at 72 hrs. Columns represent mean of triplicate experiments; error bars represent SD. Results were analyzed by one-way ANOVA, and three asterisks (***) represent p<0.0001 versus DMSO control by Bonferroni's post-test comparison.

Figure 25. Isobologram analysis of synergy for imatinib/ABT-737 combinations with respect to growth inhibition in GIST cells.



Combination indices (CI) corresponding to the Imatinib/ABT-737 combinations tested in Figure 24 were determined by isobologram analysis of synergy (Chou-Talalay method). Representative normalized isobolograms and Fraction affected (Fa)-CI plots, graphically depict the growth-inhibitory interactions between imatinib and ABT-737 in GIST-T1 (left) and GIST882 cells (right). Note that all but one imatinib/ABT-737 combination was synergistic in this analysis in GIST-T1 cells, and all combinations in GIST-T1 achieved greater than 80% growth inhibition. Similarly, only two combinations were additive/antagonistic in GIST882 cells, and all combinations achieved greater than 50% growth inhibition. Reprinted from *Molecular Oncology*, Vol 5:1(93-104). Copyright (2010), with permission from Elsevier.

ABT-737 and imatinib combine to induce apoptosis synergistically

Cell viability assays, including the MTS assay, are based on the linear relationship between metabolic activity in viable cells and reduction of MTS to formazan. While this is a highly sensitive method to detect reductions in cell viability, decreases in metabolic activity may be the result of cell cycle arrest, senescence, or quiescence, and not apoptosis. To determine whether the cell viability reductions induced by the combination of ABT-737 and imatinib were a consequence of apoptosis activation, GIST-T1 and GIST882 cells were treated with ABT-737 as a single agent and in combination with imatinib for 48 hours, and DNA fragmentation was measured by propidium iodide staining and flow cytometric cell cycle analysis (Figure 26A), as well as by TUNEL (Figure 26B).

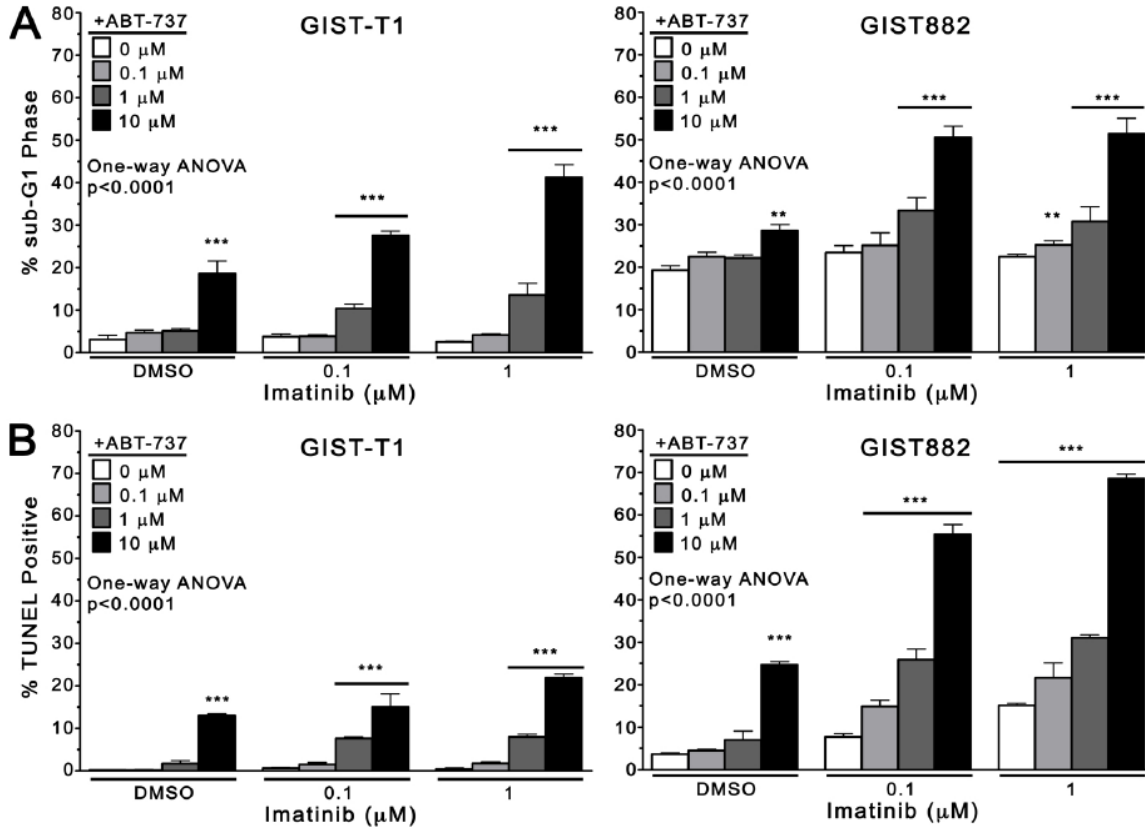
By both methodologies, combinations of ABT-737 and imatinib induced superior apoptosis as compared with DMSO or either agent alone (One-way ANOVA, $p < 0.0001$). Specifically, apoptosis (hypodiploid DNA content) was observed in 3% of DMSO-treated GIST-T1 cells, as compared with 20% of GIST-T1 cells treated with 10 μ M ABT-737 alone. Combined, 10 μ M ABT-737 + 0.1 μ M imatinib and 10 μ M ABT-737 + 1 μ M imatinib induced 28% and 41% apoptosis, respectively. By TUNEL assay, 3% apoptosis was observed with DMSO treatment in GIST-T1 cells, 13% with 10 μ M ABT-737, 15% with 10 μ M ABT-737 + 0.1 μ M imatinib, and 22% with 10 μ M ABT-737 + 1 μ M imatinib.

In GIST882 cells, 4% apoptosis was observed in the DMSO-treated group, increasing to 55% and 68%, respectively with 10 μ M ABT-737 + 0.1 μ M imatinib and 10 μ M ABT-737 + 1 μ M imatinib. Similarly, I observed a significant proportion of sub-G1

phase DMSO-treated GIST882 cells (19%), 29% with 10 μ M ABT-737, and 50% with both 10 μ M ABT-737 + 0.1 μ M imatinib and 10 μ M ABT-737 + 1 μ M imatinib.

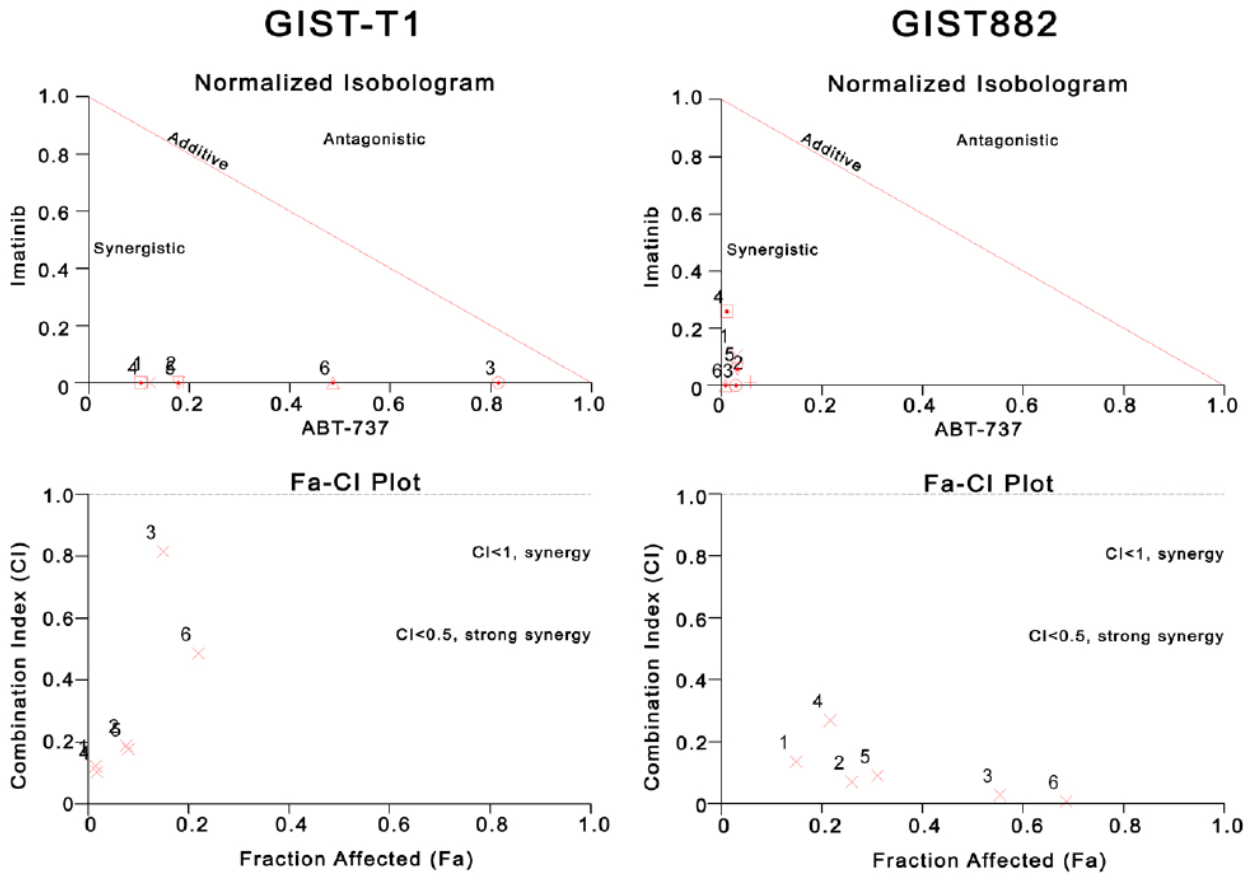
Notably, the synergy exhibited with regard to reductions in viability by MTS assay extended to apoptosis in both cell lines (Figure 27). As with cell viability reductions, isobologram analyses of apoptosis induction confirmed a synergistic interaction ($CI < 0.5$) for most combinations of ABT-737 and imatinib. Overall results of isobologram (synergy) analyses for all three cell lines are available in Table 9.

Figure 26. ABT-737 and imatinib induce apoptosis synergistically in imatinib-sensitive cells.



GIST-T1 and GIST882 cells were incubated with imatinib (0, 0.1, 1 μ M) and ABT-737 (0, 0.1, 1, 10 μ M) for 48 hrs and apoptosis was determined by (A) cell cycle analysis (sub-G1 DNA content) and (B) TUNEL (FITC+). Columns represent averages of triplicate experiments; error bars represent SD. Results were analyzed by one-way ANOVA, and three asterisks (***) represent p < 0.0001 versus DMSO control by Bonferroni's post-test.

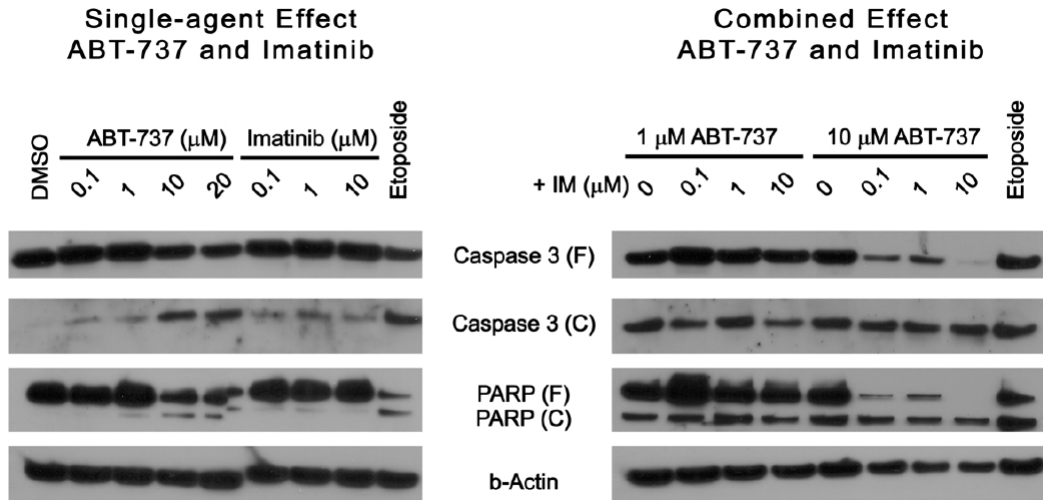
Figure 27. Isobologram analyses of synergy with respect to apoptosis for imatinib/ABT-737 combinations in GIST cells.



Combination indices (CI) corresponding to the Imatinib/ABT-737 combinations tested in Figure 25 were determined by isobologram analysis of synergy (Chou-Talalay method). Normalized isobolograms and Fraction affected (Fa)-CI plots, graphically depict the proapoptotic (% TUNEL positivity) interactions between imatinib and ABT-737 in GIST-T1 (left) and GIST882 cells (right). Normalized isobolograms (top), and Fraction affected-Combination Index (Fa-CI) plots (bottom). All combinations were strongly synergistic with regard to apoptosis in both GIST-T1 and GIST882 cells. Reprinted from *Molecular Oncology*, Vol 5:1(93-104). Copyright (2010), with permission from Elsevier.

Apoptosis was further evaluated by western blot detection of caspase 3 and PARP in whole-cell lysates of GIST882 cells after treatment with ABT-737/imatinib for 72 hours (Figure 28). ABT-737 monotherapy resulted in dose-dependent activation of caspase 3, as evidenced by cleavage of the inactive 37-kDa pro-caspase 3, coupled with detection of the 19-kDa active caspase 3. Likewise, PARP was cleaved after treatment with ABT-737 as a single-agent, but not after treatment with imatinib. Notably, imatinib treatment caused minimal cleavage of caspase 3 in GIST882 cells, with no cleavage of PARP. In contrast, combinations of 10 μ M ABT-737 + 0.1, 1, or μ M imatinib induced significant cleavage of both, in excess of the effect of 10 μ M ABT-737 alone (Figure 28, right panel). Interestingly, the cleaved species (active caspase 3 and PARP fragments) and uncleaved pro-forms were found to exhibit different rates of turnover, with the former being degraded rapidly after cleavage in GIST882 cells.

Figure 28. Single-agent and combined effect of ABT-737 and imatinib on caspase/PARP cleavage.



Representative western blots of GIST882 cells treated with ABT-737 and imatinib as single agents (left) and in combination (right). Cells were treated for 72 hours with vehicle (DMSO) or with increasing concentrations of imatinib and/or ABT-737, and caspase-3 and PARP cleavage were assessed by western blotting. Treatment with Etoposide (10 μM) was used as a positive control for caspase activation. β-actin was used to demonstrate equal protein loading. Abbreviations: (F), full length; (C), cleaved. Reprinted from *Molecular Oncology*, Vol 5:1(93-104). Copyright (2010), with permission from Elsevier.

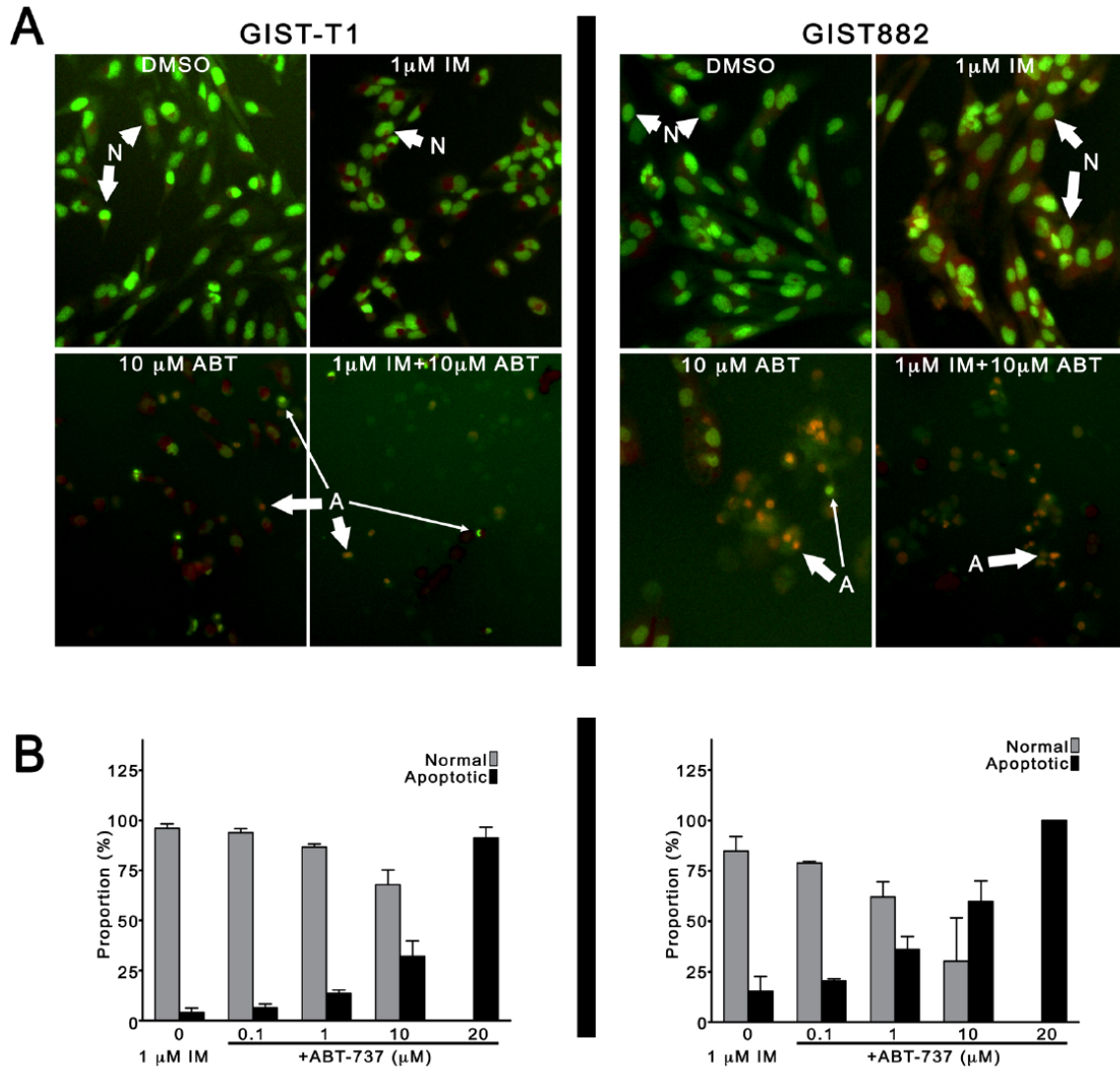
ABT-737 induces morphologic features of apoptosis in GIST cells

The gold-standard method for determination of apoptosis involves morphologic confirmation of its characteristic features, including visualization of condensation and fragmentation of nuclear contents, plasma membrane blebbing, and loss of plasma membrane integrity [153]. I evaluated apoptotic cell death after treating GIST cells with ABT-737 and/or imatinib for 72 hours, by assessing nuclear morphology with light and fluorescence microscopy of ethidium bromide/acridine orange (EB/AO) stained cells.

As seen in Figure 29A, DMSO- and imatinib-treatment result in minimal chromatin fragmentation or nuclear condensation in GIST-T1 or GIST882 cells, while treatment with 10 μ M ABT-737, or 10 μ M ABT-737 + 1 μ M imatinib results in greater apoptosis induction.

This was confirmed by quantitative assessment of nuclear morphology using ImageJ Software (Figure 29B). Specifically, treatment with 1 μ M imatinib plus any amount of ABT-737 (0.1, 1, 10, 20 μ M) for 72 hours caused superior activation of early and late apoptosis than either agent alone.

Figure 29. The morphologic features of apoptosis are induced by ABT-737 in GIST cells



GIST-T1 and GIST882 cells were treated for 72 h with 1 μ M imatinib alone, or in combination with ABT-737 (0.1, 1, 10, 20 μ M) and apoptotic cell death was evaluated by assessment of nuclear morphology after ethidium bromide/acridine orange (EB/AO) staining. (A) Representative micrographs of GIST-T1 (left) and GIST882 (right) cells treated with vehicle (DMSO), 1 μ M imatinib, 10 μ M ABT-737, or both, demonstrating nuclear fragmentation and condensation in ABT-737-treated cells. Original magnification, x200. Abbreviations: (N), normal nuclei; (Thick arrow), late apoptosis; (Thin Arrow), early apoptosis. (B) Quantitative assessment of normal and apoptotic cells treated with 1 μ M imatinib, alone or with ABT-737 (0, 0.1, 1, 10, 20 μ M). Reprinted from *Molecular Oncology*, Vol 5:1(93-104). Copyright (2010), with permission from Elsevier.

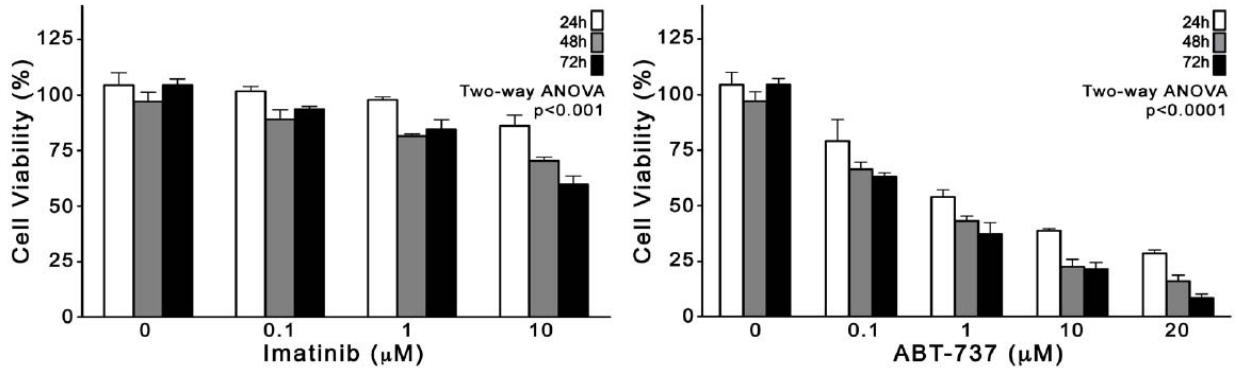
ABT-737 and imatinib combine to activate apoptosis and overcome resistance to imatinib in GIST48IM cells

Given that ABT-737 effectively augmented the cytotoxicity of imatinib in GIST cell lines that were initially susceptible to KIT inhibition (GIST-T1 and GIST882), I wondered whether this therapeutic combination could overcome imatinib-resistance in GIST48IM cells.

As with GIST-T1 and GIST882 cells, I first evaluated the anti-tumor effects imatinib and ABT-737 as single agents by MTS assay (Figure 30). In accordance with their known resistance to KIT inhibition, I observed moderate reductions in viability with single-agent imatinib for 72 hours, and the IC_{50} of imatinib was not reached (Figure 30, top). In contrast, monotherapy with ABT-737 for 72 hours resulted in significant reductions in viability of GIST48IM cells, with IC_{50} of 1 μ M (Figure 30, bottom).

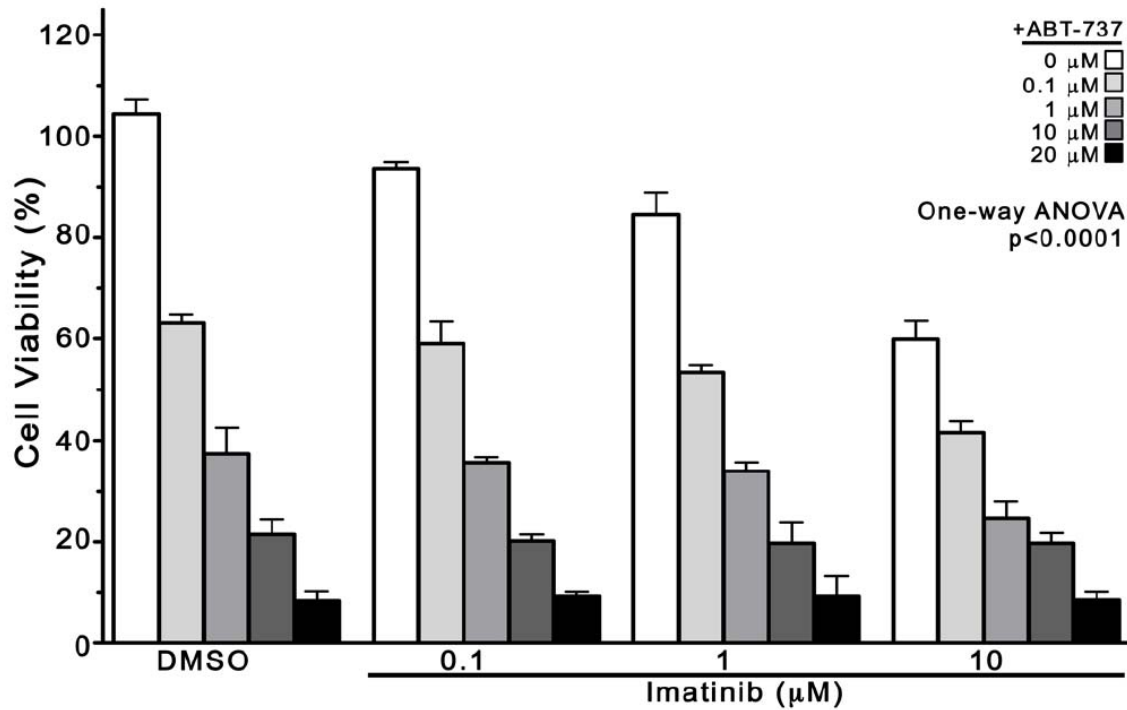
In combination (Figure 31), ABT-737 and imatinib exhibited superior inhibition of viability in GIST48IM cells, as compared with either agent alone (One-way ANOVA $p < 0.0001$). However, because single-agent imatinib has only a moderate effect on the viability of GIST48IM cells, the degree of synergy between imatinib and ABT-737 in GIST48IM was decreased (Figure 32). In particular, because the effect of ABT-737 at doses above 10 μ M is unaffected by imatinib, I observed three antagonistic, and two additive combinations in this GIST48IM cells.

Figure 30. Antiproliferative effects of imatinib and ABT-737 as single-agents in imatinib-resistant cells.



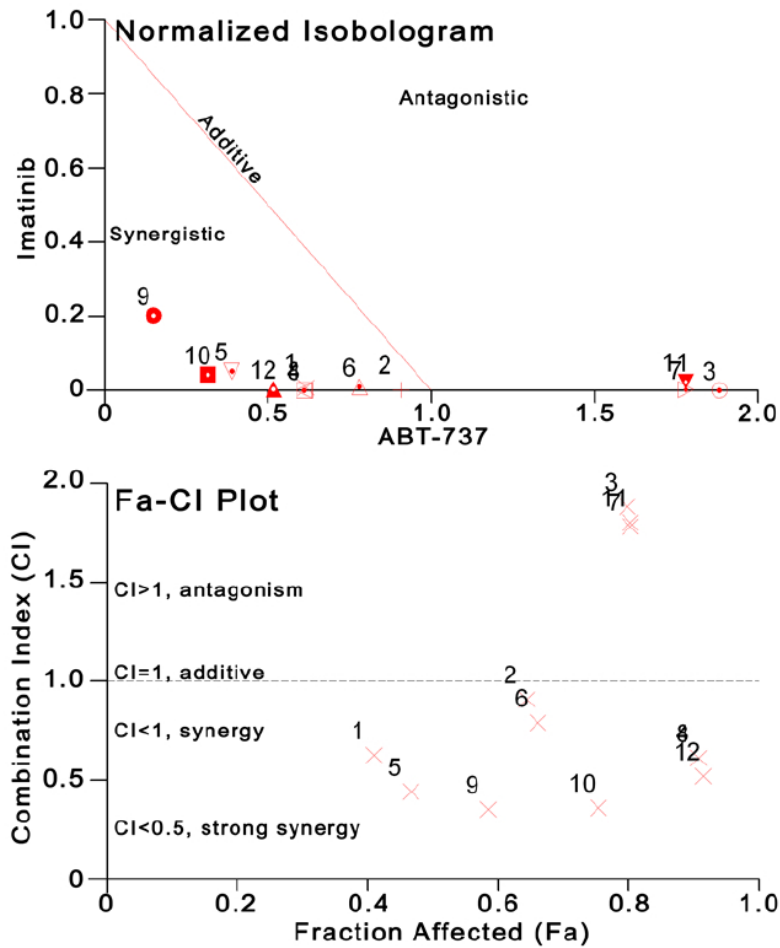
The antiproliferative effect of single-agent imatinib (top) and single-agent ABT-737 (bottom) in imatinib-resistant GIST48IM cells was examined after 24, 48 and 72 hours of treatment, using the MTS cell viability assay. Columns, mean of triplicate experiments; error bars, SD. Results were analyzed by two-way ANOVA. Reprinted from Molecular Oncology, Vol 5:1(93-104). Copyright (2010), with permission from Elsevier.

Figure 31. ABT-737 and imatinib synergistically inhibit the viability of imatinib-resistant GIST cells.



The effect of combined ABT-737 (0, 0.1, 1, 10, 20 μM) and imatinib (0, 0.1, 1, 10 μM) on the viability of GIST48IM cells at 72 h. Columns, mean of triplicate experiments; error bars, SD. Results were analyzed by one-way ANOVA. Reprinted from Molecular Oncology, Vol 5:1(93-104). Copyright (2010), with permission from Elsevier.

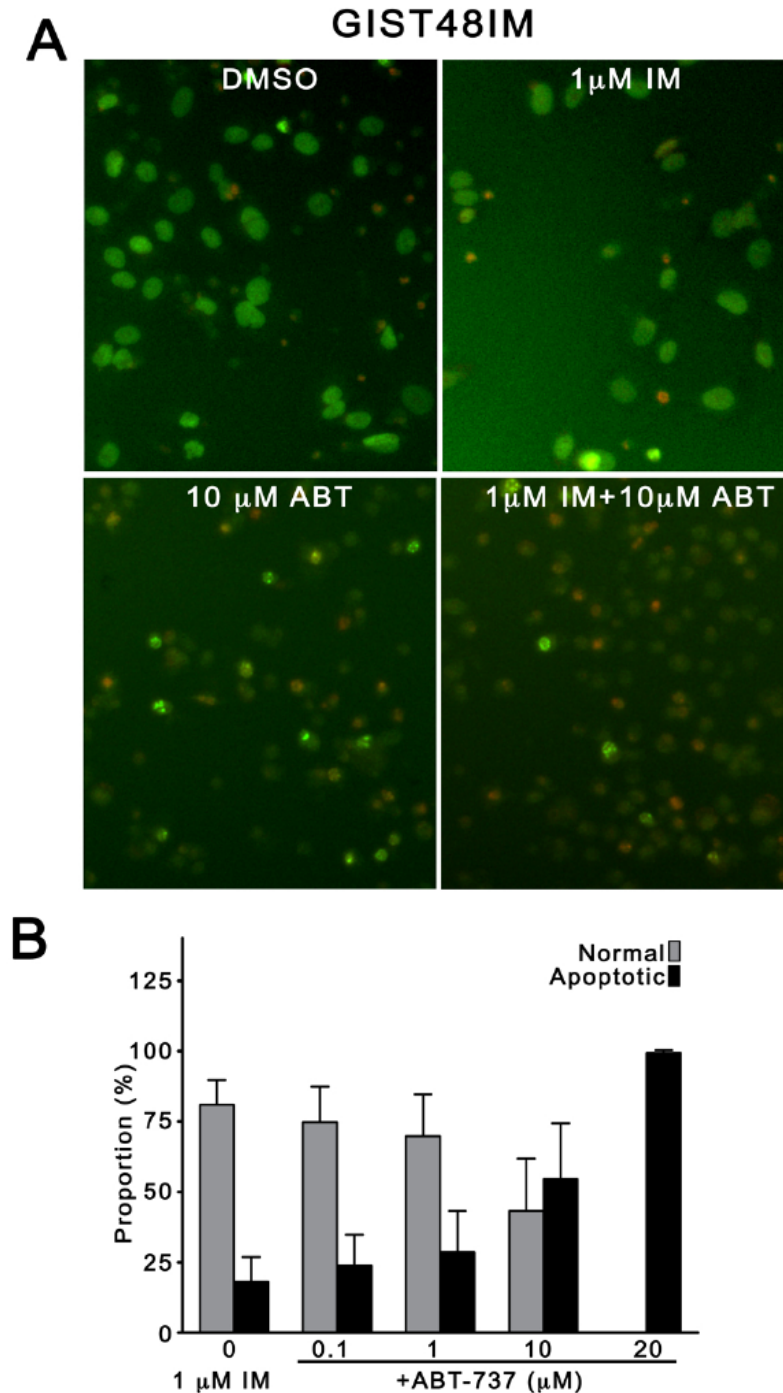
Figure 32. Analysis of synergy between imatinib and ABT-737 in imatinib-resistant GIST cells.



Normalized isobologram (top) and Fa-CI plot (bottom) of GIST48IM cells, graphically depicting synergistic, additive, and antagonistic interactions between imatinib and ABT-737 in this cell line. Reprinted from *Molecular Oncology*, Vol 5:1(93-104). Copyright (2010), with permission from Elsevier.

To further evaluate whether viability reductions in GIST48IM were caused by apoptotic cell death, I examined their nuclear morphology after treatment with DMSO or 1 μ M imatinib, in combination with ABT-737 (0, 0.1, 1, 10, 20 μ M) for 72 hours. Notably, this cell line demonstrates greater apoptosis at baseline (DMSO-treated) than either GIST-T1 or GIST882 cells (Figure 33). In addition, treatment of GIST48IM cells with 10 μ M ABT-737, with or without 1 μ M imatinib, but not with 1 μ M imatinib alone, resulted in marked nuclear fragmentation and chromatin condensation. Overall, quantitative assessment of nuclear morphology using ImageJ Software confirmed that apoptosis increased in direct proportion with ABT-737, to a maximum of 100% with 20 μ M ABT-737.

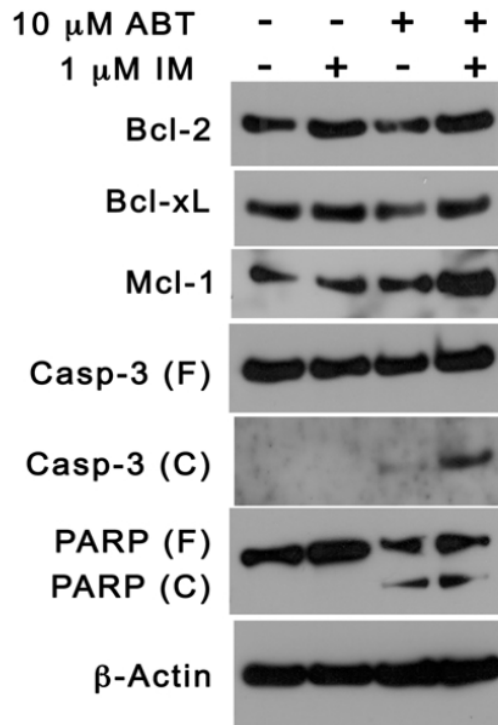
Figure 33. ABT-737 and imatinib induce morphologic apoptosis in imatinib-resistant GIST cells.



(A) Nuclear morphology was assessed by EB/AO staining after treatment with ABT-737 and imatinib for 72 h. Representative micrographs of ethidium bromide/acridine orange-stained GIST48IM cells. Original magnification, x200. (B) Quantification of normal and apoptotic cells treated with 1 μM imatinib alone, or combined with ABT-737 (0.1, 1, 10, 20 μM).

Using western blotting, expression of Bcl-2, Bcl-xL and Mcl-1, cleavage of caspase 3, and cleavage of PARP were evaluated after treatment with DMSO, 1 μ M imatinib, 10 μ M ABT-737, alone and in combination. While the protein levels of Bcl-2, Bcl-xL and Mcl-1 were unchanged under these conditions, caspase 3 and PARP were cleaved by treatment with ABT-737 monotherapy, as well as 1 μ M imatinib + 10 μ M ABT-737, but not by imatinib monotherapy.

Figure 34. Western blot detection of Bcl-2 proteins and apoptotic markers in GIST48IM cells.



Western blot analysis of Bcl-2, Bcl-xL and Mcl-1, as well as the cleavage of caspase 3 and PARP, after treatment with DMSO, 1 μ M imatinib, 10 μ M ABT-737, or a combination for 72 hours. Actin was used to demonstrate equal loading. Abbreviations: (F), full length; (C), cleaved. Reprinted from *Molecular Oncology*, Vol 5:1(93-104). Copyright (2010), with permission from Elsevier.

Table 9. Overall results from isobologram (synergy) analyses of imatinib/ABT-737 combinations in GIST cells.

COMBINATIONS		GROWTH INHIBITION							APOPTOSIS				
Imatinib	ABT-737	GIST-T1		GIST882		GIST48IM			GIST-T1		GIST882		
(μ M)	(μ M)	#	Fa	CI	Fa	CI	Fa	CI	#	Fa	CI	Fa	CI
0.1	0.1	1	0.82	0.0	0.57	0.1	0.41	0.6	1	0.15	0.1	0.02	0.1
0.1	1	2	0.82	0.1	0.63	0.3	0.64	0.9	2	0.26	0.1	0.08	0.2
0.1	10	3	0.88	0.4	0.83	<u>1.2</u>	0.80	<u>1.9</u>	3	0.55	0.0	0.15	0.8
0.1	20	4	0.98	0.2	0.98	0.2	0.91	0.6					
1	0.1	5	0.83	0.2	0.59	0.1	0.47	0.4	4	0.22	0.3	0.02	0.1
1	1	6	0.83	0.3	0.67	0.3	0.66	0.8	5	0.31	0.1	0.08	0.2
1	10	7	0.89	0.4	0.86	<i>1.0</i>	0.80	<u>1.8</u>	6	0.69	0.0	0.22	0.5
1	20	8	0.97	0.2	0.98	0.3	0.91	0.6					
10	0.1	9	0.81	<u>4.7</u>	0.70	0.1	0.58	0.4					
10	1	10	0.85	0.6	0.82	0.1	0.75	0.4					
10	10	11	0.96	0.2	0.95	0.3	0.80	<u>1.8</u>					
10	20	12	0.97	0.3	0.98	0.3	0.91	0.5					

Overall results from isobologram (synergy) analyses of imatinib/ABT-737 combinations in GIST-T1, GIST882, and GIST48IM cells, performed for growth inhibition and apoptosis. The combinations are numbered sequentially (# 1-12 for growth inhibition; # 1-6 for apoptosis) and these correspond to the numbers in the normalized isobolograms and Fa-CI plots (Figures 25, 27 and 32). Abbreviations: (CI), combination index; (Fa), fraction affected (%growth inhibition or % TUNEL-positive); Legend: #, combination identifier; CI<0.5, strong synergy; CI<1 synergy; CI=1 additive (*italics*); and CI>1, antagonism (underlined). Reprinted from Molecular Oncology, Vol 5:1(93-104). Copyright (2010), with permission from Elsevier.

Discussion

In spite of its unquestionable superiority in comparison with cytotoxic chemotherapies, current clinical evidence suggests that imatinib is unable to eradicate all viable GIST cells in tumors and produce cures. As discussed, acquired imatinib-resistance, coupled with adaptive cellular responses, enable GIST subclones to survive monotherapy with imatinib.

The therapeutic options are limited for patients with imatinib-resistant GIST. Sunitinib, and other second- and third-generation TKIs are transiently-effective treatment options for imatinib-resistance. Moreover, it is well-known that individual lesions in patients harbor diverse TKI-resistant mutations, whose capacity for adaptive selection far outpaces our pharmacologic repertoire. Thus, combining proven targeted therapies in a rational way might be a more successful therapeutic strategy to overcome imatinib-resistance or realize durable clinical remissions.

These studies evaluated whether therapeutic Bcl-2 inhibition was cytotoxic in GIST cells, and, particularly, whether it enhanced the efficacy of imatinib. Direct activation of the mitochondrial pathway of apoptosis via Bcl-2 inhibition is known to overcome resistance to TKIs in other solid and liquid tumor models, but this strategy has not been examined in the setting of GIST. One additional benefit of targeted inhibition of pro-survival Bcl-2 proteins is that normal tissues are generally not susceptible to this mode of cell death. That is, healthy tissues, by definition, do not depend on deregulated pro-survival Bcl-2 expression or function for survival and are exempt from the cytotoxic actions of Bcl-2 inhibitors.

I hypothesized that ABT-737, a BH3-mimetic inhibitor of the pro-survival Bcl-2 proteins, would complement or enhance the cytotoxicity induced by KIT inhibition in GIST cells, by specifically activating the intrinsic pathway of apoptosis downstream, and independently, of imatinib. The primary goals of this preclinical study were to examine whether ABT-737 augmented apoptosis in imatinib-sensitive GIST cell lines, and to determine whether it could overcome established imatinib-resistance in GIST cells refractory to imatinib monotherapy. Additionally, these studies sought to determine whether the effective concentrations of ABT-737 *in vitro* might be attained in GIST patients.

These studies found evidence that ABT-737 and imatinib combine synergistically to inhibit the proliferation of, and induce apoptosis in, GIST cells. The synergistic interaction between imatinib and ABT-737 in GIST cells occurs without regard to their sensitivity or resistance to imatinib. This effect may be explained by the complementary nature of the mechanisms by which these targeted therapies engage the intrinsic pathway of apoptosis. Presumably, the effect of imatinib-induced BIM upregulation combined with Bcl-2 inhibition mediated by ABT-737 achieves greater antagonism of the pro-survival Bcl-2 proteins than either agent alone.

While this study did not evaluate the degree of inhibition of Bcl-2 proteins in GIST cell lines, published reports have demonstrated that the pro-apoptotic effects of ABT-737 are the result of specific inhibition of Bcl-2, Bcl-xL, and Bcl-w [150]. Further, compound A793844, an inactive stereoisomer of ABT-737 that exhibits decreased affinity for Bcl-2 and Bcl-xL, does not exhibit cytotoxicity in GIST cells, suggesting that

GIST cell death was directly related to inhibition of pro-survival Bcl-2 proteins Bcl-2 and Bcl-xL.

The recently-published results of three phase I studies of an orally-bioavailable ABT-737 analog, ABT-263 (Navitoclax) [154], confirm the safety and biologic activity of Bcl-2 inhibition in patients with hematologic and solid tumors, including refractory chronic lymphocytic leukemia (CLL) [155], small-cell lung cancer (SCLC)/pulmonary carcinoid [156], and multidrug-resistant lymphoid tumors [157]. Wilson and colleagues found that 10 of 46 patients (22%) with relapsed or refractory lymphoid malignancies achieved partial responses with ABT-263, and the median progression-free survival (PFS) of responders was 15 months [157]. In this study, the greatest sensitivity to ABT-263 was demonstrated by patients with CLL and small lymphocytic lymphoma, two diseases characterized by increased Bcl-2 expression. Importantly, durable responses were observed with ABT-263 monotherapy in heavily pretreated patients, with a median of four previous drug regimens (range 1–12). Similarly, Roberts and colleagues observed partial responses in nine of 26 patients (35%) with relapsed or refractory CLL treated with Navitoclax >110 mg/d, with median PFS of 25 months [155]. Notably, single-agent activity was observed in patients with bulky, fludarabine-resistant del(17p) CLL. Moreover, the antitumor efficacy of ABT-263 extends to solid tumors, as Ghandi and colleagues found that 10 of 38 patients (26%) with SCLC or pulmonary carcinoid tumors achieved stable disease or partial responses [156]. In this study, however, median duration of disease control was only 5 months (range 2-35).

A corollary aim of this study was to determine whether cytotoxic concentrations of ABT-737 *in vitro* were feasible in clinical trials. Although pharmacologic data for

ABT-737 in humans is limited, C_{max} ranging from 3 to 14 μM were observed in mice and dogs gavaged with 10 to 100 mg/kg/day, in the absence of toxicity, and these concentrations constitute effective exposure in preclinical models [150]. With regards to pharmacokinetics of the orally bioavailable ABT-263 in human beings, the concentrations projected to be effective in preclinical models were achieved in humans at doses between 250 and 325 mg/day on a continuous daily dosing schedule, and these have been selected for phase II studies [155-157].

Importantly, the synergistic interaction of ABT-737 and imatinib in GIST cells was apparent with low-concentrations of either drug (0.1 and 1 μM ABT-737 and 0.1 μM and 1 μM imatinib), suggesting that a safe therapeutic index is achievable for combinations of ABT-737 and imatinib. Furthermore, whereas most cytotoxic chemotherapy regimens employed for the treatment of sarcomas and other solid tumors were developed empirically, I employed a rational approach to combine ABT-737 and imatinib. Specifically, I considered complementary mechanisms of action as the goal of therapy, so as to maximize the apoptotic effects while minimizing cross-resistance.

In sum, parallel inhibition of KIT signaling and direct engagement of the intrinsic pathway of apoptosis is an effective therapeutic strategy in GIST cells. ABT-737 synergistically augments the cytotoxicity of imatinib via apoptosis, in imatinib-sensitive GIST cells, suggesting that resistance may be preempted. Further, ABT-737 was equally efficacious against imatinib-resistant GIST cells, implying that addition of a pro-apoptotic agent may be a suitable approach to overcome established resistance. Most importantly, synergy between ABT-737 and imatinib provide rationale for clinical investigation of therapeutic combinations with independent, but complementary,

mechanisms in GIST. Multi-target studies of rational design are necessary to develop curative therapies for patients with imatinib-resistant GIST.

Chapter 4: Conclusion and Future Directions

Introduction

Most gastrointestinal soft-tissue sarcomas are GISTs. As with all cancers, GIST cells multiply uncontrollably due to mutations in genes that regulate survival, growth, and proliferation. *KIT* and *PDGFRA* mutations are required for initiation and maintenance of the malignant phenotype in GIST. Thus, they belong to a group of oncogene-addicted cancers that are absolutely dependent on specific oncogenes for survival. Until recently, most patients with advanced GIST died within two years of diagnosis due to the unrelenting growth and spread of their disease. Survival was extended by 6-9 months if reduction of tumor burden was surgically feasible, but chemo- and radiotherapy were ineffective. Over the last decade, targeted therapy with imatinib, through inhibition of KIT/ PDGFR- α , has more than doubled the life expectancy of patients.

Unlike conventional cytotoxic chemotherapies, which kill cancerous and normal cells alike, imatinib specifically inhibits the viability of GIST cells while sparing most normal cells. This is an example of the selectivity that makes targeted therapies attractive, and has contributed to their establishment as first-line treatments for oncogene-addicted cancers, including GIST and CML, as well as some lung, breast, and colon cancers. However, while imatinib in particular, and targeted therapies in general, achieve substantial disease-control by halting or reversing tumor growth, their efficacy is transient and rarely translates to cure. In GIST and CML, imatinib-resistance and disease progression afflict most patients eventually, and our pharmacologic repertoire is outpaced by the diversity of resistance mechanisms in progressing tumors. At the cellular and molecular level, evidence abounds that targeted therapies do not induce tumor cell death

exclusively, but cause a mixture of cytostatic and cytotoxic effects, which beget resistance in conjunction with secondary mutations.

Although apoptosis is an important cytotoxic effect of imatinib, the specific molecular effectors that bring about GIST cell death were only recently characterized, when the pro-apoptotic Bcl-2 protein BIM was identified as a mediator of apoptosis. However, this evidence was derived from a single study of cultured GIST cells with a genotype rarely seen in patients (*KIT* exon 13 mutant GIST882 cells), requiring confirmation. These studies examined the role of BIM, and its anti-apoptotic Bcl-2 counterparts, in the mechanism of apoptosis in GIST cells with clinically-relevant genotypes and tumors from patients, and evaluated their potential as biomarkers and/or therapeutic targets.

Summary of findings

The first set of studies (Chapter 2) examined the expression, regulation, and function of BIM in GIST cells with clinically-relevant genotypes. This is not trivial, given that genotype-specific distinctions are common among GIST [70], and effects in *KIT* exon 13 mutant GIST do not always extend to tumors harboring exon 11 mutations. These studies demonstrate that BIM-mediated, imatinib-induced apoptosis is common to GIST cells harboring *KIT* exon 11 mutations. In imatinib-sensitive GIST-T1 and imatinib-resistant GIST48IM cells, inhibition of KIT and PI3K signaling upregulates three functional isoforms of BIM at the mRNA and protein levels, in parallel with activation of apoptosis. In contrast to GIST882 cells, inhibition of MEK1/2 failed to upregulate BIM in GIST-T1 or GIST48IM, suggesting that this pathway does not

universally mediate BIM suppression in GIST. Importantly, high levels of basal BIM expression in GIST48IM cells were observed, consistent with the finding that these cells fail undergo apoptosis to the same extent as GIST-T1 cells when transfected with BIM. This suggests that, in addition to secondary *KIT* mutations, imatinib-resistant GIST may avert apoptosis by neutralizing BIM, or possibly possess additional mechanisms that inhibit caspases after BIM-mediated activation of BAX/BAK. This is consistent with the findings of Hoang and colleagues, who reported that the caspase inhibitor survivin, a member of the inhibitor of apoptosis (IAP) family, is overexpressed in GIST and correlates with potential for invasion and metastasis [158].

The patient-based studies (Chapter 2) examined whether the function of BIM extended to patients with GIST. I assessed pre- and post-treatment specimens from 28 patients treated for 3-7 days, based on the expectation that mRNA alterations induced by imatinib, if any, would be evident at early timepoints. These studies revealed that in patient tumors imatinib causes time-dependent BIM and Mcl-1 upregulation, and downregulation of Bcl-2, in parallel with activation of apoptosis. Among gene expression alterations, only upregulation of BIM correlated significantly with tumor apoptosis, although basal (pre-treatment) expression of Bcl-xL was significantly associated with post-treatment apoptosis. Given the role of BIM at the cellular level, I examined its relation with response at the whole-tumor level, and found greater upregulation of BIM in PET responders than in non-responders. Moreover, Bcl-xL upregulation was significantly associated with imatinib-resistance by PET, a finding which may explain early resistance (and immediate-progression) in some patients. Further, BIM upregulation is associated with prolonged disease-free survival in patients treated with adjuvant imatinib,

suggesting that BIM expression may have a role in suppressing GIST cells (micrometastases) lingering after surgery. In other words, the longer time to recurrence observed in patients with high post-imatinib BIM may translate to inhibition of residual GIST through activation of apoptosis.

Taken together, these studies demonstrate that the cytotoxic intracellular stresses initiated by imatinib converge upon the BIM/Bcl-2 axis, and suggested that inhibition of Bcl-2 proteins directly may be a rational approach to overcome imatinib-resistance. In the studies described in Chapter 3, the novel BH3-mimetic, ABT-737, causes significant growth-inhibition in patient-derived GIST cells, regardless of imatinib-sensitivity/resistance, and combines synergistically with imatinib to induce apoptosis. Importantly, its stereoisomer A793844, which exhibits lower affinity for Bcl-2 proteins, has no anti-tumor effects on GIST cells, suggesting that the effects of ABT-737 are target-specific. These pre-clinical studies demonstrate that combined treatment with ABT-737 and imatinib may overcome established imatinib resistance in GIST by synergistic activation of apoptotic cell death.

The guiding principle of these investigations was to acquire knowledge that contributes in a practical way to the management of patients with GIST. In the following sections, I consider the translational relevance of these findings, and discuss ways in which BIM and the Bcl-2 family may be exploited for predictive, prognostic, and therapeutic purposes. In particular, I focus the discussion on two current clinical hurdles. First, an important challenge is the inability to predict whether, or how long, individual patients will respond to imatinib. Second, patients with GIST are generally not cured with

imatinib, but rational combinations of targeted therapies have the potential for complete eradication of GIST.

Can we predict who will respond to therapy and act accordingly?

As BIM and the Bcl-2 family of proteins appear to be regulators of imatinib-induced apoptosis in GIST, one may speculate that profiling their expression in patient tumors may enable oncologists to forecast important clinical outcomes, including response or resistance to imatinib, or the extent of benefit (cure versus transient response). That is, I theorize that BIM and the Bcl-2 family may have predictive or prognostic value.

The terms ‘predictive’ and ‘prognostic’ have different meanings, but are often used interchangeably to refer to molecular biomarkers with clinical associations. A predictive biomarker offers information about response to a therapy, whereas a prognostic biomarker offers information about the natural history of a disease irrespective of treatment. To illustrate, KIT expression was the first true biomarker with diagnostic and prognostic relevance in GIST, enabling accurate diagnosis and characterization of the clinical behavior of these sarcomas, and later facilitating imatinib therapy. *KIT/PDGFRA* genotype, on the other hand, is a predictive biomarker, as patients with GIST harboring *KIT* exon 11 mutations exhibit higher imatinib-response rates and longer time to progression than wild-type tumors, or tumors harboring *KIT* exon 9 or *PDGFRA* mutations [11]. Moreover, patients with *KIT* exon 9 mutations benefit from dose-escalation to imatinib 800 mg daily, whereas patients with other genotypes do not [159].

Other than KIT expression or *KIT/PDGFRA* genotype, few biomarkers have been

characterized in the imatinib-era, and none affect clinical decision-making to the same extent. In this context, evidence that BIM is upregulated by imatinib (and correlates with tumor apoptosis, PET response, and time to progression) evokes intriguing possibilities. As patients with metastatic GIST are routinely treated with imatinib until progression ensues, and resection of metastases is increasingly used to decrease tumor burden, a wealth of clinically-informative data could be obtained from metastases profiled after resection. Knowledge of a patient's BIM/Bcl-2 expression profile might then be used to guide patients toward alternative targeted therapies or enrollment in clinical trials. For example, a patient whose GIST does not upregulate BIM may expect minimal benefit from further imatinib, warranting consideration of alternative therapy prior to overt progression. This would not only enable treatment of viable residual GIST cells earlier, but would spare the patient the adverse effects of an ineffective drug. On the other hand, a patient whose tumor responds by upregulation of BIM may be continued on imatinib after resection of metastases, with the expectation that residual disease will respond similarly to their resected lesions.

It is important to note one important limitation to molecular profiling in GIST. In particular, unlike patients with liquid tumors such as CML, tissue required for profiling solid tumors is often inaccessible to the oncologist. Requiring patients to undergo biopsy or surgical resection in order to obtain information about current or future response to therapy seems unethical and inappropriate, as the risks associated with invasive procedures may not be outweighed by the benefit of having predictive information. Nevertheless, advances in imaging technology may one day make it possible to label specific tumor biomarkers, and visualize their expression non-invasively. For instance,

Kumar and colleagues used a (64)Cu-radiolabeled peptide specific for Thomsen-Friedenreich (TF) antigen, a disaccharide expressed by human breast cancer cells, for PET imaging of breast cancer xenografts in mice. Biodistribution studies found that the radiolabeled peptide accumulated in breast cancer xenografts, but not in other organs, while *in vivo* imaging studies demonstrated tumor uptake of the antigen-specific peptide, but not of a scrambled radiolabeled peptide [160]. These findings suggest that noninvasive *in vivo* tumor imaging may be possible if specific antigens are developed. By extension, a future application of this technology may involve labeling of BIM to assess response to targeted therapies in GIST or other oncogene-addicted cancers.

In the setting of primary localized GIST, the translational implications are closer to reality, given that the standard of care for these patients already involves complete surgery, with or without adjuvant/neoadjuvant imatinib [161]. Most specialized sarcoma centers currently employ a multidisciplinary approach to manage patients with GIST, and as part of this approach many patients are treated with imatinib pre-operatively to reduce the size of their tumors or facilitate surgery [40, 162]. During this pre-operative therapy, patients are monitored via imaging (CT or MRI), and treated until ‘maximal tumor response’ is reached (or progression occurs), at which time the tumor is resected. The exact duration of therapy is not known ahead of time, but generally requires 3-12 months. Profiling tumors for imatinib-induced changes to assess response early in therapy may determine whether surgery needs to be expedited or delayed, and may help to decrease the uncertainty in management of these patients. Moreover, as responses at the time of recurrence are variable and unpredictable, a trial of neoadjuvant imatinib implemented to facilitate surgery might also yield information about subsequent response to imatinib.

Knowledge of individual tumor's BIM/Bcl-2 profiles would permit early allocation to effective therapies if, or when, recurrence occurs. For instance, tumors which fail to upregulate BIM in response to imatinib during the neoadjuvant trial may be expected to progress on imatinib upon recurrence, allowing these patients to be guided toward alternative therapies at the time of recurrence.

Can rational combinations of targeted agents cure advanced GIST?

A better understanding of the mechanism by which imatinib kills GIST cells has the potential to enable the development of more effective therapies. Many oncologists believe that the efficacy of imatinib monotherapy has already peaked (is “maxed out”), while others believe that there is room for significant improvement by optimizing dosage according to patient and tumor variables, including imatinib plasma levels [163-165], *KIT/PDGFR* genotype [166], or presence of CYP450 liver enzymes involved in imatinib metabolism [167].

Regardless of whether the efficacy of imatinib can be extended to previously-unresponsive GIST, the likelihood of cure with monotherapy is extremely low, whereas the odds of disease progression are high, a fact that motivated the study of combined KIT and Bcl-2 inhibition in GIST cells. Importantly, the high degree of synergy observed between imatinib and ABT-737 suggests that combining agents with complementary, but independent, mechanisms of action may enable permanent cures in GIST. Furthermore, in a collaborative publication, we have found that imatinib synergizes with drugs that inhibit autophagy, chloroquine and quinacrine, to effect apoptosis in GIST. These studies

provide rationale for studying the safety and efficacy of multi-target combinations in patients.

In spite of this evidence, single-agent studies of TKIs continue to predominate among clinical trials, and no trial has yet compared single-agent imatinib against a rational combination of targeted agents. Some of this may be due to pharmaceutical companies' unwillingness to compare their proprietary product(s) with others, but there is also the concern for unforeseen drug interactions and extreme adverse events. In this regard, one can look outside of cancer research to find many safe and effective combination regimens and learn from their development. For instance, current guidelines for antibiotic treatment of serious infectious conditions, including sepsis, pneumonia, meningitis, and pyelonephritis, invariably call for empiric combinations of agents in consideration of potential antimicrobial resistance [168]. Subsequently, antimicrobial susceptibility tests are routinely implemented to tailor antibiotic regimens to specific microbes. While cancer and infectious diseases are not exactly analogous, one can argue that equipoise exists to test rational combinations of targeted agents in cancer. In other words, the potential benefit of curing cancer with personalized combinations outweighs the risk of unforeseen drug interactions.

Outside of science, the challenge will be to sort and enroll patients in appropriate studies, to find the right drug for the right patient. Moreover, it will be necessary to modify or overcome the regulatory hurdles in the current drug-development process. In spite of these real obstacles, we currently stand at a turning point in cancer research, where advances in synthetic chemistry are intersecting advances in molecular biology, and the potential for cures seems possible. In this regard, clinical research in GIST has

the potential to break new ground for other cancers, by providing proof of principle for the efficacy and safety of multi-target combinations. In conclusion, over the last decade, GIST has been the subject of intense investigation out of proportion to its incidence. In spite of its rarity, however, the discoveries derived from GIST have contributed to many aspects of oncology, and their importance will continue to extend beyond the management GIST, to other soft-tissue sarcomas and cancer in general.

Bibliography

1. Cassier, P.A., A. Dufresne, S. Arifi, H. El Sayadi, I. Labidi, I. Ray-Coquard, S. Tabone, P. Meeus, D. Ranchere, M.P. Sunyach, A.V. Decouvlaere, L. Alberti, and J.Y. Blay, *Imatinib mesilate for the treatment of gastrointestinal stromal tumour*. *Expert Opin Pharmacother*, 2008. **9**(7): p. 1211-22.
2. Trent, J.C., A.J. Lazar, and W. Zhang, *Molecular approaches to resolve diagnostic dilemmas: the case of gastrointestinal stromal tumor and leiomyosarcoma*. *Future Oncol*, 2007. **3**(6): p. 629-37.
3. Mazur, M.T. and H.B. Clark, *Gastric stromal tumors. Reappraisal of histogenesis*. *Am J Surg Pathol*, 1983. **7**(6): p. 507-19.
4. Dematteo, R.P., M.C. Heinrich, W.M. El-Rifai, and G. Demetri, *Clinical management of gastrointestinal stromal tumors: before and after STI-571*. *Hum Pathol*, 2002. **33**(5): p. 466-77.
5. DeMatteo, R.P., J.J. Lewis, D. Leung, S.S. Mudan, J.M. Woodruff, and M.F. Brennan, *Two hundred gastrointestinal stromal tumors: recurrence patterns and prognostic factors for survival*. *Ann Surg*, 2000. **231**(1): p. 51-8.
6. Kindblom, L.G., H.E. Remotti, F. Aldenborg, and J.M. Meis-Kindblom, *Gastrointestinal pacemaker cell tumor (GIPACT): gastrointestinal stromal tumors show phenotypic characteristics of the interstitial cells of Cajal*. *Am J Pathol*, 1998. **152**(5): p. 1259-69.
7. Besmer, P., J.E. Murphy, P.C. George, F.H. Qiu, P.J. Bergold, L. Lederman, H.W. Snyder, Jr., D. Brodeur, E.E. Zuckerman, and W.D. Hardy, *A new acute*

- transforming feline retrovirus and relationship of its oncogene v-kit with the protein kinase gene family*. Nature, 1986. **320**(6061): p. 415-21.
8. Hirota, S., K. Isozaki, Y. Moriyama, K. Hashimoto, T. Nishida, S. Ishiguro, K. Kawano, M. Hanada, A. Kurata, M. Takeda, G. Muhammad Tunio, Y. Matsuzawa, Y. Kanakura, Y. Shinomura, and Y. Kitamura, *Gain-of-function mutations of c-kit in human gastrointestinal stromal tumors*. Science, 1998. **279**(5350): p. 577-80.
 9. Heinrich, M.C., C.L. Corless, A. Duensing, L. McGreevey, C.J. Chen, N. Joseph, S. Singer, D.J. Griffith, A. Haley, A. Town, G.D. Demetri, C.D. Fletcher, and J.A. Fletcher, *PDGFRA activating mutations in gastrointestinal stromal tumors*. Science, 2003. **299**(5607): p. 708-10.
 10. Corless, C.L., J.A. Fletcher, and M.C. Heinrich, *Biology of gastrointestinal stromal tumors*. J Clin Oncol, 2004. **22**(18): p. 3813-25.
 11. Heinrich, M.C., C.L. Corless, G.D. Demetri, C.D. Blanke, M. von Mehren, H. Joensuu, L.S. McGreevey, C.J. Chen, A.D. Van den Abbeele, B.J. Druker, B. Kiese, B. Eisenberg, P.J. Roberts, S. Singer, C.D. Fletcher, S. Silberman, S. Dimitrijevic, and J.A. Fletcher, *Kinase mutations and imatinib response in patients with metastatic gastrointestinal stromal tumor*. J Clin Oncol, 2003. **21**(23): p. 4342-9.
 12. Ullrich, A. and J. Schlessinger, *Signal transduction by receptors with tyrosine kinase activity*. Cell, 1990. **61**(2): p. 203-12.
 13. Heldin, C.H., *Dimerization of cell surface receptors in signal transduction*. Cell, 1995. **80**(2): p. 213-23.

14. Hubbard, S.R., M. Mohammadi, and J. Schlessinger, *Autoregulatory mechanisms in protein-tyrosine kinases*. J Biol Chem, 1998. **273**(20): p. 11987-90.
15. Roskoski, R., Jr., *Signaling by Kit protein-tyrosine kinase--the stem cell factor receptor*. Biochem Biophys Res Commun, 2005. **337**(1): p. 1-13.
16. Edling, C.E. and B. Hallberg, *c-Kit--a hematopoietic cell essential receptor tyrosine kinase*. Int J Biochem Cell Biol, 2007. **39**(11): p. 1995-8.
17. Huizinga, J.D., L. Thuneberg, M. Kluppel, J. Malysz, H.B. Mikkelsen, and A. Bernstein, *W/kit gene required for interstitial cells of Cajal and for intestinal pacemaker activity*. Nature, 1995. **373**(6512): p. 347-9.
18. Mol, C.D., D.R. Dougan, T.R. Schneider, R.J. Skene, M.L. Kraus, D.N. Scheibe, G.P. Snell, H. Zou, B.C. Sang, and K.P. Wilson, *Structural basis for the autoinhibition and STI-571 inhibition of c-Kit tyrosine kinase*. J Biol Chem, 2004. **279**(30): p. 31655-63.
19. Kozlowski, M., L. Larose, F. Lee, D.M. Le, R. Rottapel, and K.A. Siminovitch, *SHP-1 binds and negatively modulates the c-Kit receptor by interaction with tyrosine 569 in the c-Kit juxtamembrane domain*. Mol Cell Biol, 1998. **18**(4): p. 2089-99.
20. Babina, M., C. Rex, S. Guhl, F. Thienemann, M. Artuc, B.M. Henz, and T. Zuberbier, *Baseline and stimulated turnover of cell surface c-Kit expression in different types of human mast cells*. Exp Dermatol, 2006. **15**(7): p. 530-7.
21. Corless, C.L., L. McGreevey, A. Haley, A. Town, and M.C. Heinrich, *KIT mutations are common in incidental gastrointestinal stromal tumors one centimeter or less in size*. Am J Pathol, 2002. **160**(5): p. 1567-72.

22. Antonescu, C.R., *Gastrointestinal stromal tumor (GIST) pathogenesis, familial GIST, and animal models*. Semin Diagn Pathol, 2006. **23**(2): p. 63-9.
23. Lux, M.L., B.P. Rubin, T.L. Biase, C.J. Chen, T. Maclure, G. Demetri, S. Xiao, S. Singer, C.D. Fletcher, and J.A. Fletcher, *KIT extracellular and kinase domain mutations in gastrointestinal stromal tumors*. Am J Pathol, 2000. **156**(3): p. 791-5.
24. McAuliffe, J.C., W.L. Wang, G.M. Pavan, S. Pricl, D. Yang, S.S. Chen, A.J. Lazar, R.E. Pollock, and J.C. Trent, *Unlucky number 13? Differential effects of KIT exon 13 mutation in gastrointestinal stromal tumors*. Mol Oncol, 2008. **2**(2): p. 161-3.
25. Nishida, T., T. Kanda, A. Nishitani, T. Takahashi, K. Nakajima, T. Ishikawa, and S. Hirota, *Secondary mutations in the kinase domain of the KIT gene are predominant in imatinib-resistant gastrointestinal stromal tumor*. Cancer Sci, 2008. **99**(4): p. 799-804.
26. Wang, W.L., A. Conley, D. Reynoso, L. Nolden, A.J. Lazar, S. George, and J.C. Trent, *Mechanisms of resistance to imatinib and sunitinib in gastrointestinal stromal tumor*. Cancer Chemother Pharmacol. **67 Suppl 1**: p. S15-24.
27. Chen, L.L., J.C. Trent, E.F. Wu, G.N. Fuller, L. Ramdas, W. Zhang, A.K. Raymond, V.G. Prieto, C.O. Oyedeji, K.K. Hunt, R.E. Pollock, B.W. Feig, K.J. Hayes, H. Choi, H.A. Macapinlac, W. Hittelman, M.A. Velasco, S. Patel, M.A. Burgess, R.S. Benjamin, and M.L. Frazier, *A missense mutation in KIT kinase domain 1 correlates with imatinib resistance in gastrointestinal stromal tumors*. Cancer Res, 2004. **64**(17): p. 5913-9.

28. Ylipaa, A., K.K. Hunt, J. Yang, A.J. Lazar, K.E. Torres, D.C. Lev, M. Nykter, R.E. Pollock, J. Trent, and W. Zhang, *Integrative genomic characterization and a genomic staging system for gastrointestinal stromal tumors*. *Cancer*. **117**(2): p. 380-9.
29. Breiner, J.A., J. Meis-Kindblom, L.G. Kindblom, E. McComb, J. Liu, M. Nelson, and J.A. Bridge, *Loss of 14q and 22q in gastrointestinal stromal tumors (pacemaker cell tumors)*. *Cancer Genet Cytogenet*, 2000. **120**(2): p. 111-6.
30. Yang, J., X. Du, A.J. Lazar, R. Pollock, K. Hunt, K. Chen, X. Hao, J. Trent, and W. Zhang, *Genetic aberrations of gastrointestinal stromal tumors*. *Cancer*, 2008. **113**(7): p. 1532-43.
31. Sabah, M., R. Cummins, M. Leader, and E. Kay, *Altered expression of cell cycle regulatory proteins in gastrointestinal stromal tumors: markers with potential prognostic implications*. *Hum Pathol*, 2006. **37**(6): p. 648-55.
32. Chen, Y., C.C. Tzeng, C.P. Liou, M.Y. Chang, C.F. Li, and C.N. Lin, *Biological significance of chromosomal imbalance aberrations in gastrointestinal stromal tumors*. *J Biomed Sci*, 2004. **11**(1): p. 65-71.
33. Druker, B.J., M. Talpaz, D.J. Resta, B. Peng, E. Buchdunger, J.M. Ford, N.B. Lydon, H. Kantarjian, R. Capdeville, S. Ohno-Jones, and C.L. Sawyers, *Efficacy and safety of a specific inhibitor of the BCR-ABL tyrosine kinase in chronic myeloid leukemia*. *N Engl J Med*, 2001. **344**(14): p. 1031-7.
34. Joensuu, H., P.J. Roberts, M. Sarlomo-Rikala, L.C. Andersson, P. Tervahartiala, D. Tuveson, S. Silberman, R. Capdeville, S. Dimitrijevic, B. Druker, and G.D. Demetri, *Effect of the tyrosine kinase inhibitor STI571 in a patient with a*

- metastatic gastrointestinal stromal tumor*. N Engl J Med, 2001. **344**(14): p. 1052-6.
35. van Oosterom, A.T., I. Judson, J. Verweij, S. Stroobants, E. Donato di Paola, S. Dimitrijevic, M. Martens, A. Webb, R. Sciot, M. Van Glabbeke, S. Silberman, and O.S. Nielsen, *Safety and efficacy of imatinib (STI571) in metastatic gastrointestinal stromal tumours: a phase I study*. Lancet, 2001. **358**(9291): p. 1421-3.
36. Demetri, G.D., M. von Mehren, C.D. Blanke, A.D. Van den Abbeele, B. Eisenberg, P.J. Roberts, M.C. Heinrich, D.A. Tuveson, S. Singer, M. Janicek, J.A. Fletcher, S.G. Silverman, S.L. Silberman, R. Capdeville, B. Kiese, B. Peng, S. Dimitrijevic, B.J. Druker, C. Corless, C.D. Fletcher, and H. Joensuu, *Efficacy and safety of imatinib mesylate in advanced gastrointestinal stromal tumors*. N Engl J Med, 2002. **347**(7): p. 472-80.
37. Verweij, J., P.G. Casali, J. Zalcberg, A. LeCesne, P. Reichardt, J.Y. Blay, R. Issels, A. van Oosterom, P.C. Hogendoorn, M. Van Glabbeke, R. Bertulli, and I. Judson, *Progression-free survival in gastrointestinal stromal tumours with high-dose imatinib: randomised trial*. Lancet, 2004. **364**(9440): p. 1127-34.
38. Blanke, C.D., G.D. Demetri, M. von Mehren, M.C. Heinrich, B. Eisenberg, J.A. Fletcher, C.L. Corless, C.D. Fletcher, P.J. Roberts, D. Heinz, E. Wehre, Z. Nikolova, and H. Joensuu, *Long-term results from a randomized phase II trial of standard- versus higher-dose imatinib mesylate for patients with unresectable or metastatic gastrointestinal stromal tumors expressing KIT*. J Clin Oncol, 2008. **26**(4): p. 620-5.

39. Dematteo, R.P., K.V. Ballman, C.R. Antonescu, R.G. Maki, P.W. Pisters, G.D. Demetri, M.E. Blackstein, C.D. Blanke, M. von Mehren, M.F. Brennan, S. Patel, M.D. McCarter, J.A. Polikoff, B.R. Tan, and K. Owzar, *Adjuvant imatinib mesylate after resection of localised, primary gastrointestinal stromal tumour: a randomised, double-blind, placebo-controlled trial*. *Lancet*, 2009. **373**(9669): p. 1097-104.
40. Reynoso, D., V. Subbiah, J.C. Trent, B.A. Guadagnolo, A.J. Lazar, R. Benjamin, R.E. Pollock, and J.A. Ludwig, *Neoadjuvant treatment of soft-tissue sarcoma: a multimodality approach*. *J Surg Oncol*. **101**(4): p. 327-33.
41. Liegl, B., I. Kepten, C. Le, M. Zhu, G.D. Demetri, M.C. Heinrich, C.D. Fletcher, C.L. Corless, and J.A. Fletcher, *Heterogeneity of kinase inhibitor resistance mechanisms in GIST*. *J Pathol*, 2008. **216**(1): p. 64-74.
42. Mahadevan, D., L. Cooke, C. Riley, R. Swart, B. Simons, K. Della Croce, L. Wisner, M. Iorio, K. Shakalya, H. Garewal, R. Nagle, and D. Bearss, *A novel tyrosine kinase switch is a mechanism of imatinib resistance in gastrointestinal stromal tumors*. *Oncogene*, 2007. **26**(27): p. 3909-19.
43. Thao le, B., H.A. Vu, K. Yasuda, S. Taniguchi, F. Yagasaki, T. Taguchi, T. Watanabe, and Y. Sato, *Cas-L was overexpressed in imatinib-resistant gastrointestinal stromal tumor cells*. *Cancer Biol Ther*, 2009. **8**(8): p. 683-8.
44. Liegl, B., J.L. Hornick, C.R. Antonescu, C.L. Corless, and C.D. Fletcher, *Rhabdomyosarcomatous differentiation in gastrointestinal stromal tumors after tyrosine kinase inhibitor therapy: a novel form of tumor progression*. *Am J Surg Pathol*, 2009. **33**(2): p. 218-26.

45. de Lavallade, H., J.F. Apperley, J.S. Khorashad, D. Milojkovic, A.G. Reid, M. Bua, R. Szydlo, E. Olavarria, J. Kaeda, J.M. Goldman, and D. Marin, *Imatinib for newly diagnosed patients with chronic myeloid leukemia: incidence of sustained responses in an intention-to-treat analysis*. J Clin Oncol, 2008. **26**(20): p. 3358-63.
46. Bixby, D. and M. Talpaz, *Mechanisms of resistance to tyrosine kinase inhibitors in chronic myeloid leukemia and recent therapeutic strategies to overcome resistance*. Hematology Am Soc Hematol Educ Program, 2009: p. 461-76.
47. Pao, W., V.A. Miller, K.A. Politi, G.J. Riely, R. Somwar, M.F. Zakowski, M.G. Kris, and H. Varmus, *Acquired resistance of lung adenocarcinomas to gefitinib or erlotinib is associated with a second mutation in the EGFR kinase domain*. PLoS Med, 2005. **2**(3): p. e73.
48. Mahon, F.X., M.W. Deininger, B. Schultheis, J. Chabrol, J. Reiffers, J.M. Goldman, and J.V. Melo, *Selection and characterization of BCR-ABL positive cell lines with differential sensitivity to the tyrosine kinase inhibitor STI571: diverse mechanisms of resistance*. Blood, 2000. **96**(3): p. 1070-9.
49. Wang, L., A. Giannoudis, S. Lane, P. Williamson, M. Pirmohamed, and R.E. Clark, *Expression of the uptake drug transporter hOCT1 is an important clinical determinant of the response to imatinib in chronic myeloid leukemia*. Clin Pharmacol Ther, 2008. **83**(2): p. 258-64.
50. Liu, Y., S.A. Perdreau, P. Chatterjee, L. Wang, S.F. Kuan, and A. Duensing, *Imatinib mesylate induces quiescence in gastrointestinal stromal tumor cells*

- through the CDH1-SKP2-p27Kip1 signaling axis. Cancer Res, 2008. 68(21): p. 9015-23.*
51. Gupta, A., S. Roy, A.J. Lazar, W.L. Wang, J.C. McAuliffe, D. Reynoso, J. McMahon, T. Taguchi, G. Floris, M. Debiec-Rychter, P. Schoffski, J.A. Trent, J. Debnath, and B.P. Rubin, *Autophagy inhibition and antimalarials promote cell death in gastrointestinal stromal tumor (GIST)*. Proc Natl Acad Sci U S A. **107**(32): p. 14333-8.
52. Le Cesne, A., I. Ray-Coquard, B.N. Bui, A. Adenis, M. Rios, F. Bertucci, F. Duffaud, C. Chevreau, D. Cupissol, A. Cioffi, J.F. Emile, S. Chabaud, D. Perol, and J.Y. Blay, *Discontinuation of imatinib in patients with advanced gastrointestinal stromal tumours after 3 years of treatment: an open-label multicentre randomised phase 3 trial*. Lancet Oncol. **11**(10): p. 942-9.
53. Kelley, R.K. and A.P. Venook, *Nonadherence to imatinib during an economic downturn*. N Engl J Med. **363**(6): p. 596-8.
54. Demetri, G.D., A.T. van Oosterom, C.R. Garrett, M.E. Blackstein, M.H. Shah, J. Verweij, G. McArthur, I.R. Judson, M.C. Heinrich, J.A. Morgan, J. Desai, C.D. Fletcher, S. George, C.L. Bello, X. Huang, C.M. Baum, and P.G. Casali, *Efficacy and safety of sunitinib in patients with advanced gastrointestinal stromal tumour after failure of imatinib: a randomised controlled trial*. Lancet, 2006. **368**(9544): p. 1329-38.
55. Goodman, V.L., E.P. Rock, R. Dagher, R.P. Ramchandani, S. Abraham, J.V. Gobburu, B.P. Booth, S.L. Verbois, D.E. Morse, C.Y. Liang, N. Chidambaram, J.X. Jiang, S. Tang, K. Mahjoob, R. Justice, and R. Pazdur, *Approval summary:*

- sunitinib for the treatment of imatinib refractory or intolerant gastrointestinal stromal tumors and advanced renal cell carcinoma. Clin Cancer Res, 2007. 13(5): p. 1367-73.*
56. Hanahan, D. and R.A. Weinberg, *The hallmarks of cancer. Cell, 2000. 100(1): p. 57-70.*
57. Wyllie, A.H., "Where, O death, is thy sting?" *A brief review of apoptosis biology. Mol Neurobiol. 42(1): p. 4-9.*
58. Kim, R., M. Emi, and K. Tanabe, *Caspase-dependent and -independent cell death pathways after DNA damage (Review). Oncol Rep, 2005. 14(3): p. 595-9.*
59. Tuveson, D.A., N.A. Willis, T. Jacks, J.D. Griffin, S. Singer, C.D. Fletcher, J.A. Fletcher, and G.D. Demetri, *STI571 inactivation of the gastrointestinal stromal tumor c-KIT oncoprotein: biological and clinical implications. Oncogene, 2001. 20(36): p. 5054-8.*
60. McAuliffe, J.C., K.K. Hunt, A.J. Lazar, H. Choi, W. Qiao, P. Thall, R.E. Pollock, R.S. Benjamin, and J.C. Trent, *A randomized, phase II study of preoperative plus postoperative imatinib in GIST: evidence of rapid radiographic response and temporal induction of tumor cell apoptosis. Ann Surg Oncol, 2009. 16(4): p. 910-9.*
61. Bauer, S., A. Duensing, G.D. Demetri, and J.A. Fletcher, *KIT oncogenic signaling mechanisms in imatinib-resistant gastrointestinal stromal tumor: PI3-kinase/AKT is a crucial survival pathway. Oncogene, 2007. 26(54): p. 7560-8.*
62. Rossi, F., I. Ehlers, V. Agosti, N.D. Socci, A. Viale, G. Sommer, Y. Yozgat, K. Manova, C.R. Antonescu, and P. Besmer, *Oncogenic Kit signaling and*

- therapeutic intervention in a mouse model of gastrointestinal stromal tumor. Proc Natl Acad Sci U S A, 2006. 103(34): p. 12843-8.*
63. Miselli, F., T. Negri, A. Gronchi, M. Losa, E. Conca, S. Brich, E. Fumagalli, M. Fiore, P.G. Casali, M.A. Pierotti, E. Tamborini, and S. Pilotti, *Is autophagy rather than apoptosis the regression driver in imatinib-treated gastrointestinal stromal tumors?* Transl Oncol, 2008. **1**(4): p. 177-86.
64. Sambol, E.B., G. Ambrosini, R.C. Geha, P.T. Kennealey, P. Decarolis, R. O'Connor, Y.V. Wu, M. Motwani, J.H. Chen, G.K. Schwartz, and S. Singer, *Flavopiridol targets c-KIT transcription and induces apoptosis in gastrointestinal stromal tumor cells.* Cancer Res, 2006. **66**(11): p. 5858-66.
65. Nakatani, H., K. Araki, T. Jin, M. Kobayashi, T. Sugimoto, T. Akimori, T. Namikawa, K. Okamoto, T. Nakano, T. Okabayashi, N. Hokimoto, H. Kitagawa, and T. Taguchi, *STI571 (Glivec) induces cell death in the gastrointestinal stromal tumor cell line, GIST-T1, via endoplasmic reticulum stress response.* Int J Mol Med, 2006. **17**(5): p. 893-7.
66. Noma, K., Y. Naomoto, M. Gunduz, J. Matsuoka, T. Yamatsuji, Y. Shirakawa, T. Nobuhisa, T. Okawa, M. Takaoka, Y. Tomono, O. Hiroyuki, E. Gunduz, and N. Tanaka, *Effects of imatinib vary with the types of KIT-mutation in gastrointestinal stromal tumor cell lines.* Oncol Rep, 2005. **14**(3): p. 645-50.
67. Tarn, C., Y.V. Skorobogatko, T. Taguchi, B. Eisenberg, M. von Mehren, and A.K. Godwin, *Therapeutic effect of imatinib in gastrointestinal stromal tumors: AKT signaling dependent and independent mechanisms.* Cancer Res, 2006. **66**(10): p. 5477-86.

68. Trent, J.C., L. Ramdas, J. Dupart, K. Hunt, H. Macapinlac, E. Taylor, L. Hu, A. Salvado, J.L. Abbruzzese, R. Pollock, R.S. Benjamin, and W. Zhang, *Early effects of imatinib mesylate on the expression of insulin-like growth factor binding protein-3 and positron emission tomography in patients with gastrointestinal stromal tumor*. *Cancer*, 2006. **107**(8): p. 1898-908.
69. McAuliffe, J.C., A.J. Lazar, D. Yang, D.M. Steinert, W. Qiao, P.F. Thall, A.K. Raymond, R.S. Benjamin, and J.C. Trent, *Association of intratumoral vascular endothelial growth factor expression and clinical outcome for patients with gastrointestinal stromal tumors treated with imatinib mesylate*. *Clin Cancer Res*, 2007. **13**(22 Pt 1): p. 6727-34.
70. Duensing, A., F. Medeiros, B. McConarty, N.E. Joseph, D. Panigrahy, S. Singer, C.D. Fletcher, G.D. Demetri, and J.A. Fletcher, *Mechanisms of oncogenic KIT signal transduction in primary gastrointestinal stromal tumors (GISTs)*. *Oncogene*, 2004. **23**(22): p. 3999-4006.
71. Liu, Y., M. Tseng, S.A. Perdreau, F. Rossi, C. Antonescu, P. Besmer, J.A. Fletcher, S. Duensing, and A. Duensing, *Histone H2AX is a mediator of gastrointestinal stromal tumor cell apoptosis following treatment with imatinib mesylate*. *Cancer Res*, 2007. **67**(6): p. 2685-92.
72. Schultz, D.R. and W.J. Harrington, Jr., *Apoptosis: programmed cell death at a molecular level*. *Semin Arthritis Rheum*, 2003. **32**(6): p. 345-69.
73. Adams, J.M. and S. Cory, *Bcl-2-regulated apoptosis: mechanism and therapeutic potential*. *Curr Opin Immunol*, 2007. **19**(5): p. 488-96.

74. Green, D.R. and J.C. Reed, *Mitochondria and apoptosis*. Science, 1998. **281**(5381): p. 1309-12.
75. Vaux, D.L., S. Cory, and J.M. Adams, *Bcl-2 gene promotes haemopoietic cell survival and cooperates with c-myc to immortalize pre-B cells*. Nature, 1988. **335**(6189): p. 440-2.
76. Strasser, A., A.W. Harris, and S. Cory, *bcl-2 transgene inhibits T cell death and perturbs thymic self-censorship*. Cell, 1991. **67**(5): p. 889-99.
77. Gibson, L., S.P. Holmgreen, D.C. Huang, O. Bernard, N.G. Copeland, N.A. Jenkins, G.R. Sutherland, E. Baker, J.M. Adams, and S. Cory, *bcl-w, a novel member of the bcl-2 family, promotes cell survival*. Oncogene, 1996. **13**(4): p. 665-75.
78. Kozopas, K.M., T. Yang, H.L. Buchan, P. Zhou, and R.W. Craig, *MCL1, a gene expressed in programmed myeloid cell differentiation, has sequence similarity to BCL2*. Proc Natl Acad Sci U S A, 1993. **90**(8): p. 3516-20.
79. Oltvai, Z.N., C.L. Milliman, and S.J. Korsmeyer, *Bcl-2 heterodimerizes in vivo with a conserved homolog, Bax, that accelerates programmed cell death*. Cell, 1993. **74**(4): p. 609-19.
80. Chittenden, T., E.A. Harrington, R. O'Connor, C. Flemington, R.J. Lutz, G.I. Evan, and B.C. Guild, *Induction of apoptosis by the Bcl-2 homologue Bak*. Nature, 1995. **374**(6524): p. 733-6.
81. Willis, S.N. and J.M. Adams, *Life in the balance: how BH3-only proteins induce apoptosis*. Curr Opin Cell Biol, 2005. **17**(6): p. 617-25.

82. Scorrano, L. and S.J. Korsmeyer, *Mechanisms of cytochrome c release by proapoptotic BCL-2 family members*. Biochem Biophys Res Commun, 2003. **304**(3): p. 437-44.
83. Willis, S.N., J.I. Fletcher, T. Kaufmann, M.F. van Delft, L. Chen, P.E. Czabotar, H. Ierino, E.F. Lee, W.D. Fairlie, P. Bouillet, A. Strasser, R.M. Kluck, J.M. Adams, and D.C. Huang, *Apoptosis initiated when BH3 ligands engage multiple Bcl-2 homologs, not Bax or Bak*. Science, 2007. **315**(5813): p. 856-9.
84. Weinstein, I.B., *Cancer. Addiction to oncogenes--the Achilles heel of cancer*. Science, 2002. **297**(5578): p. 63-4.
85. Weinstein, I.B. and A. Joe, *Oncogene addiction*. Cancer Res, 2008. **68**(9): p. 3077-80; discussion 3080.
86. Arends, J.W., *Molecular interactions in the Vogelstein model of colorectal carcinoma*. J Pathol, 2000. **190**(4): p. 412-6.
87. Sollars, V.E., *Epigenetic modification as an enabling mechanism for leukemic transformation*. Front Biosci, 2005. **10**: p. 1635-46.
88. Felsher, D.W. and J.M. Bishop, *Reversible tumorigenesis by MYC in hematopoietic lineages*. Mol Cell, 1999. **4**(2): p. 199-207.
89. Huettner, C.S., P. Zhang, R.A. Van Etten, and D.G. Tenen, *Reversibility of acute B-cell leukaemia induced by BCR-ABL1*. Nat Genet, 2000. **24**(1): p. 57-60.
90. Aoki, K., T. Yoshida, N. Matsumoto, H. Ide, T. Sugimura, and M. Terada, *Suppression of Ki-ras p21 levels leading to growth inhibition of pancreatic cancer cell lines with Ki-ras mutation but not those without Ki-ras mutation*. Mol Carcinog, 1997. **20**(2): p. 251-8.

91. Druker, B.J., S. Tamura, E. Buchdunger, S. Ohno, G.M. Segal, S. Fanning, J. Zimmermann, and N.B. Lydon, *Effects of a selective inhibitor of the Abl tyrosine kinase on the growth of Bcr-Abl positive cells*. Nat Med, 1996. **2**(5): p. 561-6.
92. Gambacorti-Passerini, C., P. le Coutre, L. Mologni, M. Fanelli, C. Bertazzoli, E. Marchesi, M. Di Nicola, A. Biondi, G.M. Corneo, D. Belotti, E. Pogliani, and N.B. Lydon, *Inhibition of the ABL kinase activity blocks the proliferation of BCR/ABL+ leukemic cells and induces apoptosis*. Blood Cells Mol Dis, 1997. **23**(3): p. 380-94.
93. Chin, L., A. Tam, J. Pomerantz, M. Wong, J. Holash, N. Bardeesy, Q. Shen, R. O'Hagan, J. Pantginis, H. Zhou, J.W. Horner, 2nd, C. Cordon-Cardo, G.D. Yancopoulos, and R.A. DePinho, *Essential role for oncogenic Ras in tumour maintenance*. Nature, 1999. **400**(6743): p. 468-72.
94. O'Dwyer, M.E., M.J. Mauro, and B.J. Druker, *STI571 as a targeted therapy for CML*. Cancer Invest, 2003. **21**(3): p. 429-38.
95. Lynch, T.J., D.W. Bell, R. Sordella, S. Gurubhagavatula, R.A. Okimoto, B.W. Brannigan, P.L. Harris, S.M. Haserlat, J.G. Supko, F.G. Haluska, D.N. Louis, D.C. Christiani, J. Settleman, and D.A. Haber, *Activating mutations in the epidermal growth factor receptor underlying responsiveness of non-small-cell lung cancer to gefitinib*. N Engl J Med, 2004. **350**(21): p. 2129-39.
96. Sharma, S.V., P. Gajowniczek, I.P. Way, D.Y. Lee, J. Jiang, Y. Yuza, M. Classon, D.A. Haber, and J. Settleman, *A common signaling cascade may underlie "addiction" to the Src, BCR-ABL, and EGF receptor oncogenes*. Cancer Cell, 2006. **10**(5): p. 425-35.

97. Gillings, A.S., K. Balmanno, C.M. Wiggins, M. Johnson, and S.J. Cook, *Apoptosis and autophagy: BIM as a mediator of tumour cell death in response to oncogene-targeted therapeutics*. *Febs J*, 2009. **276**(21): p. 6050-62.
98. Cartlidge, R.A., G.R. Thomas, S. Cagnol, K.A. Jong, S.A. Molton, A.J. Finch, and M. McMahon, *Oncogenic BRAF(V600E) inhibits BIM expression to promote melanoma cell survival*. *Pigment Cell Melanoma Res*, 2008. **21**(5): p. 534-44.
99. Kuroda, J., H. Puthalakath, M.S. Cragg, P.N. Kelly, P. Bouillet, D.C. Huang, S. Kimura, O.G. Ottmann, B.J. Druker, A. Villunger, A.W. Roberts, and A. Strasser, *Bim and Bad mediate imatinib-induced killing of Bcr/Abl+ leukemic cells, and resistance due to their loss is overcome by a BH3 mimetic*. *Proc Natl Acad Sci U S A*, 2006. **103**(40): p. 14907-12.
100. Belloc, F., F. Moreau-Gaudry, M. Uhalde, L. Cazalis, M. Jeanneteau, F. Lacombe, V. Praloran, and F.X. Mahon, *Imatinib and nilotinib induce apoptosis of chronic myeloid leukemia cells through a Bim-dependant pathway modulated by cytokines*. *Cancer Biol Ther*, 2007. **6**(6): p. 912-9.
101. Kuribara, R., H. Honda, H. Matsui, T. Shinjyo, T. Inukai, K. Sugita, S. Nakazawa, H. Hirai, K. Ozawa, and T. Inaba, *Roles of Bim in apoptosis of normal and Bcr-Abl-expressing hematopoietic progenitors*. *Mol Cell Biol*, 2004. **24**(14): p. 6172-83.
102. Aichberger, K.J., K.V. Gleixner, I. Mirkina, S. Cerny-Reiterer, B. Peter, V. Ferenc, M. Kneidinger, C. Baumgartner, M. Mayerhofer, A. Gruze, W.F. Pickl, C. Sillaber, and P. Valent, *Identification of proapoptotic Bim as a tumor suppressor*

- in neoplastic mast cells: role of KIT D816V and effects of various targeted drugs.* Blood, 2009. **114**(26): p. 5342-51.
103. Sheridan, C., G. Brumatti, and S.J. Martin, *Oncogenic B-RafV600E inhibits apoptosis and promotes ERK-dependent inactivation of Bad and Bim.* J Biol Chem, 2008. **283**(32): p. 22128-35.
104. Costa, D.B., B. Halmos, A. Kumar, S.T. Schumer, M.S. Huberman, T.J. Boggon, D.G. Tenen, and S. Kobayashi, *BIM mediates EGFR tyrosine kinase inhibitor-induced apoptosis in lung cancers with oncogenic EGFR mutations.* PLoS Med, 2007. **4**(10): p. 1669-79; discussion 1680.
105. Gordon, P.M. and D.E. Fisher, *Role for the proapoptotic factor BIM in mediating imatinib-induced apoptosis in a c-KIT-dependent gastrointestinal stromal tumor cell line.* J Biol Chem. **285**(19): p. 14109-14.
106. Dupart, J.J., J.C. Trent, H.Y. Lee, K.R. Hess, A.K. Godwin, T. Taguchi, and W. Zhang, *Insulin-like growth factor binding protein-3 has dual effects on gastrointestinal stromal tumor cell viability and sensitivity to the anti-tumor effects of imatinib mesylate in vitro.* Mol Cancer, 2009. **8**: p. 99.
107. U, M., T. Miyashita, Y. Shikama, K. Tadokoro, and M. Yamada, *Molecular cloning and characterization of six novel isoforms of human Bim, a member of the proapoptotic Bcl-2 family.* FEBS Lett, 2001. **509**(1): p. 135-41.
108. Taguchi, T., H. Sonobe, S. Toyonaga, I. Yamasaki, T. Shuin, A. Takano, K. Araki, K. Akimaru, and K. Yuri, *Conventional and molecular cytogenetic characterization of a new human cell line, GIST-T1, established from gastrointestinal stromal tumor.* Lab Invest, 2002. **82**(5): p. 663-5.

109. Bauer, S., L.K. Yu, G.D. Demetri, and J.A. Fletcher, *Heat shock protein 90 inhibition in imatinib-resistant gastrointestinal stromal tumor*. *Cancer Res*, 2006. **66**(18): p. 9153-61.
110. Rossi, S., W. Ou, D. Tang, N. Bhattacharya, A.P. Dei Tos, J.A. Fletcher, and M. Loda, *Gastrointestinal stromal tumours overexpress fatty acid synthase*. *J Pathol*, 2006. **209**(3): p. 369-75.
111. Rikhof, B., W.T. van der Graaf, C. Meijer, P.T. Le, G.J. Meersma, S. de Jong, J.A. Fletcher, and A.J. Suurmeijer, *Abundant Fas expression by gastrointestinal stromal tumours may serve as a therapeutic target for MegaFasL*. *Br J Cancer*, 2008. **99**(10): p. 1600-6.
112. Livak, K.J. and T.D. Schmittgen, *Analysis of relative gene expression data using real-time quantitative PCR and the 2(-Delta Delta C(T)) Method*. *Methods*, 2001. **25**(4): p. 402-8.
113. Riccardi, C. and I. Nicoletti, *Analysis of apoptosis by propidium iodide staining and flow cytometry*. *Nat Protoc*, 2006. **1**(3): p. 1458-61.
114. Reynoso, D., L.K. Nolden, D. Yang, S.N. Dumont, A.P. Conley, A.G. Dumont, K. Zhou, A. Duensing, and J.C. Trent, *Synergistic induction of apoptosis by the Bcl-2 inhibitor ABT-737 and imatinib mesylate in gastrointestinal stromal tumor cells*. *Mol Oncol*. **5**(1): p. 93-104.
115. Papadopulos, F., M. Spinelli, S. Valente, L. Foroni, C. Orrico, F. Alviano, and G. Pasquinelli, *Common tasks in microscopic and ultrastructural image analysis using ImageJ*. *Ultrastruct Pathol*, 2007. **31**(6): p. 401-7.

116. Luciano, F., A. Jacquel, P. Colosetti, M. Herrant, S. Cagnol, G. Pages, and P. Auberger, *Phosphorylation of Bim-EL by Erk1/2 on serine 69 promotes its degradation via the proteasome pathway and regulates its proapoptotic function.* Oncogene, 2003. **22**(43): p. 6785-93.
117. Zheng, W.H., S. Kar, and R. Quirion, *Insulin-like growth factor-1-induced phosphorylation of the forkhead family transcription factor FKHRL1 is mediated by Akt kinase in PC12 cells.* J Biol Chem, 2000. **275**(50): p. 39152-8.
118. Eisenberg-Lerner, A. and A. Kimchi, *The paradox of autophagy and its implication in cancer etiology and therapy.* Apoptosis, 2009. **14**(4): p. 376-91.
119. Pattingre, S., A. Tassa, X. Qu, R. Garuti, X.H. Liang, N. Mizushima, M. Packer, M.D. Schneider, and B. Levine, *Bcl-2 antiapoptotic proteins inhibit Beclin 1-dependent autophagy.* Cell, 2005. **122**(6): p. 927-39.
120. Stroobants, S., J. Goeminne, M. Seegers, S. Dimitrijevic, P. Dupont, J. Nuyts, M. Martens, B. van den Borne, P. Cole, R. Sciot, H. Dumez, S. Silberman, L. Mortelmans, and A. van Oosterom, *18FDG-Positron emission tomography for the early prediction of response in advanced soft tissue sarcoma treated with imatinib mesylate (Glivec).* Eur J Cancer, 2003. **39**(14): p. 2012-20.
121. O'Connor, L., A. Strasser, L.A. O'Reilly, G. Hausmann, J.M. Adams, S. Cory, and D.C. Huang, *Bim: a novel member of the Bcl-2 family that promotes apoptosis.* EMBO J, 1998. **17**(2): p. 384-95.
122. Suster, S., C. Fisher, and C.A. Moran, *Expression of bcl-2 oncoprotein in benign and malignant spindle cell tumors of soft tissue, skin, serosal surfaces, and gastrointestinal tract.* Am J Surg Pathol, 1998. **22**(7): p. 863-72.

123. Cunningham, R.E., S.L. Abbondanzo, W.S. Chu, T.S. Emory, L.H. Sobin, and T.J. O'Leary, *Apoptosis, bcl-2 expression, and p53 expression in gastrointestinal stromal/smooth muscle tumors*. *Appl Immunohistochem Mol Morphol*, 2001. **9**(1): p. 19-23.
124. Noguchi, T., T. Sato, S. Takeno, Y. Uchida, K. Kashima, S. Yokoyama, and W. Muller, *Biological analysis of gastrointestinal stromal tumors*. *Oncol Rep*, 2002. **9**(6): p. 1277-82.
125. Wong, N.A., R. Young, R.D. Malcomson, A.G. Nayar, L.A. Jamieson, V.E. Save, F.A. Carey, D.H. Brewster, C. Han, and A. Al-Nafussi, *Prognostic indicators for gastrointestinal stromal tumours: a clinicopathological and immunohistochemical study of 108 resected cases of the stomach*. *Histopathology*, 2003. **43**(2): p. 118-26.
126. Steinert, D.M., M. Oyarzo, X. Wang, H. Choi, P.F. Thall, L.J. Medeiros, A.K. Raymond, R.S. Benjamin, W. Zhang, and J.C. Trent, *Expression of Bcl-2 in gastrointestinal stromal tumors: correlation with progression-free survival in 81 patients treated with imatinib mesylate*. *Cancer*, 2006. **106**(7): p. 1617-23.
127. Schittenhelm, M.M., S. Shiraga, A. Schroeder, A.S. Corbin, D. Griffith, F.Y. Lee, C. Bokemeyer, M.W. Deininger, B.J. Druker, and M.C. Heinrich, *Dasatinib (BMS-354825), a dual SRC/ABL kinase inhibitor, inhibits the kinase activity of wild-type, juxtamembrane, and activation loop mutant KIT isoforms associated with human malignancies*. *Cancer Res*, 2006. **66**(1): p. 473-81.
128. Dewaele, B., B. Wasag, J. Cools, R. Sciot, H. Prenen, P. Vandenberghe, A. Wozniak, P. Schoffski, P. Marynen, and M. Debiec-Rychter, *Activity of dasatinib*,

- a dual SRC/ABL kinase inhibitor, and IPI-504, a heat shock protein 90 inhibitor, against gastrointestinal stromal tumor-associated PDGFRAD842V mutation. Clin Cancer Res, 2008. 14(18): p. 5749-58.*
129. Ikezoe, T., Y. Yang, C. Nishioka, K. Bandobashi, H. Nakatani, T. Taguchi, H.P. Koeffler, and H. Taguchi, *Effect of SU11248 on gastrointestinal stromal tumor-T1 cells: enhancement of growth inhibition via inhibition of 3-kinase/Akt/mammalian target of rapamycin signaling. Cancer Sci, 2006. 97(9): p. 945-51.*
130. Huynh, H., J.W. Lee, P.K. Chow, V.C. Ngo, G.B. Lew, I.W. Lam, H.S. Ong, A. Chung, and K.C. Soo, *Sorafenib induces growth suppression in mouse models of gastrointestinal stromal tumor. Mol Cancer Ther, 2009. 8(1): p. 152-9.*
131. Muhlenberg, T., Y. Zhang, A.J. Wagner, F. Grabellus, J. Bradner, G. Taeger, H. Lang, T. Taguchi, M. Schuler, J.A. Fletcher, and S. Bauer, *Inhibitors of deacetylases suppress oncogenic KIT signaling, acetylate HSP90, and induce apoptosis in gastrointestinal stromal tumors. Cancer Res, 2009. 69(17): p. 6941-50.*
132. Ou, W.B., M.J. Zhu, G.D. Demetri, C.D. Fletcher, and J.A. Fletcher, *Protein kinase C-theta regulates KIT expression and proliferation in gastrointestinal stromal tumors. Oncogene, 2008. 27(42): p. 5624-34.*
133. Tarn, C., L. Rink, E. Merkel, D. Flieder, H. Pathak, D. Koumbi, J.R. Testa, B. Eisenberg, M. von Mehren, and A.K. Godwin, *Insulin-like growth factor 1 receptor is a potential therapeutic target for gastrointestinal stromal tumors. Proc Natl Acad Sci U S A, 2008. 105(24): p. 8387-92.*

134. Sakurama, K., K. Noma, M. Takaoka, Y. Tomono, N. Watanabe, S. Hatakeyama, O. Ohmori, S. Hirota, T. Motoki, Y. Shirakawa, T. Yamatsuji, M. Haisa, J. Matsuoka, N. Tanaka, and Y. Naomoto, *Inhibition of focal adhesion kinase as a potential therapeutic strategy for imatinib-resistant gastrointestinal stromal tumor*. Mol Cancer Ther, 2009. **8**(1): p. 127-34.
135. Bauer, S., J.A. Parry, T. Muhlenberg, M.F. Brown, D. Seneviratne, P. Chatterjee, A. Chin, B.P. Rubin, S.F. Kuan, J.A. Fletcher, S. Duensing, and A. Duensing, *Proapoptotic activity of bortezomib in gastrointestinal stromal tumor cells*. Cancer Res. **70**(1): p. 150-9.
136. Agaram, N.P., G.C. Wong, T. Guo, R.G. Maki, S. Singer, R.P. Dematteo, P. Besmer, and C.R. Antonescu, *Novel V600E BRAF mutations in imatinib-naive and imatinib-resistant gastrointestinal stromal tumors*. Genes Chromosomes Cancer, 2008. **47**(10): p. 853-9.
137. Wardelmann, E., S. Merkelbach-Bruse, K. Pauls, N. Thomas, H.U. Schildhaus, T. Heinicke, N. Speidel, T. Pietsch, R. Buettner, D. Pink, P. Reichardt, and P. Hohenberger, *Polyclonal evolution of multiple secondary KIT mutations in gastrointestinal stromal tumors under treatment with imatinib mesylate*. Clin Cancer Res, 2006. **12**(6): p. 1743-9.
138. Sattler, M., H. Liang, D. Nettlesheim, R.P. Meadows, J.E. Harlan, M. Eberstadt, H.S. Yoon, S.B. Shuker, B.S. Chang, A.J. Minn, C.B. Thompson, and S.W. Fesik, *Structure of Bcl-xL-Bak peptide complex: recognition between regulators of apoptosis*. Science, 1997. **275**(5302): p. 983-6.

139. Oltersdorf, T., S.W. Elmore, A.R. Shoemaker, R.C. Armstrong, D.J. Augeri, B.A. Belli, M. Bruncko, T.L. Deckwerth, J. Dinges, P.J. Hajduk, M.K. Joseph, S. Kitada, S.J. Korsmeyer, A.R. Kunzer, A. Letai, C. Li, M.J. Mitten, D.G. Nettesheim, S. Ng, P.M. Nimmer, J.M. O'Connor, A. Oleksijew, A.M. Petros, J.C. Reed, W. Shen, S.K. Tahir, C.B. Thompson, K.J. Tomaselli, B. Wang, M.D. Wendt, H. Zhang, S.W. Fesik, and S.H. Rosenberg, *An inhibitor of Bcl-2 family proteins induces regression of solid tumours*. Nature, 2005. **435**(7042): p. 677-81.
140. Vogler, M., K. Weber, D. Dinsdale, I. Schmitz, K. Schulze-Osthoff, M.J. Dyer, and G.M. Cohen, *Different forms of cell death induced by putative BCL2 inhibitors*. Cell Death Differ, 2009. **16**(7): p. 1030-9.
141. Jayanthan, A., S.C. Howard, T. Trippett, T. Horton, J.A. Whitlock, L. Daisley, V. Lewis, and A. Narendran, *Targeting the Bcl-2 family of proteins in Hodgkin lymphoma: in vitro cytotoxicity, target modulation and drug combination studies of the Bcl-2 homology 3 mimetic ABT-737*. Leuk Lymphoma, 2009. **50**(7): p. 1174-82.
142. Kuroda, J., S. Kimura, M. Andreeff, E. Ashihara, Y. Kamitsuji, A. Yokota, E. Kawata, M. Takeuchi, R. Tanaka, Y. Murotani, Y. Matsumoto, H. Tanaka, A. Strasser, M. Taniwaki, and T. Maekawa, *ABT-737 is a useful component of combinatory chemotherapies for chronic myeloid leukaemias with diverse drug-resistance mechanisms*. Br J Haematol, 2008. **140**(2): p. 181-90.
143. Cragg, M.S., E.S. Jansen, M. Cook, C. Harris, A. Strasser, and C.L. Scott, *Treatment of B-RAF mutant human tumor cells with a MEK inhibitor requires Bim and is enhanced by a BH3 mimetic*. J Clin Invest, 2008. **118**(11): p. 3651-9.

144. Yang, Y., T. Ikezoe, C. Nishioka, T. Taguchi, W.G. Zhu, H.P. Koeffler, and H. Taguchi, *ZD6474 induces growth arrest and apoptosis of GIST-T1 cells, which is enhanced by concomitant use of sunitinib*. *Cancer Sci*, 2006. **97**(12): p. 1404-9.
145. Ribble, D., N.B. Goldstein, D.A. Norris, and Y.G. Shellman, *A simple technique for quantifying apoptosis in 96-well plates*. *BMC Biotechnol*, 2005. **5**: p. 12.
146. Chou, T.C., *Preclinical versus clinical drug combination studies*. *Leuk Lymphoma*, 2008. **49**(11): p. 2059-80.
147. Chou, T.C. and P. Talalay, *Generalized equations for the analysis of inhibitions of Michaelis-Menten and higher-order kinetic systems with two or more mutually exclusive and nonexclusive inhibitors*. *Eur J Biochem*, 1981. **115**(1): p. 207-16.
148. Reynolds, C.P. and B.J. Maurer, *Evaluating response to antineoplastic drug combinations in tissue culture models*. *Methods Mol Med*, 2005. **110**: p. 173-83.
149. Gordon, P.M. and D.E. Fisher, *Role for the pro-apoptotic factor BIM in mediating imatinib-induced apoptosis in a c-KIT dependent gastrointestinal stromal tumor cell line*. *J Biol Chem*.
150. Tse, C., A.R. Shoemaker, J. Adickes, M.G. Anderson, J. Chen, S. Jin, E.F. Johnson, K.C. Marsh, M.J. Mitten, P. Nimmer, L. Roberts, S.K. Tahir, Y. Xiao, X. Yang, H. Zhang, S. Fesik, S.H. Rosenberg, and S.W. Elmore, *ABT-263: a potent and orally bioavailable Bcl-2 family inhibitor*. *Cancer Res*, 2008. **68**(9): p. 3421-8.
151. Paoluzzi, L., M. Gonen, G. Bhagat, R.R. Furman, J.R. Gardner, L. Scotto, V.D. Gueorguiev, M.L. Heaney, K. Manova, and O.A. O'Connor, *The BH3-only*

- mimetic ABT-737 synergizes the antineoplastic activity of proteasome inhibitors in lymphoid malignancies.* Blood, 2008. **112**(7): p. 2906-16.
152. Shoemaker, A.R., A. Oleksijew, J. Bauch, B.A. Belli, T. Borre, M. Bruncko, T. Deckwirth, D.J. Frost, K. Jarvis, M.K. Joseph, K. Marsh, W. McClellan, H. Nellans, S. Ng, P. Nimmer, J.M. O'Connor, T. Oltersdorf, W. Qing, W. Shen, J. Stavropoulos, S.K. Tahir, B. Wang, R. Warner, H. Zhang, S.W. Fesik, S.H. Rosenberg, and S.W. Elmore, *A small-molecule inhibitor of Bcl-XL potentiates the activity of cytotoxic drugs in vitro and in vivo.* Cancer Res, 2006. **66**(17): p. 8731-9.
153. Squier, M.K. and J.J. Cohen, *Standard quantitative assays for apoptosis.* Mol Biotechnol, 2001. **19**(3): p. 305-12.
154. Park, C.M., M. Bruncko, J. Adickes, J. Bauch, H. Ding, A. Kunzer, K.C. Marsh, P. Nimmer, A.R. Shoemaker, X. Song, S.K. Tahir, C. Tse, X. Wang, M.D. Wendt, X. Yang, H. Zhang, S.W. Fesik, S.H. Rosenberg, and S.W. Elmore, *Discovery of an orally bioavailable small molecule inhibitor of prosurvival B-cell lymphoma 2 proteins.* J Med Chem, 2008. **51**(21): p. 6902-15.
155. Roberts, A.W., J.F. Seymour, J.R. Brown, W.G. Wierda, T.J. Kipps, S.L. Khaw, D.A. Carney, S.Z. He, D.C. Huang, H. Xiong, Y. Cui, T.A. Busman, E.M. McKeegan, A.P. Krivoshik, S.H. Enschede, and R. Humerickhouse, *Substantial Susceptibility of Chronic Lymphocytic Leukemia to BCL2 Inhibition: Results of a Phase I Study of Navitoclax in Patients With Relapsed or Refractory Disease.* J Clin Oncol.

156. Gandhi, L., D.R. Camidge, M. Ribeiro de Oliveira, P. Bonomi, D. Gandara, D. Khaira, C.L. Hann, E.M. McKeegan, E. Litvinovich, P.M. Hemken, C. Dive, S.H. Enschede, C. Nolan, Y.L. Chiu, T. Busman, H. Xiong, A.P. Krivoshik, R. Humerickhouse, G.I. Shapiro, and C.M. Rudin, *Phase I study of Navitoclax (ABT-263), a novel Bcl-2 family inhibitor, in patients with small-cell lung cancer and other solid tumors*. J Clin Oncol. **29**(7): p. 909-16.
157. Wilson, W.H., O.A. O'Connor, M.S. Czuczman, A.S. LaCasce, J.F. Gerecitano, J.P. Leonard, A. Tulpule, K. Dunleavy, H. Xiong, Y.L. Chiu, Y. Cui, T. Busman, S.W. Elmore, S.H. Rosenberg, A.P. Krivoshik, S.H. Enschede, and R.A. Humerickhouse, *Navitoclax, a targeted high-affinity inhibitor of BCL-2, in lymphoid malignancies: a phase I dose-escalation study of safety, pharmacokinetics, pharmacodynamics, and antitumour activity*. Lancet Oncol. **11**(12): p. 1149-59.
158. Hoang, T.C., T.K. Bui, T. Taguchi, T. Watanabe, and Y. Sato, *All-trans retinoic acid inhibits KIT activity and induces apoptosis in gastrointestinal stromal tumor GIST-T1 cell line by affecting on the expression of survivin and Bax protein*. J Exp Clin Cancer Res. **29**: p. 165.
159. Heinrich, M.C., K. Owzar, C.L. Corless, D. Hollis, E.C. Borden, C.D. Fletcher, C.W. Ryan, M. von Mehren, C.D. Blanke, C. Rankin, R.S. Benjamin, V.H. Bramwell, G.D. Demetri, M.M. Bertagnolli, and J.A. Fletcher, *Correlation of kinase genotype and clinical outcome in the North American Intergroup Phase III Trial of imatinib mesylate for treatment of advanced gastrointestinal stromal*

- tumor: CALGB 150105 Study by Cancer and Leukemia Group B and Southwest Oncology Group. *J Clin Oncol*, 2008. **26**(33): p. 5360-7.
160. Kumar, S.R., F.A. Gallazzi, T.P. Quinn, and S.L. Deutscher, (64)*Cu-labeled peptide for PET of breast carcinomas expressing the Thomsen-Friedenreich carbohydrate antigen*. *J Nucl Med*. **52**(11): p. 1819-26.
161. Eisenberg, B.L., *Combining imatinib with surgery in gastrointestinal stromal tumors: rationale and ongoing trials*. *Clin Colorectal Cancer*, 2006. **6 Suppl 1**: p. S24-9.
162. Reynoso, D. and J.C. Trent, *Neoadjuvant and adjuvant imatinib treatment in gastrointestinal stromal tumor: current status and recent developments*. *Curr Opin Oncol*. **22**(4): p. 330-5.
163. von Mehren, M. and N. Widmer, *Correlations between imatinib pharmacokinetics, pharmacodynamics, adherence, and clinical response in advanced metastatic gastrointestinal stromal tumor (GIST): an emerging role for drug blood level testing?* *Cancer Treat Rev*. **37**(4): p. 291-9.
164. George, S. and J.C. Trent, *The role of imatinib plasma level testing in gastrointestinal stromal tumor*. *Cancer Chemother Pharmacol*. **67 Suppl 1**: p. S45-50.
165. Demetri, G.D., Y. Wang, E. Wehrle, A. Racine, Z. Nikolova, C.D. Blanke, H. Joensuu, and M. von Mehren, *Imatinib plasma levels are correlated with clinical benefit in patients with unresectable/metastatic gastrointestinal stromal tumors*. *J Clin Oncol*, 2009. **27**(19): p. 3141-7.

166. Marrari, A., J.C. Trent, and S. George, *Personalized cancer therapy for gastrointestinal stromal tumor: synergizing tumor genotyping with imatinib plasma levels*. *Curr Opin Oncol*. **22**(4): p. 336-41.
167. van Schaik, R.H., *CYP450 pharmacogenetics for personalizing cancer therapy*. *Drug Resist Updat*, 2008. **11**(3): p. 77-98.
168. O'Donnell, E.P., K.M. Hurt, M.H. Scheetz, M.J. Postelnick, and K.K. Scarsi, *Empiric antibiotic selection for infectious emergencies: bacterial pneumonia, meningitis and sepsis*. *Drugs Today (Barc)*, 2009. **45**(5): p. 379-93.

VITA

David Reynoso Gaytan was born in Mexico City, Mexico on February 6, 1982 to parents Micaela Gaytan Perez and Ebodio Reynoso Santamaria. Together, his family immigrated to the United States and settled in Houston, Texas in 1989. He is an alumnus of the University of Texas at Austin, where he obtained a Bachelor of Science degree in Biology in 2004. He has been active in biomedical research since 2002, with the Department of Molecular Genetics & Microbiology at UT-Austin from 2002 to 2004, and with the Laboratory of Malaria and Vector Research at the National Institutes of Health from 2004 to 2005. From 2005 to 2012, he received medical and research training through the M.D./Ph.D. Program at the University of Texas Medical School at Houston. His dissertation research was conducted with the sponsorship of The University of Texas Graduate School of Biomedical Sciences, M. D. Anderson Cancer Center, under the supervision of Jonathan C. Trent, M.D., Ph.D. in the Department of Sarcoma Medical Oncology. He will pursue a medical residency in internal medicine beginning July 2012, and is forever grateful for the unconditional love and support of his family and friends.

Permanent address:
1404 Walton Street
Houston, TX 77009

Permanent e-mail:
david.reynoso@gmail.com